PhD thesis:

Novel gene therapeutic approaches to prolong corneal allograft survival

A thesis submitted to the National University of Ireland in fulfillment of the requirement for the degree of

Doctor of Philosophy

by

Mieszko Wilk, M.Sc.

Supervisors: Dr. Thomas Ritter (REMEDI, NCBES)

Institution: Regenerative Medicine Institute, National Centre for Biomedical Engineering Science (REMEDI/NCBES)

Submitted: September 2012

For those who waited the most

My parents Barbara and Zbigniew

and my beloved partner, Ewa

Table of contents:

TABLE OF CONTENTS I
ACKNOWLEDGEMENTS III
ABBREVIATIONS V
SUMMARY VIII

1 GENERAL INTRODUCTION 1
1.1 Anatomy of the cornea 1
1.1.1 The endothelium 2
1.2 Corneal immune privilege 3
1.2.1 Inhibition of the afferent arm 4
1.2.2 Inhibition of the efferent arm 5
1.3 Corneal allograft rejection 8
1.3.1 Afferent arm – allorecognition 8
1.3.2 Immune effectors 9
1.4 Gene-therapeutic applications for cornea transplantation 12
1.4.1 Experimental strategies for preventing immune rejection 13
1.4.2 Local gene transfer to the cornea 15
1.5 Aims and hypothesis of the PhD Project 16
1.5.1 Anti-apoptotic strategy 16
1.5.2 Inhibition of immune cells infiltration 17

2 MATERIALS AND METHODS 18
2.1 Plasmid constructs 18
2.1.1 Plasmids 18
2.1.2 Primer design 18
2.1.3 Amplifying mNGF sequence by Polymerase Chain Reaction 19
2.1.4 DNA Gel Electrophoresis 20
2.1.5 Extraction of DNA fragments from agarose gel 21
2.1.6 Plasmid DNA isolation 21
2.1.7 Bacteria transformation 22
2.1.8 Selection of transformed bacteria 22
2.1.9 Ligation with intermediate plasmid 23
2.1.10 Ligation with destination plasmid 23
2.1.11 Restriction enzyme analysis 25
2.1.12 Generation of PD-L1 expressing lentiviral plasmid 26
2.2 Cell culture, transduction and treatment 26
2.2.1 Cell lines 26
2.2.2 Lentiviral vector production and titration 27
2.2.3 Verification of functional NGF expression 29
2.2.4 Microscopic examination of neurite outgrowth of PC12 cells 29
2.2.5 Apoptosis detection assay 30
2.2.6 Protein preparation and Western blotting 30
2.2.7 Quantification of NGF concentration 31

2.3 Rat corneal transplantation 32
2.3.1 Rat strains 32
2.3.2 Surgical procedure 32
2.3.3 Ex vivo gene transfer into cultured corneas 33
2.3.4 Isolation of lymphocytes from corneas, LNs and PBMCs 33
2.3.5 Flow cytometry 34
2.3.6 Histology and histochemistry 35
2.3.7 RNA isolation and reverse transcription of mRNA 36
2.3.8 Quantitive Real-Time PCR (qRT-PCR) 37
2.3.9 Statistics 38
2.4 General consumables 39

3 ROLE OF LOCAL OVER-EXPRESSION OF NGF ON CORNEAL ALLOGRAFT SURVIVAL 40
3.1 Introduction 40
3.2 Results 43
3.2.1 Generation of lentiviral vectors encoding for nerve growth factor 43
3.2.2 Detection of NGF protein and functional activity assay 45
3.2.3 Role of NGF overexpression on corneal endothelial cell protection 56
3.2.4 The effect of local lentiviral-mediated NGF gene transfer on corneal allograft survival .. 69
3.2.5 *Ex vivo* LV-mediated gene transfer of NGF into the donor cornea 75
3.3 Discussion 79

4 ROLE OF LENTIVIRUS-MEDIATED OVEREXPRESSION OF PD-L1 ON CORNEAL ALLOGRAFT SURVIVAL 89
4.1 Introduction 89
4.2 Results 91
4.2.1 Local overexpression of PD-L1 leads to prolongation of corneal allograft survival 91
4.2.2 Flow cytometric characterization of immune cells from transplanted animals 97
4.3 Discussion 107

5 GENERAL DISCUSSION 114

BIBLIOGRAPHY 119

APPENDIX 135
I. Publications by the author 135

Acknowledgements

I would like to express my deepest appreciation to several people that have inspire and motivate me during the best and worst moments of my Ph.D. The printed version of this dissertation does not reflect the amount of work and encouragement of numerous people who made this thesis possible. Completing my Ph.D. degree has been one of the most challenging activities I have ever undertaken and an unforgettable experience. I am very fortunate that I could spend all these years working at the Regenerative Medicine Institute in Galway and look back fondly on my time there.

First and foremost, I would like to thank to my supervisor, Dr. Thomas Ritter for giving me the opportunity to conduct this work but also for his guidance and encouragement throughout the course of my studies. I am also thankful for allowing me the freedom to pursue independent work.

I am also extremely indebted to Dr. Mikhail Nosov for his valuable suggestions and constructive criticism that allowed me to successfully overcome many difficulties and learn a lot. His contribution to my work was invaluable.

I gratefully acknowledge Dr. Martin Maenz who introduced me to a Ph.D. pathway at the beginning of my studies and served as a role model of a Ph.D. student until he graduated. Also other members of the laboratory deserve my sincerest thanks. Their friendship and assistance has been very important throughout all my Ph.D. Special thanks to Oliver Treacy and Marese Cregg for helping me to “polish my English” and for their willingness to edit this thesis. I could not omit Lisa O’Flynn who is close to completing her thesis – good luck!

I would like to express my sincere gratitude to the members of the Discipline of Biochemistry, Dr. Katarzyna Mnich and Dr. Adrienne Gorman. I could not have

completed my work without their invaluable technical knowledge, support and expert opinion in relation to on the NGF work.

A special thanks to Mourice Morcos for performing all animal surgical procedures and to the administrative staff of the Regenerative Medicine Institute and the National Centre for Biomedical Engineering Sciences for day-to-day assistance.

I would also like to take this opportunity to acknowledge the Irish Research Council for Science, Engineering and Technology (IRCSET) for providing financial assistance in the form of the EMBARK Postgraduate Scholarship Scheme, which gave me the opportunity to expand my scientific skills by participating in several workshops.

There is also “normal” life outside of a Ph.D., there really is. I take this opportunity to thank my housemates from 37 Gleann Dara, Rahoon. I would also like to expand my thanks to all my friends from the Polish Society and also to those friends who have been impatiently waiting for my return to Kraków. They were sources of laughter, joy and support during my studies.

I wish to thank my parents, Barbara and Zbigniew, and my closest family. Their unconditional love was my true driving force. I hope that this work makes them proud of me.

It finally want to gratefully acknowledge my beloved partner Ewa Oleszycka who has brought harmony to my life. She positively inspired me for further work. Without her day-to-day closeness, patience and kindness, as well as valuable advice and moral support, this thesis would not have been possible.

Abbreviations

293T	Human Embrionic Kidney 293T cells
AAV	Adeno-Associated Viruses
ACAID	Anterior Chamber-Associated Immune Deviation
AH	Aqueous humor
APC	Antigen presenting cells
Bag-1	BAG family molecular chaperone regulator 1
bcl-xL	B-cell lymphoma-extra large
BSA	Bovine serum albumin
CD	Cluster of differentiation
cDMEM	DMEM with L-glutamine supplemented with 10% FCS and P/S
cDNA	Complementary DNA
CGRP	Calcitonin gene-related peptide
CMV.IE	Human cytomegalovirus immediate early
CRP	Complement regulatory protein
Crry	Complement receptor related protein
CTL	Cytotoxic T lymphocytes
CTLA	Cytotoxic T lymphocyte antigen
DA	Dark Agouti rat
DAPI	4',6-diamidino-2-phenylindole
DEVD-MCA	Acetyl-L-Aspartyl-L-Glutamyl-L-Valyl-L-Aspartic Acid α-(4-Methyl-Coumaryl-7-Amide)
DMEM	Dulbecco's modified Eagle's medium
DNA	Deoxyribonucleic acid
dNTP	Deoxyribonucleotide triphosphate
DTH	Delayed-type hypersensitivity
E::K-5	Endostatin::kringle-5
EF-1α	Elongation factor - 1α
EGFP	Enhanced green fluorescent protein
EIAV	Equine infectious anaemia virus
ELISA	Enzyme linked immuno – sorbent assay
ER	Endoplasmatic reticulum
EYFP	Enhanced yellow fluorescent protein
FACS	Fluorescence – activated cell sorting – flow cytometry
FCS	Fetal calf serum
HCEC	Human corneal endothelial cells
HCEpC	Human corneal epithelial cell
HEPES	4-(2-hydroxyethyl)-1-piperazineethanesulfonic acid
HIV	Human immunodeficiency virus

HS	Horses serum
HSC	Hematopoietic stem cell
hsDMEM	DMEM with L-glutamine supplemented with 10% HS, 5% FCS and P/S antibiotics
ICOS	Inducible T-cell costimulator
IDO	Indoleamine 2,3-dioxygenase
IFN-γ	Interferon - gamma
iHCEC	Immortalized HCEC
IL	Interleukin
IM	Insertional mutagenesis
IPTG	Isopropyl-beta-D-thiogalactopyranoside
KIR	Killer inhibitory receptors
KO	Knockout
LB	Luria broth
LEW	Lewis rat
LINE	Long interspersed nuclear elements
LV	Lentiviral vectors
LV.NGF	Lentiviral vector expressing NGF
LV.PD-L1	Lentiviral vector expressing PD-L1
mAbs	Monoclonal antibodies
mHAg	Minor histocompatibility antigens
MHC	Major histocompatibility complex
MIF	Migration inhibitory factor
MLR	Mixed lymphocyte reaction
MST	Median survival time
NCBI	National Center for Biotechnology Information
NGF	Nerve growth factor
NK	Natural killer cells
NKT	Natural killer T cells
NO^-	Nitric oxide
NT	Neurotrophin
NV	Neovascularogenesis
OP	Opacity
P/S	Penicillin/streptomycin
PBMCs	Peripheral blood mononuclear cells
PBS	Phosphate buffored saline
PC12	Rat adrenal phaeochromocytoma
PCR	Polymerase chain reaction
PD-1	Programmed death - 1
PD-L1	Programmed death - ligand 1

pDNA	Plasmid DNA
PEI	Polyethylenimine
PFA	Paraformaldehyde
PI	Propidium Iodide
POD	Postoperative day
qRT-PCR	Real-Time quantitative reverse transcription PCR
RCL	Replication-competent lentivirus
RNA	Ribonucleic acid
rNGF	Recombinant
RPE	Retinal pigment epithelium
RPMI	Roswell Park Memorial Institute medium
RT	Room temperature
SCID	Severe combined immunodeficiency
SDS-PAGE	Sodium dodecyl sulfate polyacrylamide gel electrophoresis
SIN	Self-inactivating
TAE	Tris-acetate-EDTA buffer
TG	Thapsigargin
TGF-β	Transforming growth factor - beta
Th	T-helper cell
TNF-α	Tumor necrosis factor - alfa
Trk	Tyrosine kinase
TU	Transducing unit
UV	Ultraviolet
VEGF	Vascular endothelial growth factor
VIP	Vasoactive intestinal peptide
VSV-G	Vesicular stomatitis virus G
WPRE	Woodchuck posttranscriptional regulatory element
Xgal	5-bromo-4-chloro-3-indolyl-beta-D-galactopyranoside
Z-VAD-fmk	Pan-caspase inhibitor
α-MSH	α-melanocyte-stimulating hormone

Summary

Cornea transplantation (penetrating keratoplasty) is the most frequent form of allograft transplantation in humans with a 90 % success rate in the first 2 years, however, the rate of survival decreases over time and drops to approximately 62% after 10 years. The predictions for "high risk" graft survival are even poorer. Despite advances in microsurgery and immunosuppressive treatment protocols a significant number of corneal grafts still undergo immune-mediated allograft rejection. Therefore, alternative approaches are needed to prevent corneal transplant rejection such as genetic modification of donor corneas.

Gene therapy has been widely applied in preclinical studies to manipulate the corneal graft rejection process. The main goal of corneal gene therapy is to achieve long-term allograft survival without the need for other treatments or only restricted to short periods of time thereby reducing undesired side effects. Herein, two distinctive strategies in a preclinical model of rat cornea transplantation to prevent allograft rejection were investigated using lentiviral (LV) vectors as vehicles for therapeutic gene delivery and overexpression in the corneal allograft.

The first part of this work was based on known anti-apoptotic properties of nerve growth factor (NGF). As previously reported, adenovirus (Ad)-mediated NGF overexpression reduces apoptosis in corneal endothelial cells and prolongs allograft survival in an *in vivo* rat model, however, the mechanisms were not fully understood and the use of adenoviral vectors raised concern. The aim of this part of the project was to develop an anti-apoptotic strategy using alternative, low immunogenic LV vectors expressing NGF (LV.NGF) for rat cornea transplantation and investigation of the underlying mechanisms of cytoprotection. It was shown that LV.NGF transduced corneal endothelial cells secreted biologically active NGF. In addition, supernatants from LV.NGF transduced immortalized human corneal endothelial cells (HCEC) significantly reduced thapsigargin (TG)-induced apoptosis in control PC12 cells, however, no protective effect of either recombinant NGF or supernatant containing NGF could be observed in HCEC. Subsequently, a protocol for LV-mediated transduction of *ex vivo* cultured corneas was established. However, in contrast to previous results showing that Ad.NGF gene transfer in cultured corneas resulted in significant prolongation of allograft survival, donor corneas transduced with

LV.NGF did not show any protective effect *in vivo*. Different expression levels of the therapeutic gene after Ad- or LV gene transfer may account for these results.

The second part of this project was to investigate the role of LV-mediated overexpression of Programmed Death Ligand-1 (PD-L1) on rat corneal allograft survival. In contrast to LV.NGF treatment, allogeneic LV.PD-L1 transduced corneas showed a high percentage (83%) of graft survival. This striking result was associated with a reduction of natural killer T (NKT) cell and cytotoxic CD8+ T cell infiltration to the graft as measured by flow cytometry. Graft opacity, as an indicator of cell infiltration, was present but was significantly reduced in PD-L1 transduced corneas compared to control or EGFP expressing corneas.

Herein, the data provide evidence that therapeutic applications of LV-based cornea gene therapy might be a valuable clinical approach for treatment of corneal endothelium failure and/or graft rejection.

Chapter 1:

General introduction

1 General introduction

Cornea transplantation holds the unique advantage for gene therapy to modify allografts *ex-vivo* prior to transplantation. In contrast to other tissues that are routinely transplanted, the cornea can be kept in culture for up to 4 weeks without significant loss of function which allows sufficient time for *ex-vivo* manipulation. Moreover, local expression of therapeutic genes may be sufficient to achieve a therapeutic effect thus making systemic (genetic) intervention either unnecessary or required only at reduced doses thereby avoiding undesired side effects.

1.1 Anatomy of the cornea

The cornea is the anterior part of the eye protecting the inner environment from harmful substances, foreign particle penetration or pathogen infection. As it is a highly light-refractive element of the eye, it also plays a crucial role in producing the initial image, focusing it and passing light rays to the retina. The smoothness, shape and clearness of the corneal tissue are essential for visual acuity. Any disruption of corneal structure may result in a loss of function and subsequent risk of sight problems.

The cornea consists of three cellular layers and two basement membranes devoid of cells lying between them (1). The epithelium contains six to eight non-keratinized cell layers placed on the Bowman's membrane. The deeper epithelial cells constantly undergo mitosis and eventually replace the superficial cells in about 7-10 days (2). The Bowman's acellular membrane is formed from irregularly-arranged collagen fibers in contrast to the stromal fiber organization. The stroma is located between two acellular membranes and is mostly formed of tightly packed and precisely aligned collagen populated by scattered keratocytes. The Descemet's layer is a relatively thick basement membrane secreted by the endothelial monolayer cells. The corneal endothelium, that forms a boundary between the stroma and anterior chamber, is critical to the functioning of the cornea and will be described in more detail (3).

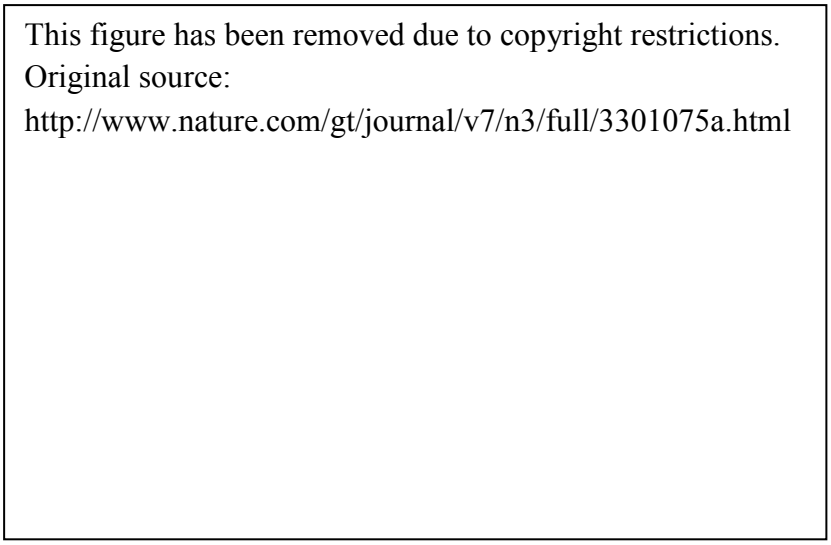

Fig. 1.1. A schematic diagram of the anterior part of the human eye with a close up of the cornea indicating all three cell layers and the two membranes that make up this transparent tissue (1)**.**

1.1.1 The endothelium

The corneal endothelial monolayer originates from neural crest-derived mesenchymal cells (4). The mature and fully developed layer is built from polygon-shaped cells with limited proliferation capacity, which is believed to be inhibited by cell-cell contact inhibition and G1 phase arrest (5). The two major functions of the endothelium are: i) to supply the avascular cornea with nutrients from the aqueous humor and ii) to act as a barrier protecting the stroma from swelling by removal of excess stromal fluid (6).

The clearness of the cornea is due in part to maintenance of epithelial integrity, a lack of blood vessels and spatial arrangement of the collagen fibers within the stroma, however, the epithelium plays the role in maintenance of transparency. The maintenance of cornea transparency directly depends on the barrier and “pump” functions which can be disturbed by an integrity disruption of the endothelial layer. The number of endothelial cells declines by age (7-9), however, trauma (surgical or otherwise) is a main cause of irreversible decline in the endothelial cell number which might result in edema, clouding and as a final consequence – a loss of vision

(10, 11). This must be considered in the context of cornea storage and keratoplasty where the quality and density of the endothelial cells are critical factors.

From the cornea transplantation perspective, endothelial decompensation is the main contributor to graft failure. This can occur during cornea storage, as a consequence of surgical trauma or the early postoperative inflammation. A further acute loss in cell number is described during rejection episodes as a result of immunological damage (12, 13). Despite the fact that any cellular layer of the cornea can be vulnerable to the rejection process, the epithelium can be restored by recipient cells and stromal destruction can be reversed with intensive application of topical steroid. Only rejection of the endothelium is irreversible due to its reduced proliferative capacity. Therefore, it is of high importance to investigate the nature of endothelial cell decompensation as well as to develop novel strategies to prevent cell loss (3, 14).

1.2 Corneal immune privilege

Immune privilege is a mechanism restricted only to several sites and tissues in the organism defined as sites (e.g. brain, testicles, eyes) that allow foreign grafts to survive for extended, often indefinite periods. These immune privileged tissues are also accepted for extended and often indefinite periods when transplanted orthotopically (15). This phenomenon was observed by Eduard Zirm when the first successful keratoplasty in a human subject was performed more than 100 years ago and re-discovered 50 years later by Peter Medawar based on new findings and evidence (16). The cornea is constantly threatened by injuries or infections which may provide a risk of inflammation and tissue damage. Any distortion of the ocular surface may result in the loss of visual acuity. It is postulated that immune privilege evolved as a natural equilibrium between elimination of the threat and protection against immunopathogenic tissue damage (15). There are several immunological mechanisms as well as microenvironmental solutions that ensure the immune-privileged status of the eye. Overall, these result in a higher success rate than other forms of organ transplantation and often reach 90% success rate after surgery (17). The favourable prognosis of corneal transplants in humans or experimental animals

in the absence of risk factors is attributed to the immune privilege of the eye (16). There are several pathways that induce and maintain the immune privilege of the eye.

1.2.1 Inhibition of the afferent arm

As mentioned previously, the normal cornea is an avascular structure. This avascular microenvironment plays a profound role in suppressing the immune response by reducing the possibility of antigen presentation by the lymphatic-drainage pathway and infiltration of effector cells into the cornea through the blood vessels (18). In the setting of cornea transplantation, pre-existing or secondary neovascularization (NV) is one of the most important predisposing factors for immunological corneal allograft rejection and correlate with lower success rate in both humans and mice (18). Moreover, induction of corneal NV leads to loss of immune privilege in the anterior segment (19), thus proving that the avascular microenvironment contributes to maintenance of ocular immune privilege.

The constitutive expression of soluble vascular endothelial growth factor (VEGF) receptor 1 by the cornea (20) and VEGF receptor 3 by intact epithelium inhibits non-specific neovascularization (21, 22). Furthermore, lymphangiogenesis is locally suppressed by the constitutive production of VEGF receptor 2 by epithelial cells and keratocytes (23). This is supported by findings that high vascular bed or surgical trauma (either suture or wound healing) during keratoplasty stimulates both blood and lymph vessel growth and promotes a rapid immune rejection. On the other hand, administration of exogenous soluble VEGF receptor 2 doubles the corneal allograft survival rate in a “high risk” rat model (23), suggesting that the lymphatic-drainage pathway but not absence of blood vessels, is important to maintaining corneal immune privilege (24).

The blood-ocular barrier provides additional support to the protection of the unique eye environment. To gain access to the eye, the cells have to pass through tight junctions within the iris pigment epithelial layer. These cells constitutively express the co-stimulatory molecule CD86 that binds to CD28 and CTLA4 on activated T

cells. This cell-cell interaction blocks T-cell proliferation and IFN-γ production as well as converts them into regulatory T cells (25).

1.2.2 Inhibition of the efferent arm

There is no doubt that lack of blood vessels in the cornea greatly reduces infiltration of the effector cells, however, it does not fully eliminate the risk of acute immune response. Consequently, other mechanisms have developed to maintain ocular immune privilege.

1.2.2.1 Components of aqueous humor

The soluble factors in aqueous humor (AH) are able not only to suppress effector cells of both innate and adaptive immunity, but also to modulate the response to create a tolerogenic milieu. The immunosuppressive activity of AH is orchestrated by cytokines, growth factors and neuropeptides that are able to selectively inhibit innate and adaptive immune effector cells that threaten the eye by mediating inflammation (15). Indeed, natural killer (NK) cell-mediated cytolysis, that can occur because of lack of MHC class I expression on endothelial cells, is suppressed by macrophage migration inhibitory factor (MIF) and transforming growth factor-β (TGF-β) present in AH (26, 27). In addition, soluble complement regulatory protein (CRP) abrogates the effect of complement-mediated cytolysis.

An important group of modulating factors in the anterior chamber are neuropeptides. Many of these factors are constantly present in AH and contribute to the creation and maintenance of an immunosuppressive microenvironment. It was suggested that the endothelium, as a neural crest-derived layer, can play a neuroendocrine function by expressing neurotrophic factors such as vasoactive intestinal peptide (VIP) (28). Moreover, VIP is able to protect endothelial cells from the acute killing effect of hydrogen peroxide and modulates the cell death pathway by switching necrosis to apoptosis (29, 30). This is important in the context of inflammation which is caused by necrosis but not apoptotic cells. Also, the presence of α-melanocyte-stimulating hormone (α-MSH) is critical for immune inhibitory function of AH. It was shown that the production of inflammatory cytokines by adaptive effector $CD4^+$ T cells is abrogated by α-MSH (31). Moreover, activated

T cells are converted by α-MSH into regulatory cells that help to strengthen immunological ignorance (32). The importance of α-MSH in AH is supported by the discovery that subconjunctival α-MSH injections after cornea transplantation significantly reduce allorejection in mice (33). Calcitonin gene-related peptide (CGRP), constitutively present in AH, inhibits the production of nitric oxide (NO^-) by activated macrophages (34). Pro-inflammatory cytokines, which are released by alloreactive infiltrating cells, cause apoptosis of corneal endothelium also via the NO^- pathway (35). It is possible that CGRP protects endothelium from apoptosis by inhibiting NO^- production. Overall, soluble factors play a crucial role in maintenance of the anti-inflammatory state of the aqueous humor and, in turn, contribute to the immune privilege status of the eye.

1.2.2.2 Corneal endothelium barrier

Molecules that are expressed on the surface of endothelial cells form a unique barrier that protects the cornea from effector T cells or complement activation (16). It was shown that FasL (CD95L), as well as its soluble form are responsible for apoptosis induction of infiltrating neutrophils and activated T cells into the AH (36-38). Moreover, constitutive expression of membrane-associated CRP acts to disable complement-mediated cytolysis (39). It was reported that neutralization of complement receptor related protein (Crry) in rat leads to spontaneous inflammation of the anterior segment (40). Programmed Death–Ligand 1 (PD-L1) was also detected on endothelial cell membrane. Further studies revealed that it is involved in neutralizing T lymphocytes by apoptosis induction, inhibition of their proliferation and blocking of IFN-γ production (41, 42) and will be described in more detail later.

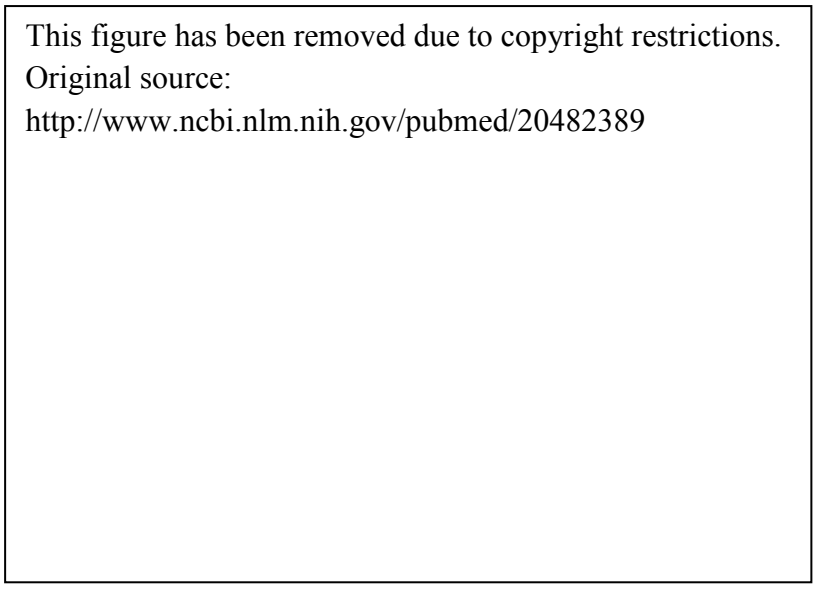

Fig. 1.2. Cell membrane-bound molecules expressed on the corneal endothelium block the expression of effector T cells and complement activation (16).

1.2.2.3 Anterior Chamber-Associated Immune Deviation (ACAID)

In addition to local immunosuppressive mechanisms in the eye, the unique process of peripheral immune tolerance induction also contributes to maintaining immune privilege. ACAID is defined as antigen-specific suppression of a delayed-type hypersensitivity response which arose as a consequence of exogenous antigen presentation in the anterior chamber. The mechanisms involve migration of intraocular APCs to the spleen and formation of multicellular clusters that activate antigen-specific 'afferent' $CD4^+$ and 'efferent' $CD8^+$ regulatory T cells (15). In agreement with this mechanism, it has been proposed that during keratoplasty corneal alloantigens could be sloughed or shed into the AC and induce ACAID, however, Cunnusamy et al showed that there are two different forms of immune tolerance involved in the induction of ACAID and corneal allograft survival (43). ACAID $CD4^+$ T regs are required to generate $CD8^+$ T regs that inhibit delayed-type sensitivity (DTH) responses to the donor's alloantigen, however, alone are not able to suppress DTH reactions. By contrast $CD4^+$ T regs which are induced by corneal allograft, act independently on $CD8^+$ T cells to suppress T-cell proliferation and DTH (44, 45).

1.3 Corneal allograft rejection

As described earlier, the avascular corneal microenvironment and mechanisms maintaining immune privilege do not fully protect corneal allografts from rejection. Moreover, other factors like surgical trauma, uncontrolled inflammation, allergies or the need for re-transplantation predispose the graft to rejection process. The primary initial mechanism that leads to graft rejection is allorecognition. Appropriate detection and recognition of the alloantigens from grafted organs are necessary to provide an adequate and effective response against non-self tissue.

1.3.1 Afferent arm – allorecognition

In the context of allogeneic transplantation, recipient $CD4^+$ T cells are considered to be the main cell type involved in allorecognition (46). This is due to their ability to recognize major histocompatibility complex (MHC) molecules presented by donor cells. T lymphocytes are also able to recognize minor histocompatibility antigens (mHAg) processed by host antigen presenting cells and presented in the groove of MHC class I and II molecules. The strength and mechanism of the T-cell alloresponse varies due to the nature of transplanted tissue and placement site in the recipient body. There are two distinct, but not mutually exclusive, pathways of allorecognition. The direct pathway, which is ascribed to the acute rejection process, involves activation of the recipient $CD4^+$ T cells in the regional lymph nodes by allogeneic MHC class II molecules presented on donor passenger leucocytes. The indirect route, however, is also mediated by recipient $CD4^+$ T lymphocytes but activated by recipient APCs that process and present donor antigens in the context of “self” MHC. This type of allorecognition is thought to be involved in the late acute or chronic forms of rejection due to the delayed tempo of response to alloantigens (47-49).

The rejection process of corneal allografts differs from other solid tissue grafts (50). It was shown that the main, but not exclusive, route of corneal allograft recognition by recipient $CD4^+$ T cells is mediated through the indirect pathway, in contrast to, for example, skin allograft recognition (51). Moreover, Sano et al have reported that minor H antigens are considered to be the prime source of peptides recognized

through the indirect pathway (52). These results were confirmed by a direct comparison of minor Ag and MHC antigen contribution to the indirect alloresponse by $CD4^+$ T lymphocytes in transplanted mouse corneas (51). The possible explanation is that reduced expression of MHC antigens on the corneal cells restrict alloantigen recognition to the indirect pathway with minor H antigens as a main source of peptides. Also, donor immature APCs that migrate to the recipient's draining lymph nodes may activate a sort of tolerogenicity.

Other aspects of corneal alloantigen recognition have to be considered when the graft is placed onto the inflamed and/or vascularized bed. The rejection rate is dramatically increased and the tempo is reminiscent of acute rejection of other solid and vascularized tissues and organs. Similar to low risk grafts, donor APCs migrate to the draining LN, however, the trafficking is enhanced (53) and the APC activation markers (CD40, CD80, CD86), as well as MHC class II on donor cells, are significantly upregulated (54). Furthermore, despite the indirect activation of effector cells, inhibition of the indirect pathway in high risk grafts fails to abrogate the rejection process (55, 56). In addition, the direct pathway was found to play a profound role in a high risk setting in parallel with the indirect response (54).

It is claimed that the absence or reduced expression of MHC class I molecules on ocular cells (in particular endothelium) developed during evolution as part of immune privilege mechanisms to prevent them from cytotoxic T lymphocytes (CTL)-mediated lysis in the event of viral infection (57). However, lack of MHC class I molecules is recognized by killer inhibitory receptors (KIR) expressed on NK cells and provide a signal for NK cell-mediated cytolysis. This non-self discrimination, known as the 'missing self hypothesis' (58), plays a crucial role in non-clasical allorecognition in parallel to the classical pathway.

1.3.2 Immune effectors

The primary effector cells in the corneal rejection process are $CD4^+$ T cells. A number of investigations have reported that *in vivo* depletion of $CD4^+$ T cells either with anti-CD4 mAbs or by gene deletion resulted in a significant decrease of corneal allograft rejection (59-63). $CD4^+$ T cell-depleted mice or rats, however, do

not fully accept the corneal allograft suggesting other, $CD4^+$ T cell-independent mechanisms may play a role in this process. Overall, there are many possible mechanisms of immune rejection that are complementary to each other and their activation depends on several factors like allorecognition pathway, degree of histocompatibility, low/high risk grafts, infection or allergies.

The first T-cell subtype that has been proposed to mediate corneal graft rejection is $CD4^+$ Th1 cells. Th1 cells produce a range of cytokines including IFN-γ and TNF-α that are required for DTH responses to the donor's histocompatibility antigens. Indeed, Th1 cells are activated either by indirect (low risk graft) or direct (high risk graft) pathways of allosensitization (54, 62). Moreover, IFN-γ and TNF-α, which are capable of causing corneal tissue damage, were detected in rejected corneas (64-66). There is also evidence that these cytokines have impact on other cells which might direct cytotoxicity to allografts. It was revealed that several adhesion molecules which are necessary for mononuclear cell recruitment, are upregulated in the presence of IFN-γ and TNF-α in corneal cells (67).

Conflicting results have been reported when experiments with IFN-γ knockout mice or IFN-γ-depleted animals revealed that inhibition of the Th1 arm results in accelerated immune rejection of the cornea with Th2-immune bias (44, 68), however, the mechanism strictly depends on the animal model used (68, 69). In MHC-matched, minor H-mismatched grafts lack of IFN-γ prevents the development of conventional Th1 responses to minor H antigens and rejection. On the other hand, MHC-mismatched, minor H-matched grafts were rejected equally in both wild-type and IFN-γ KO mice showing the importance of the Th1-independent mechanism of rejection. Further investigations related this type of rejection to pronounced eosinophilic inflammatory infiltrate and a Th2-form of immune response (68, 70), which is in agreement with the observation in patients with atopic keratoconus who display a higher rate of corneal graft rejection when MHC-mismatched allografts are transplanted (71).

Recent studies have shed new light on the interplay between Th1 and Th2 responses in the context of keratoplasty. The elimination of $CD4^+$ Th17 cells with anti-IL-17A Ab treatment results in an enhanced rejection rate and tempo and

promotes Th2 immune responses. This indicates that IL-17A, together with IFN-γ, plays an important role in immune privilege maintenance and is necessary for corneal allograft survival (43, 44). Moreover, IL-17A is necessary for the generation of corneal allograft-induced Tregs which suppress the efferent arm of the immune response (45).

The other T-cell subtype that has been proposed to mediate corneal graft rejection is the $CD8^+$ CTL. This cell type was found in rejecting corneas as well as in aqueous humor as early as two days post-transplantation (72). The nature of rejection, described as "piecemeal necrosis", suggests involvement of $CD8^+$ T cells in contact-dependent cytolysis of corneal cells (73, 74). These findings are supported by *in vitro* data showing that $CD8^+$ CTL are able to kill allogeneic corneal cells (75). Interestingly, low risk grafts fail to induce donor-specific cytotoxic T cells. In contrast, in high risk allografts donor-specific $CD8^+$ CTL were detected and were able to mediate rejection when adoptively transferred to SCID hosts (76).

Natural killer (NK) cells, due to their cytolytic activity, are also known to mediate corneal rejection. It was shown that $CD3^-/CD161^+$ cells are not only present in the aqueous humor already at two days post-op, but also the number of cells constantly increase up to the moment of rejection. Moreover, up to day six after keratoplasty the number and percentage of cell subsets between syngeneic and allogeneic groups was similar except for the percentage of NK and NKT lymphocytes in AH (77). In other studies, NK cells were also detected in the allograft seven days after surgery and in rejecting corneas (78). The most profound evidence with regard to the contribution of NK cells in the rejection process was obtained from experiments where $CD8^+$ or $CD161^+$ cells were depleted. Depletion of the $CD161^+$ subset, but not the $CD8^+$, resulted in a decrease in cytotoxicity of the AH lymphocytes. Moreover, isolation of $CD3^-CD161^+$ cells from the AH revealed that this population has strong cytotoxic activity (77). The contribution of NK cells in corneal allograft rejection was also revealed in young rats. The depletion of NK cells resulted in a significant delay in rejection, however, lack of NK cells seems to strengthen other mechanisms which mediate allograft rejection (79).

Lastly, the role of B-cells was investigated and found that neither antibody nor complement are necessary in mediating rejection of allogeneic corneas in mice (80). This conclusion was based on findings indicating that B-cell and C3 deficient animals rejected corneal grafts with the same incidence as wild-type control subjects. However, it is important to note that a low-risk model of keratoplasty was assessed in this study. Others showed that the role of B cells is masked by robust T-cell-mediated effector mechanism (81) and might be important in specific conditions like keratoplasties performed in high-risk human eyes which have been reported to elicit donor-specific antibodies associated with graft rejection (82). On the other hand, it was described that B cells are important during the establishment of peripheral tolerance and maintaining the ocular immune privilege (83, 84).

1.4 Gene-therapeutic applications for cornea transplantation

The majority of pre-clinical gene-therapeutic studies to improve cornea transplant survival utilize recombinant viral vectors derived from Adenoviruses (Ad), Lentiviruses (LV) or Adeno-Associated Viruses (AAV) as gene transfer vehicles (85-87). Non-viral gene transfer would avoid many issues concerning unwanted immune responses against the viral vector and/or the therapeutic gene and also with regard to general safety aspects such as reversion to potentially pathogenic wild type virus. However, the efficiency of gene transfer into corneal cells is reportedly low (86). In contrast, viral vectors are generally characterized by their high transduction efficiency of different cell types and tissues, although transduction efficiency may vary, depending on the cell type. Ad-vectors predominantly transduce the corneal endothelium, whereas the epithelium and stroma are refractive to Ad-mediated gene transfer (88-91). Due to the genetic DNA backbone of the Ad-vector (first generation Ad) used in many studies, Ad-transduced cells remain capable of expressing adenoviral proteins. These antigens can be presented via MHC molecules on endothelial cells or keratocytes and stimulate T cell-mediated immunity. This may result in short-term, transient expression of the therapeutic gene which, in some circumstances, might be sufficient or even desired in certain situations when long-term expression of the therapeutic gene might not be beneficial. Unlike Ad,

AAV- and LV-vectors are generally considered as gene therapy vehicles leading to long-term gene expression in target cells due to their low immunogenic profile and their integration into the cellular genome (92). AAV vectors are thought to remain mostly episomal in post-mitotic cells, however, a significant proportion of AAV vectors do integrate (93). Although integration does not seem to lead to pathological consequences when using AAV-vectors, cellular integration of lentiviral vectors in chromosomal areas harboring tumor genes has led to insertional mutagenesis (IM) and tumor formation (94).

1.4.1 Experimental strategies for preventing immune rejection

Keratoplasty is the most frequent form of allograft transplantation with a success rate of 90 % in the first 2 years. However, the rate of survival decreases over time and is reduced to approximately 62% after 10 years (95). The predictions for high risk graft survival are even poorer. The main cause of graft failure is immune rejection despite the immune privileged status of the eye. Furthermore, commonly used immunosuppressive therapies have not resulted in improved long-term survival rates as observed in solid organ transplantation. Moreover, local or systemic immunosuppression may be required for several years and will expose the patient to the risk of side effects without the possibility of achieving general tolerance.

Gene therapy has been widely applied in preclinical studies to manipulate the corneal graft rejection process. There are several advantages to be attained from a genetic modification to prolong corneal graft survival approach. Firstly, the cornea is an easy accessible organ which can be stored for a prolonged time period. This provides necessary time for *ex vivo* manipulations prior to the graft transplantation. Additionally, the clarity of the cornea gives an opportunity to directly monitor the rejection process.

Despite some controversial aspects with regards to the use of viral vectors for gene delivery, there are already successful results from phase I clinical trials on people suffering from Leber congenital amaurosis (96-99). This indicates a great need for gene therapy and the beneficial aspects of this approach over some conventional

treatment strategies. The reasons to investigate and improve virus-based gene delivery techniques for cornea transplantation include the variety of viral vectors that can be used as well as the variety of strategies that can be implemented to enhance allograft survival. Virus-based gene therapy may provide a long-term effect, which can be regulated by inducible or tissue-specific promoters, without the need for life-long treatment. Indeed, many experimental gene therapies have already been described which have resulted in prolongation of corneal allograft survival (87). The variety of therapeutic transgenes and strategies applied for target different mechanisms of immune rejection will be described here in more details.

Immunosuppression and tolerance induction

One example of a successful approach to corneal gene therapy was achieved through delivery of T cell activation and proliferation suppressors. The intraperitoneal administration of Ad.CTLA4-Ig prevented graft rejection (100), in contrast to another study which used the co-stimulatory fusion molecule ICOS-Ig delivered systemically by adenovirus vector (101). Similarly, over-expression of indoleamine 2,3-dioxygenase (IDO), that is known to be involved in T cell suppression and tolerance induction, by *ex vivo* transduction of the cornea with EIAV-IDO vectors showed prolonged graft survival (102).

Cytokines

Cytokines or their soluble receptors have also shown the ability to inhibit rejection. Local adenovirus-mediated delivery of ovine IL-12p40 to the sheep cornea resulted in extension of graft survival in the absence of any additional immunosuppression (103). This prolongation, however, was not confirmed in a rat model either after local or systemic administration of Ad.IL-12p40 (104).

Anti-angiogenic molecules

Inhibition of angiogenesis is another interesting target for gene therapy to prevent allograft rejection. Preexisting vascularisation of recipient corneal beds is one of the factor for immune rejection after keratoplasty (105). It was shown by Murthy et al.

(106) that lentiviral-mediated over-expression of an endostatin::kringle-5 (E::K-5) fusion gene has an anti-angiogenic effect and inhibits graft failure. This therapy might be particularly useful for high risk corneal transplants.

Anti-apoptotic molecules

Apoptosis is potentially a main cause of endothelial cell death either during storage, surgery or post-operative trauma and inflammation. Several strategies were tested to protect corneal endothelium from programmed cell death. The most successful was performed by Barcia et al. (107) showing a significant increase in corneal survival rate after lentiviral-mediated delivery of the bcl-xL gene to the corneal endothelium. Anti-apoptotic strategies might also be beneficial with regard to retention of cell viability and physiological cell morphology during storage conditions used in eye banking. This is of high importance when one considers that 30% of corneal tissues are discarded because of endothelial cell loss during storage (108). It is also estimated that 25% of all failed grafts within 15 years post-op are as a result of considerable and progressive endothelial cell loss (109). In support of this hypothesis two anti-apoptotic genes, baculoviral p35 and mammalian bcl-xL, were transferred to the corneal endothelium by lentivirus vectors in different storage conditions. The results confirmed that over-expression of both genes in endothelium resulted in prolongation of cell viability and retention of endothelium morphology (110, 111).

1.4.2 Local gene transfer to the cornea

The most frequent strategy for virus-mediated gene transfer is *ex vivo* transduction of the donor cornea. This is not only due to its successful application for preventing corneal graft rejection, but also because of the need to enhance specificity and biosafety if to be considered as a future human therapy. The main goal for corneal gene therapy is long-term graft survival without the need for other treatment regimens or, if required, that they be restricted only to short periods post-op. Several studies have shown that systemic administration of virus vectors prolong graft survival (100), however, this application is not specific and is unlikely that it

will be accepted in human therapies for non-life threatening diseases. In addition, there is an increased probability of transgene silencing and unwanted immune responses to the transgene product or viral vector itself. In contrast, local expression of therapeutic genes can be better controlled and should, in theory, have less of an impact on the body system as a whole thereby decreasing the chance of immune recognition. The anatomic location and the immune-privileged nature of the cornea provide an additional advantage for gene therapy. Indeed, it was shown that transgene expression in immune-privileged sites was prolonged and persistent in comparison to other organs and tissues (112, 113). Moreover, the blood-eye barrier limits any systemic spillover of the vector if still present on donor cornea. Similarly, *ex vivo* manipulations before transplantation minimize the risk of viral vector spread to other tissues and an overall reduction in the risk of *in vivo* application of viral vectors.

1.5 Aims and hypothesis of the PhD Project

As described above, novel therapeutic strategies are required to improve allogeneic corneal graft survival. Lentiviral-mediated gene transfer to *ex vivo* cultured corneas is a promising approach for the prolongation of allograft survival and attenuation of graft rejection. Therefore, the purpose of this research project was to develop and investigate two distinct strategies in a preclinical model of rat cornea transplantation to prevent allograft rejection.

1.5.1 Anti-apoptotic strategy

As previously reported, Ad-mediated over-expression of nerve growth factor (NGF) resulted in endothelial cell protection from apoptosis and prolongation of allograft survival (114). Together with successful experiments that took advantage of other anti-apoptotic molecules (107, 110, 111), anti-apoptotic gene therapy seems to be an attractive approach to improve graft survival rate. The aim of the first part of the project was to develop alternative lentiviral vectors expressing NGF with a low immunogenic profile for their application in rat cornea transplantation and to investigate the underlying mechanisms of cytoprotection. It was hypothesised that

lentivirus-mediated over-expression of NGF is able to protect endothelial cells from apoptosis *in vitro* and prolong allograft survival *in vivo* in a fully allogeneic rat cornea transplant model.

1.5.2 Inhibition of immune cells infiltration

Since the successful application of co-stimulatory blockade therapy in cornea transplantation has been described, these immune-modulatory molecules have become attractive targets for novel strategies including gene therapies. One of the most important molecules expressed on endothelial cells that contribute to maintenance of the immune privilege of the anterior chamber is programmed death – ligand 1 (PD-L1) (115). There is strong *in vivo* evidence that PD-L1 expression on corneal parenchymal cells is an important immune-inhibitory factor (42). This discovery raises the question of whether over-expression of PD-L1 can be an enhance factor for cornea allograft survival. The goal for the second part of the project was to develop a novel strategy and investigate the role of lentivirus-mediated over-expression of PD-L1 on rat corneal allograft survival. It was hypothesised that lentivirus-mediated over-expression of PD-L1 in *ex vivo* cultured corneas leads to long term allogeneic graft survival by reduction of effector cells infiltrating into the graft and proinflammatory cytokine production during the rejection process.

Chapter 2:

Materials and Methods

2 Materials and Methods

2.1 Plasmid constructs

2.1.1 Plasmids

pWPT-GFP – was obtained from Addgene (cat. no. 12255). It can be used for constitutive transgene expression. Plasmid contains reporter gene, enhanced green fluorescent protein (EGFP), under the human elongation factor-1 alpha (EF-1 alpha) promoter.

cPPT-GFP – derived from cloning vector pHR'-CMVLacZ (GenBank: AF105229). LacZ sequence was replaced by EGFP gene and central polypurine tract (cPPT) sequence was added. Reporter gene expression is driven by the human cytomegalovirus immediate early (CMV.IE) promoter.

pLenti6/V5-DEST – was obtained from Invitrogen (cat. no. V499–10). Plasmid contains the human ubiquitin C (UbC) promoter which drives constitutive but physiological levels of expression of the target gene. It was used as a lentiviral expression vector for PD-L1 gene.

psPAX2.2 – 2nd generation packaging vector was obtained from Addgene (cat. no. 12260)

pMD2.G – the fusiogenic envelope G glycoprotein of the vesicular stomatitis virus (VSV-G) plasmid was obtained from Addgene (cat. no. 12259);

pRSV-Rev – helper plasmid with rev sequence was obtained from Addgene (cat. no. 12253);

pTZ57R/T – linearized TA cloning vector was obtained from Fermentas (cat. no. K1213);

2.1.2 Primer design

Two sets of primer pairs were designed for the cloning process of NGF fragment to pWPT and cPPT plasmid backbones: primers which allowed for the verification of the insert sequence and primers which were used to clone NGF fragment in its correct orientation. The primers for sequencing were designed according to

published sequences of pWPT or cPPT plasmid backbones. The NGF-flanking primers were designed with appropriate restriction sites necessary to subclone the NGF gene in the correct orientation into the destination plasmids. The reverse primer had the same sequence for both plasmids with BamHI restriction site at the 5'-end of the primer, however, the forward primer sequence differ between two destination plasmids. For pWPT backbone SalI restriction site was added at the 5'-end of the primer, whereas cPPT required XhoI restriction site. The primer sequences, which were used during cloning process, are presented in table 2.1.

The sequenced DNA fragments were compared to the mouse NGF sequence obtained from NCBI GenBank (Ref. Seq. NM_013609.2) using Pairwise Sequence Aligment (European Bioinformatics Institute, Hinxton, Cambridgeshire, UK). Primers and insert sequencing were assigned to EurofinsMWG Operon, Germany.

	primer	sequence (5' → 3')
CLONING	forward NGF'SalI	5'-ACGT**GTCGAC**GCAGGCAAGTCAGCCTCTTCT-3'
	forward NGF'XhoI	5'-GT**CTCGAG**GCAGGCAAGTCAGCCTCTTCT-3'
	reverse NGF'BamHI	5'-TA**GGATCC**GAACATGCTGTGCCTCAAGC-3'
	primer	**sequence (5' → 3')**
SEQUENCING	forward pWPT	5'-GTGCAGTAGTCGCCGTGAAC-3'
	reverse pWPT	5'-AAGCAGCGTACTCACATAGCG-3'
	forward cPPT	5'- ATTCTGCAAGCCTCCGGAGC-3'
	reverse cPPT	5'- GCTAAGATCTACAGCTGCCTTG-3'

Table 2.1. Primers used for verification insert identity and for cloning NGF fragment into the appropriate destination plasmids.

2.1.3 Amplifying mNGF sequence by Polymerase Chain Reaction

A PCR method was used to amplify the NGF sequence in the correct orientation and additionally flank the fragment with specific restriction sites that allowed cloning the NGF gene into destination plasmids. Two separate reactions were performed for two sets of primers (table 2.1). Similar reaction mixes were used to obtain NGF products specific for pWPT and cPPT destination plasmids and presented in Table 2.2. The PCR conditions were described in Fig. 2.1. All reagents used for PCR assay were obtained from New Engand Biolabs, UK.

Reaction Mix	Stock concentration	Volume [µl]
plasmid template	app. 1 µg/µl	0.5
forward primer	10 µM	5.0
reverse primer	10 µM	5.0
dNTP Mix	2 mM	5.0
reaction Taq buffer (KCl, 15 mM $MgCl_2$)	10 ×	5.0
Taq pomymerase	5 U/µl	0.5
nuclease-free dH_2O		28.5
TOTAL		**50.0**

Table 2.2. Reaction mix used for amplification NGF fragment by PCR.

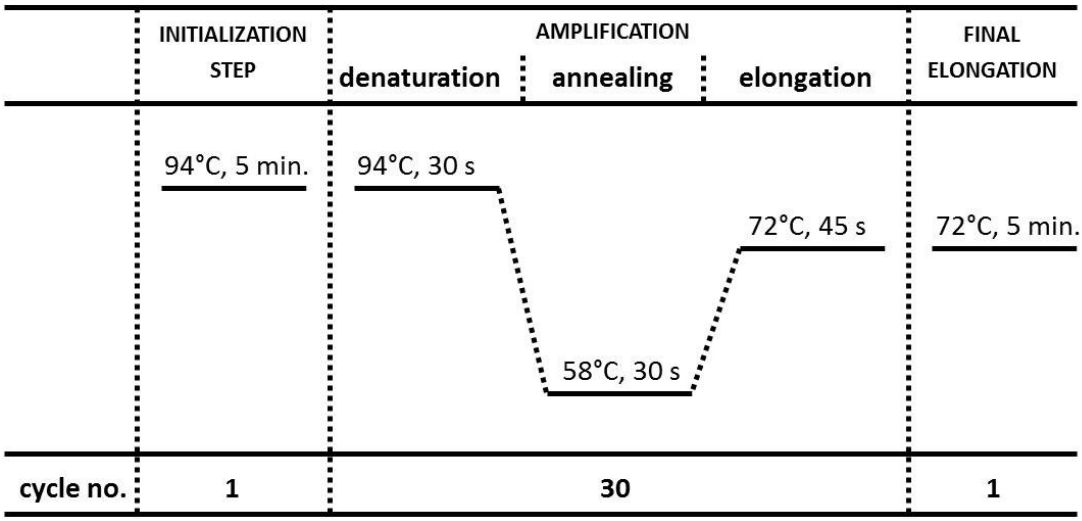

Fig. 2.1. Conditions of PCR used for amplification of NGF fragment.

2.1.4 DNA Gel Electrophoresis

The PCR products or other samples were separated through 1% w/v agarose gel (agarose in 1 × TAE buffer) placed in 1 × TAE buffer in the presence of 1 × SYBR DNA gel stain. For DNA fragment electrophoresis, a 100 V electrical field was applied for 30 min. The 100 bp or 1 kb DNA size markers (Fermentas) were used to determine

the product sizes. The results were analyzed by visualizing the gel with UV light using ultraviolet transilluminator.

2.1.5 Extraction of DNA fragments from agarose gel

The DNA fragments were extracted from the agarose gel using QIAquick Gel Extraction Kit according to the manufacturer's protocol (Qiagen, UK). Briefly, the appropriate DNA bands after PCR or pDNA restriction enzyme digestion were cut out from the agarose gel by a scalpel on the UV transilluminator and transferred to 1.5 ml tubes. Weight of the gel slice was determined and 3 volumes of buffer QG was added to 1 volume of gel slice. Next, the tube was incubated at 50°C for 10 min and the sample was applied to the QIAquick column and centrifuged at 13,000 rpm for 1 min. Then, the flow-through was discarded and the column was washed with 0.75 ml of buffer PE at 13,000 rpm for 1 min. After flow-through removal the column was centrifuged again and placed into a clean 1.5 ml tube. Lastly, DNA was eluted with 30 µl of nuclease-free water. The concentration of extracted DNA was determined by NanoDrop spectrophotometer.

2.1.6 Plasmid DNA isolation

The plasmid DNA required for cloning process was isolated by alkaline lysis of E. coli bacteria using Qiagen® buffers. Briefly, 3 ml of bacteria overnight culture was spun down at 3500 rpm for 5 min. The pellet was resuspended in 300 µl of buffer P1 and left for 2 min at room temperature (RT). Next, 300 µl of buffer P2 was added and the sample was incubated for 10 min at RT. At that point, 300 µl of buffer N3 was added and the sample was incubated on ice for 5 min. After this the tube was centrifuged at 10,000 rpm for 5 min and supernatant was transferred to the clean 1.5 ml tube. pDNA was precipitated with 640 µl of isopropanol, left for 5 min at RT and pDNA was pelleted at 10,000 rpm for 20 min. Supernatant was aspirated and the pellet was washed with 1 ml of 70% ethanol and centrifuged for 5 min. The pellet was air-dried for 15 min and resuspended in 30 µl of nuclease-free water. The concentration of extracted pDNA was determined by NanoDrop spectrophotometer.

2.1.7 Bacteria transformation

The competent bacteria Escherichia coli strain Top50 was thawed on ice (50 µl per vial). Soon after, 10 µl of ligation reaction was added directly to the competent cells and mixed by gently tapping. Cells were incubated on ice for 30 min. Next, the tube was incubated in water bath at 42°C for 45 s and immediately placed on ice for another 5 min. 250 µl of pre-warmed S.O.C medium was added to the vial and then, cells were shaken horizontally at 37°C for 1 h at 225 rpm in a rotory shaker-incubator.

2.1.8 Selection of transformed bacteria

(i) Blue/white screening

40 µl of IPTG and 40 µl of Xgal were spread on top of the pre-made agar plates with a hockey stick spreader. Then, the plates were dried for 1 h. Next, 100 µl of transformed bacteria were spread on the plates and kept in an incubator overnight at 37°C. Presence of white bacteria colonies on the plate suggested successful cloning procedure. Single colonies were picked and grown in 5 ml of LB medium at 37°C for 16 h at 225 rpm in a rotory shaker-incubator. Thereafter, pDNA was isolated by alkaline lysis method as described before.

IPTG (isopropyl-beta-D-thiogalactopyranoside) (#R0391, #R0392) stock solution (0.1M): 1.2g IPTG, add water to 50ml final volume. Filter-sterilize and store at 4°C.
X-Gal (5-bromo-4-chloro-3-indolyl-beta-D-galactopyranoside) (#R0401, #R0402) stock solution: 20mg/ml in N,N-dimethylformamide.

(ii) Antibiotic selection

100 µl of competent bacteria were spread on agar plate containing ampicillin (100 µg/ml). The plate was kept in an incubator at 37°C overnight. Presence of bacteria colonies on the plate suggested successful uptake of plasmid DNA. Single colonies were picked and grown in 5 ml of LB medium at 37°C for 16 h at 225 rpm in a rotory shaker-incubator. Thereafter, pDNA was isolated by alkaline lysis method.

2.1.9 Ligation with intermediate plasmid

The InsTAclone™ PCR Cloning Kit (Fermentas) was used for direct cloning of the NGF fragments (NGF/BamSal and NGF/BamXho) obtained by PCR and extracted from the agarose gel. The PCR products had a single 3'-A overhang on both ends which favored direct cloning into a linearized cloning vector pTZ57R/T with single 3'-ddT overhangs. The ligation reaction was performed according to the manufacturer's instructions. Briefly, ligation mix was prepared in 0.5 ml tube (see Table 2.3) and the sample was incubated for 1 h at RT. Competent bacteria were transformed with 10 µl of ligation mix. Recombinant clones were selected based on blue/white screening. pDNA was isolated from positive colonies and analyzed by restriction enzymes. Two plasmids were obtained after ligation reactions: pTZ/NGF'BamSal and pTZ/NGF'BamXho.

Ligation Mix	
Components	**Volume**
PCR product	180 ng
Vector pTZ57R/T	165 ng
5 × ligation buffer	2.0 µl
nuclease-free dH_2O	to 9.0 µl
T4 DNA ligase	1.0 µl
TOTAL	**10.0 µl**

Table. 2.3. Ligation mix used for a direct cloning of PCR product into an intermediate plasmid.

2.1.10 Ligation with destination plasmid

First, intermediate plasmids with the NGF insert as well as destination vectors (pWPT-GFP and cPPT-GFP) were digested with endonucleases specific for the restriction sites which were added to NGF sequence during PCR amplification. The reaction mixes (Table 2.4) were incubated for 2 h at 37°C and electrophoresis was performed. NGF fragments and linearized destination vector backbones were extracted from the agarose gel and the concentration was determined. Next, ligation mixes were prepared as described in Table 2.5. The samples were incubated overnight at 4°C. Competent bacteria were transformed with 10 µl of ligation mix. Antibiotic selection was used to identify recombinant clones. pDNA was isolated

from positive colonies and analyzed by restriction enzymes. Two plasmids were received after ligation reactions: pWPT-NGF and cPPT-NGF. Confirmation of correct sequence and orientation of NGF inserts was achieved by sequencing both plasmids using primers as indicated in Table 2.1.

A)

Intermediate plasmid hydrolysis	
Components	**Volume**
pTZ/NGF'BamSal	4 µg
H_2O	up to 20 µl
b. BamHI	2.0 µl
BamHI	0.5 µl
SalI	1.0 µl

Destination plasmid hydrolysis	
Components	**Volume**
pWPT-GFP	4 µg
H_2O	up to 20 µl
b. BamHI	2.0 µl
BamHI	0.5 µl
SalI	1.0 µl

B)

Intermediate plasmid hydrolysis	
Components	**Volume**
pTZ/NGF'BamXho	4 µg
H_2O	up to 20 µl
b. BamHI	2.0 µl
BamHI	0.5 µl
XhoI	0.5 µl

Destination plasmid hydrolysis	
Components	**Volume**
cPPT-GFP	4 µg
H_2O	up to 20 µl
b. BamHI	2.0 µl
BamHI	0.5 µl
XhoI	0.5 µl

Table 2.4. Reaction mixes for hydrolysis with indicated restriction enzymes of both intermediate and destination plasmid to obtain NGF fragments and linear destination vector backbones. **(A)** pWPT vector and **(B)** cPPT vector.

pWPT ligation mix	
Components	**Volume**
NGF'BamSal	100 ng
pWPT'BamSal	100 ng
ligation buffer	1x
T4 DNA ligase	1.0 µl
H_2O	up to 25 µl

cPPT ligation mix	
Components	**Volume**
NGF'BamXho	100 ng
cPPT'BamXho	100 ng
ligation buffer	1x
T4 DNA ligase	1.0 µl
H_2O	1.0 µl

Table 2.5. Ligation mixes used for cloning NGF fragments obtained from intermediate plasmid after endonucleases digestion into the appropriate destination plasmids.

2.1.11 Restriction enzyme analysis

Restriction enzyme analysis was performed to confirm the correct size of NGF fragments by testing both restriction enzymes used for cloning and also to reveal correct insert orientation using ApaI enzyme. Reaction mixes for both plasmids are presented in Table 2.4. Samples were incubated for 2 h at 37°C and electrophoresis was performed. The results were analyzed by visualizing the gel with UV light using Kodak Image Station 4000MM Pro.

A)

Restriction analysis for pWPT-NGF plasmid					
Components	**no digestion**	**BamHI**	**SalI**	**BamHI+SalI**	**ApaI**
pWPT-NGF	250 ng	250 ng	250 ng	250 ng	250 ng
H_2O	up to 10 µl	up to 10 µl	up to 10 µl	up to 10 µl	up to 10 µl
b. BamHI	1.0 µl	1.0 µl	1.0 µl	1.0 µl	×
buffer 4	×	×	×	×	1.0 µl
BamHI	×	0.25 µl	×	0.25 µl	×
SalI	×	×	0.25 µl	0.25 µl	×
ApaI	×	×	×	×	0.25 µl
Sample	**1**	**2**	**3**	**4**	**5**

B)

Restriction analysis for cPPT-NGF plasmid					
Components	**no digestion**	**BamHI**	**XhoI**	**BamHI+SalI**	**ApaI**
pWPT-NGF	250 ng	250 ng	250 ng	250 ng	250 ng
H_2O	up to 10 µl	up to 10 µl	up to 10 µl	up to 10 µl	up to 10 µl
b. BamHI	1.0 µl	1.0 µl	1.0 µl	1.0 µl	×
buffer 4	×	×	×	×	1.0 µl
BamHI	×	0.25 µl	×	0.25 µl	×
XhoI	×	×	0.25 µl	0.25 µl	×
ApaI	×	×	×	×	0.25 µl
Sample	**1**	**2**	**3**	**4**	**5**

Table 2.6. Restriction enzyme analysis of final cloning products. **(A)** pWPT-NGF vector and **(B)** cPPT-NGF vector.

2.1.12 Generation of PD-L1 expressing lentiviral plasmid

Rat PD-L1 mRNA was isolated from LEWIS rat heart and converted to cDNA using RT-PCR. Amplified PD-L1 cDNA was cloned into pLenti6/V5-DEST (Invitrogen, Dun Laoghaire, Ireland) and sequence identity was confirmed by sequencing (Source Bioscience, Dublin, Ireland) using reference sequence from the NCBI database (NM_001191954). The cloning process of PD-L1 sequence into a destination plasmid was performed by Dr. Mikhail Nosov.

2.2 Cell culture, transduction and treatment

2.2.1 Cell lines

(i) Human Embrionic Kidney 293T cells (293T) were grown in high glucose Dulbecco's modified Eagle's medium (DMEM) with L-glutamine supplemented with 10% fetal calf serum (FCS) and 100 U/ml penicillin, 100µg/ml streptomycin and incubated at 37°C in 5% CO_2. The cells were maintained in culture using standard method. Briefly, when cells reached 80-90% of confluence they were washed with PBS, detached from the flask by 1 × trypsin/EDTA, pelleted at 400 x g for 5 min, resuspended in fresh medium and split into new flasks in a 1:10 ratio. 293T cells were cultured up to passage 20 and mainly used for lentiviral vector generation.

(ii) HeLa cells were cultured in the same conditions as 293T cells. The cells were passaged every 3rd day when their confluence reached 80 – 90% and split in 1:10 ratio. HeLa cells were used as a reference cell line for lentivirus titration and also for optimizing transduction efficiency of produced lentivectors.

(iii) Human Corneal Endothelial Cells (HCEC) were isolated from a donor cornea and immortalized with SV40 vector. This cell line is a kind gift from Dr. J. Bednarz from Department of Ophthalmology, University Eye Clinic Eppendorf, Hamburg, Germany. HCEC were grown similarly to other two cell lines. HCEC cells were used as an *in vitro* model of corneal endothelium.

(iv) Rat adrenal phaeochromocytoma PC12 cells were grown in DMEM with L-glutamine supplemented with 10% horse serum (HS), 5% fetal calf serum (FCS) and penicillin/streptomycin (P/S) antibiotics and incubated at 37°C in 5% CO_2. PC12 cells were trypsinized and split in 1:10 ratio when their confluence reached 80-90%. The cells were used as the NGF-responsive indicator cells which are able to differentiate into neuronal-like cells and induce neurite outgrowth in the presence of NGF and also as a reference cell line for experiments on anti-apoptotic effect of NGF. The experiments were performed on cells below passage 20.

(v) All cell lines were stored in liquid nitrogen and thawed when needed for experiments. The cells were cryopreserved in 10% DMSO and 90% FCS solution and aliquoted in cryovials at concentration 1×10^6 cells/ vial.

cDMEM – DMEM with L-glutamine supplemented with 10% fetal calf serum (FCS) and 100 U/ml penicillin, 100µg/ml streptomycin. FCS was heat inactivated at 56°C for 30 min.

hsDMEM – DMEM with L-glutamine supplemented with 10% horse serum (HS), 5% fetal calf serum (FCS) and penicillin/streptomycin (P/S) antibiotics. Both FCS and HS were heat inactivated at 56°C for 30 min.

2.2.2 Lentiviral vector production and titration

Lentiviral vectors used in this studies are based on Tat-dependent, second generation self-inactivating (SIN) human immunodeficiency virus-1 (HIV). The lentiviral packaging and production plasmids were obtained from Prof. Didier Trono (Lausanne, Switzerland). Recombinant lentiviruses were generated by co-transfection of 293T cells with expression plasmids containing either EGFP, NGF or PD-L1 sequences as well as with gag-pol (psPAX2.2 - Addgene plasmid 12260), VSV-G envelope plasmids (pMD2.G - Addgene plasmid 12259) and supplemented with helper plasmid with rev sequence (pRSV-Rev – Addgene plasmid 12253) using a standard protocol. Briefly, the 293T cells (4.6 x 10^6 cells/15cm dish) were co-

transfected with plasmids using JetPEI transfection reagent (Polyplus Transfection Inc, NY, USA) according to manufacturer's protocol. The next day culture medium was replaced. Supernatants containing viral particles were harvested 48 and 72 hours post-transfection, filtered through 0,45 μm pore size filters and concentrated by ultracentrifugation at 27000 x g for 2.30 h at 4°C. LV were resuspended in 1% albumin in PBS, aliquoted and stored at -80°C. As a final result five different LV vectors were generated: $LV_{ef}GFP$, $LV_{cmv}GFP$, $LV_{ef}NGF$, $LV_{cmv}NGF$ and LV.PD-L1.

For titration of LV.EGFP HeLa cells at the density of $5x10^4$ cells/well were seeded on 24-well plate in 1ml of cDMEM and incubated overnight. Dilution of LV.EGFP vectors were prepared in duplicates in 0.5ml of cDMEM containing 5, 1, 0.5, 0.1 and 0.05 μl of lentivirus and medium was replaced in all wells. Untransduced cells were used as a negative control. Cells from two wells were trypsinized and counted to estimate the accurate cells number on time of transduction. After 24h transduction media were replaced by fresh culture DMEM and left for another day. Flow cytometric method was used to determine LV.EGFP virus titer. A following equation was used to determine viral titer:

$$\text{Titer} = [(F \times C_n) / V] \times D_F$$

F – the frequency of GFP-positive cells determined by flow cytometry from the range between 1 - 20 % of GFP-positive cells

C_n – the total number of target cells infected

V – the volume of the inoculum

D_F – the virus dilution factor

Moreover, two step quantitative real-time PCR based on viral RNA from LV.EGFP, LV.NGF and LV.PD-L1 viruses was performed to determine LV.NGF and LV.PD-L1 titer by comparing C_t values of common shared woodchuck posttranscriptional regulatory element (WPRE) sequence between LV.EGFP with known titer and yet untitered LV.NGF or LV.PD-L1 vectors. The primers used for WPRE were: forward 5'-GGACCTGAAAGCGAAAGGG-3'; reversed 5'-CATCTCTCTCCTTCTAGCCTCCG-3'; probe 5'-Fam-CTCGACGCAGGACTCGGCTTGC-Tamra-3'. All qRT-PCR was performed

according to the standard program on the ABI onestep machine (Applied Biosystem, Foster City, CA, USA) and is described in more details below.

2.2.3 Verification of functional NGF expression

To examine NGF expression levels after transfection HeLa cells were seeded in 24-well plates at a density 6.0×10^4 cells/well 24 h prior transfection. Cells were transfected with 1μg of NGF-bearing plasmids using JetPEI reagent according to the manufacturer's protocol. Supernatants were harvested 72 h post-transfection and analyzed by specific ELISA. Untransfected supernatants were used as a control.

To examine NGF expression level after LV.NGF transduction HeLa cells were seeded on 24-well plates at a density 6.0×10^4 cells/well 24 h prior to transduction. Cells were transduced with 2.0×10^5 TU of LV.NGF and incubated overnight. 24 h after transduction medium was replaced. Supernatants were collected 24, 48 and 72 h after medium replacement and analyzed by specific ELISA. Supernatants from untransduced cells were used as a control.

2.2.4 Microscopic examination of neurite outgrowth of PC12 cells

To examine the biological activity of lentivirally delivered NGF, PC12 cells were seeded on poly-L-lysine coated (10 μg/ml) 24-well plates at a density of 8.0×10^4 cells/well 24 h prior neurite outgrowth induction in 1 ml of hsDMEM. Next, medium was replaced with supernatants from transduced HCEC cells with $LV_{ef}GFP$, $LV_{ef}NGF$ and $LV_{cmv}NGF$ vectors. Cells cultured in complete PC12 medium served as a negative control and cells cultured in complete PC12 medium treated with 100 ng/ml rNGF were used as a positive control of neurite outgrowth. Cells morphology was assessed using Olympus IX71 Inverted Fluorescent Microscope 48 h after induction of neurite outgrowth.

For apoptosis induction experiments, PC12 cells were seeded on PLL-coated 24-well plates whereas HCEC cells were seeded on uncoated 24-well plates at a required density. Prior to the experiments, NGF concentration in supernatants from transduced HCECs was determined by ELISA. The final concentration of NGF in the supernatants from HCECs transduced with both LV.NGF vectors used in the experiments was 1ng/ml.

HCEC and PC12 cells were cultured in supernatants from transduced (with LV_{ef}GFP, LV_{ef}NGF and LV_{cmv}NGF), untransduced HCECs or in complete medium for 48 h before induction of apoptosis. Cells cultured in complete medium were pre-treated with rNGF (100 ng/ml) 24 h before apoptosis induction or with pan-caspase inhibitor (Z-VAD-fmk, 50µM) for 30min before thapsigargin treatment. Then, medium was replaced and new induction medium containing 1.5 µM TG was added to the cells. PC12 cells were harvested 24 h and HCECs 48 h after apoptosis induction. Untreated cells served as a control. Before harvesting for Western blotting or apoptotic assays, cell morphology was assessed using Olympus IX71 Inverted Fluorescent Microscope.

2.2.5 Apoptosis detection assay

The Propidium Iodide (PI) flow cytometric assay was used for evaluation of apoptotic cell levels as previously described (116). Briefly, PC12 cells were seeded at a density of 8.0×10^4 cells/well on 24-well plates in triplicates while HCEC at 5.0×10^4 cells/well and treated as described above. After treatment, cells were harvested 24 h (PC12 cells) or 48 h (HCEC cells) after apoptosis induction, washed twice in PBS and resuspended in cold fluorochrome solution (0.1 % sodium citrate, 0.1 % Triton X-100, 50 µg/ml PI). After incubation at 4° C for 16 h, cells were analyzed by flow cytometry for DNA content. The cells with hypodiploid DNA content were defined as apoptotic cells. Specific apoptosis was calculated by subtracting values of basal apoptosis of untreated cells from values of thapsigargin-induced cells.

2.2.6 Protein preparation and Western blotting

PC12 cells were seeded at 1.8×10^5 and HCEC at 1.5×10^5 cells/well on 6-well plates in triplicates. After treatment, cells were harvested by scraping them off the wells, pulled together and centrifuged. The cell pellet was lysed in 100 µl of lysis buffer as previously described (117). Protein concentration was measured using Bradford method. 50 µg of protein were denatured with Laemmli's buffer and boiled for 5 min. Proteins were separated by SDS-PAGE using 15% acrylamide gel and transferred onto nitrocellulose membrane. The membrane was blocked for 1 h in blocking solution (PBS, 0.05% Tween 20, 5% non-fat dried milk) and then incubated for

1 h at RT with antibodies to actin (1:1,000; Sigma) or overnight at 4°C with antibodies to caspase-3 (1:1,000; Cell Signaling Technologies). The appropriate goat IgG secondary antibody (1:10,000 dilution for actin, 1:5,000 for caspase-3) was added for 2 h. Protein were visualized using SuperSignal (Pierce Biotechnology) on X-ray film (Agfa).

2.2.7 Quantification of NGF concentration

NGF protein in cell cultured supernatants was detected by ELISA specific for rat NGF, according to the manufacturer's instructions (R&D Systems Europe, Abingdon, UK). Briefly, a 96-well plate was coated with 100 µl of capture antibody diluted in 1 × PBS to working concentration and incubated overnight at RT. Next, the plate was washed three times with 200 µl of Washing buffer and blotted against clean paper towel after each wash. To block unspecific binding the plate was incubated for at least 1 h at RT with 100 µl of Reagent Diluent. The plate was washed and 100 µl of sample or standards diluted in Reagent Diluent were added to each well and incubated for 2 h at RT. After washing, the plate was coated with 100 µl of detection antibodies which were diluted in Reagent Diluent and incubated for additional 2 h at RT. After this time, the plate was washed and 100 µl of the working dilution of streptavidin-HRP was added to each well and incubated for 20 min. The plate was washed again and 100 µl of Substrate solution was added for 20 min. Finally, 50 µl of Stop solution was added to stop the reaction. Optical density was determined on a microplate reader set to 450 nm. Sample concentration was calculated based on a standard curve.

PBS 10x – 800g NaCl, 116g Na_2HPO_4, 20g KH_2PO_4 and 20g KCl dissolved in 10L dH_20 and brought up to pH 7.2

Reagent Diluent – w/v 1% BSA in 1 × PBS

Substrate Solution – 1:1 mixture of Color Reagent A (H2O2) and Color Reagent B (Tetramethylbenzidine) (R&D Systems Catalog # DY999).

Washing buffer – v/v 0.05% Tween (Sigma) in $1 \times$ PBS

Stop solution – 1M H_2SO_4 (Sigma)

2.3 Rat corneal transplantation

2.3.1 Rat strains

A well-established, fully allogeneic, major histocompatibility class (MHC) I/II disparate transplant model was applied for these studies. Lewis (LEW) rats served as recipients of Dark Agouti (DA) grafts leading almost 100% rejection in untreated animals (114). All animals were males at the age of 8-14 weeks-old and obtained from Harlan Laboratories UK. All procedures performed were conducted under animal license granted from the Department of Health, Ireland and were approved by the Animals Ethics Committee of the National University of Ireland, Galway. The animals were housed under specific pathogen free conditions with food and water ad lib.

2.3.2 Surgical procedure

(i) The keratoplasty was performed by a fully trained and licensed ophthalmic surgeon (Mr. Maurice Morcos). Briefly, donor animals were euthanized by CO_2 inhalation. Donor corneas were excised using a 3 mm trephine and angled scissors. The excised donor corneas were incubated in 6-well plates for 4 hours at 37°C and 5% CO_2 with 20 µl DMEM containing lentivirus vectors in a concentration ranged between 3,4 x 10^7 and 1,0 x 10^9 TU/ml. Thereafter, corneas were washed 3 times and left on ice in 20 µl of PBS for subsequent transplantation. Next, recipient animals were pre-anaesthetized before keratoplasty with Isoflurane (5% anaesthetic in 2 l / min medical oxygen) until rats were fully immobilised. In the meantime, pupile dilating drops and Tetracaine drops were applied. Fully anaesthetized animals were transferred onto an operating table and deep anaesthesia was maintained by administration between 1.5 – 2.5 % of Isoflurane with the flow rate of 2 l / min oxygen. Next, the graft bed was prepared using 2.5 mm trephine to mark central cornea and angled scissors to excise corneal tissue. Finally, the transduced donor cornea was placed on the recipient eye and sutured with 8 – 9 stitches. After the surgery atropine and chloramphenicol drops were administered onto the eye surface and the animals were carefully placed into clean

cages lined with paper tissue towels and covered with operating drapes. The animals remained in the recovery cage until fully awake and afterwards were transferred into freshly lined cages and kept for indicated time. Post-op graft transparency and neovascularization was monitored under an operating microscope every 2 – 3 days. Animals considered to display any surgical complications were excluded from the study and euthanized.

(ii) Graft transparency as an indicator of rejection was evaluated every second day and graded as follow: 0 – completely transparent cornea; 0,5 – slight corneal opacity, iris structure easily visible; 1,0 – low opacity with visible iris details; 1,5 – modest corneal opacity, iris vessels still visible; 2,0 – moderate opacity, only some iris details visible; 2,5 – high corneal opacity, only pupil margin visible; 3,0 – complete corneal opacity, anterior chamber not visible. Neovascularization was evaluated on the basis of the number of quaternary segments of donor corneas in which vessels were present.

The opacity above 2.5 in combination with edema and correlating changes of transplant geometry (degree of convex contour, shrinking and surface roughness of graft) was considered as graft rejection.

2.3.3 Ex vivo gene transfer into cultured corneas

The donor corneas were excised as described before and incubated in 6-well plates for 4 hours at 37°C and 5% CO_2 with 20 µl DMEM containing either LV.GFP, LV.NGF or LV.PDL1 in a concentration ranged between 3,4 x 10^7 and 1,0 x 10^9 TU/ml. Thereafter, corneas were washed 3 times and left on ice in 20 µl of PBS for subsequent transplantation.

2.3.4 Isolation of lymphocytes from corneas, LNs and PBMCs

Single cell suspension from transplanted corneas was prepared by digestion of corneal buttons with 5% w/v Collagenase D in RPMI containing 25 mM HEPES (Lonza) plus 1% fetal calf serum (Sigma) at 37°C for 90 min at 900 shakes per minute. Corneal tissue was carefully poured into a 100 µM cell strainer and

disrupted by grinding with a syringe plunger. Cell suspensions were transferred into 1,5 ml Eppendorf tubes, spun at 400 x g for 5 min and washed again with PBS.

Ipsi- and contra-lateral lymph nodes were disintegrated with the syringe plunger and passed through a 100 µM cell strainer. Cell suspensions were transferred into 15 ml tubes, spun at 400 x g for 5 min, washed again with PBS.

Lymphocytes from peripheral blood mononuclear cells (PBMCs) were isolated by mixing 5 ml of whole rat blood with 625 µl of OptiPrep™ (Axis-Shield) and adding 500 µl of PBS on top. Blood samples were centrifuged at 1300 x g for 30 min at 20°C. PBMCs were collected from the meniscus downwards, diluted with two volumes of PBS and spun at 400 x g for 5 min.

Cell suspensions from individual corneas, lymph nodes and PBMCs were used for subsequent multicolor flow cytometry analysis.

2.3.5 Flow cytometry

The following monoclonal antibodies and their appropriate isotype controls were used to characterize lymphocyte subpopulations in transplanted corneas, cervical lymph nodes and PBMCs (Table 2.7). All antibodies were obtained from Biolegend, Cambridge, UK.

For staining, single cell suspensions were aliquoted into V-shaped 96-well plates and centrifuged for 3 min at 400 x g. Next, the supernatant was removed from the plate and cells were washed twice with FACS buffer following centrifugation. Then, a mix of mAbs was prepared in FACS buffer and the cells were resuspended in 50 µl/well of antibodies mix. The plate was incubated for 30 min on ice. Finally, unbound reagents were removed by washing twice with FACS buffer and the cells were resuspended in 200µl of FACS buffer and transferred into 5ml FACS tubes for further analysis using a FACS Canto (BD Biosciences). Data were compensated and analysed using FlowJo software (Tree Star, Inc.).

FACS buffer – PBS containing 2 % heat-inactivated FCS and 0.1 % NaN_3.

antibody	label	clone	isotype	cat. no.
CD3	FITC	1F4	mouse IgM, κ	201403
CD4	APC	W3/25	mouse IgG, κ	201509
CD25	FITC	OX-39	mouse IgG1, κ	202103
CD152 (CTLA4)	PE	WKH203	mouse IgG1, κ	203008
CD134	PE	OX40	mouse IgG2b, κ	204508
CD8	PE	OX-8	mouse IgG1, κ	201706
CD161	Alexa647	10/78	mouse IgG1, κ	203110
CD45RA	PE	OX-33	mouse IgG1, κ	202307
MHCII	FITC	OX-6	mouse IgG1, κ	205305
CD11b/c	APC	OX-42	mouse IgG2b, κ	201809
CD86	PE	24F	mouse IgG1, κ	200308

isotype control	label	clone	cat. no.
mouse IgG1, κ	Alexa647	MOPC-21	400130
mouse IgG1, κ	APC	MOPC-21	400122
mouse IgG1, κ	PE	MOPC-21	400111
mouse IgG2a, κ	APC	MOPC-173	400222
mouse IgG2a, κ	PE	MG2b-57	401208
mouse IgM, κ	FITC	MM-30	401607

Table 2.7. Monoclonal antibodies and their appropriate isotype controls used for characterization lymphocyte subpopulations in transplanted corneas, ipsi- and contra-lateral lymph nodes and PBMCs.

2.3.6 Histology and histochemistry

Fixation and Embedding

The eyes were enucleated at day 14 after transplantation for all groups and at the end of the observation period for long-term survivors. The eyes were dissected from the animals as soon after death as possible and fixed in 4% paraformaldehyde (PFA) in PBS for 24 h at 4 °C. Next, the eye was transferred into 70% ethanol. The fixed eyes stayed in the ethanol until further processing.

Paraffin-wax embedding was performed using automatic tissue-processor (Leica Microsystems). The fixed eyes were transferred into the cassettes and routine overnight program was applied. To complete the embedding process the wax-impregnated eyes were positioned with cornea orientated to the left and

embedded in the wax blocks. Before taking sections wax blocks were placed corneal side down on the Cold Plate (Leica Microsystems).

Haematoxylin Eosin Staining

Briefly, the eyes embedded in paraffin were cut in 5 µm thick sections, dried overnight at 56°C and then twice deparaffinized in xylene for 10 min, followed by hydration through graded alcohols. Slides were incubated for 40 s in Harris haematoxylin, washed in tap water for 2 min, then stained in eosine for 7 min, washed again in water for 2 min and dehydrated through graded alcohols. Next, sections were cleared twice for 10 min in xylene and mounted in DPX (Sigma-Aldrich).

Histological instruments used for preparing eye sections:

Heated Paraffin Embedding Module – The Leica EG1150 H, Leica Microsystems, Asbourne, Ireland

Cold Plate for Modular Tissue Embedding System – Leica EG1150 C, Leica Microsystems, Asbourne, Ireland

Tissue processor - The Leica ASP300, Leica Microsystems, Asbourne, Ireland

Manual Rotary Microtome – The Leica RM2235, Leica Microsystems, Asbourne, Ireland

2.3.7 RNA isolation and reverse transcription of mRNA

Total RNA from rat cornea samples was isolated using TRIZOL reagent (Invitrogen) according to the manufacturer's protocol. Briefy, cornea buttons were cut in small fragments and transferred to 1.5 ml tubes. Next, 0.5 ml of TRIZOL reagent was added to the tissue. The samples were passed through pipette several times to lyse small corneal fragments. At this stage the lysates were frozen at -80°C. To complete RNA isolation the samples were thawed and incubated for 5 min at RT. Then, 0.1 ml of chloroform was added to the tubes following vigorously shaking for 15 s by hand and further incubation for 3 min. All samples were centrifuged at 12000 x g for

15 min at 4°C. Aqueous phase was transferred to a fresh tube and 0.25 ml of isopropyl alcohol was used to precipitate the RNA. The samples were incubated for 10 min at RT and centrifuged at 12000 x g for 10 min at 4°C. The supernatants were discarded and 0.5 ml of 75% ethanol was added. The sample was mixed by vortexing and centrifuged at 7500 x g for 5 min at 4°C. The RNA pellet was air-dried for 10 min and resuspended in 11 µl of nuclease-free water.

cDNA was synthesized using RevertAid^{TM} H Minus Reverse Transcriptase (Fermentas, York, UK) with random primers straight after the RNA isolation. The reaction mix was prepared in a fresh nuclease-free tube by adding 4 µl of 5 x Reaction Buffer, 1 µl of RiboLock^{TM} RNase Inhibitor (40 u), 2 µl of 10 mM dNTP mix and 1 µl of RevertAid^{TM} H Minus Reverse Transcriptase (200 u). The mix was kept on ice. The RNA resuspended in 11 µl of nuclease-free water was mixed with 1 µl of Random hexamer primers and incubated for 5 min at 65°C. Next, it was centrifuged briefly and transferred to the reaction mix tube. The reaction was performed according to the program described in Table 2.8 using Verti® 96-well Thermal Cycler (Applied Biosystems). cDNA was diluted 8 times and kept in -20°C.

Step	Time [min]	Temp. [°C]
Initialization	10	25
Transcription	60	42
Termination	5	70
	for ever	4

Table 2.8. Conditions used for reverse transcription reaction.

2.3.8 Quantitive Real-Time PCR (qRT-PCR)

Two step qRT-PCR based on corneal RNA from LV.EGFP and LV.PDL1 transduced corneas on day 7 after transplantation was performed to confirm EGFP and PD-L1 mRNA expression. cDNA from transduced corneas was mixed with 2 x TaqMan master mix and primer mix containing forward primer, reverse primer and a probe.

The change in gene expression was normalized to β-actin expression from the corresponding sample (Ct_{Gene}–$Ct_{\beta\text{-actin}}$=ΔCt). Relative expression was determined

with ΔΔCt method described by Livak and Schmittgen (118). Fold induction was calculated as $2^{(-\Delta\Delta Ct)}$. All quantitative real time PCR was performed according to the standard program on the ABI StepOnePlus™ Real-Time PCR instrument.

gene	primer	sequence (5' → 3')
EGFP	forward	GCCACAAGTTCAGCGTGTCC
	reverse	GCTTCATGTGGTCGGGGTAC
	probe	FAM-CGGCAAGCTGACCCTGAA-TAMRA
PD-L1	forward	TGGAGTATGGCAGCAATGTC
	reverse	CCTCCACAAACTGAATAACT
	probe	FAM-ATGCAGATTCCCAGTAGAACAGA-TAMRA

Table 2.9. Primers used for detecting genes transferred into the corneas by qRT-PCR.

2.3.9 Statistics

Statistical analysis was performed by GraphPad Prism software (La Jolla, USA) using non-parametric Mann–Whitney or parametric Student T test. Differences were considered significant if $p \leq 0.05$.

2.4 General consumables

Material	Supplier code	Manufacturer, supplier
15ml screw cap centrifugation tube	62.554.502 PP	Sarstedt Ltd, Ireland
50ml screw cap centrifugation tube	62.547.254 PP	Sarstedt Ltd, Ireland
T-75 TC flasks	83.1813.002	Sarstedt Ltd, Ireland
T-175 TC flasks	83.1812.002	Sarstedt Ltd, Ireland
5 ml, 10 ml, 25ml sterile, single-use serological pipettes		Sarstedt Ltd, Ireland
10 µl, 20 µl, 200 µl, 1000 µl aerosol-resistant pipetting tips		StarLab, Germany
50ml syringes (Luer-lock)	613-3925	BD Falcon, UK
0.45µm syringe filters	83.1826	Sarstedt Ltd, Ireland
0.2µm syringe filters	83.1826.001	Sarstedt Ltd, Ireland
96 MicroWell Plates Nunclon flat bottom wells	734-2073	Nunc, Roskilde, Denmark
24-well plates		
12-well plates	150628	Nunc, Roskilde, Denmark
6-well plates	83.1839	Sarstedt Ltd, Ireland
1,8 ml sterile cryo-tubes	368632	Nunc, Roskilde, Denmark
high glucose DMEM with L-glutamine	BE12-604F	Lonza Biologics, UK
DPBS 1x, w/o Ca2+,Mg2+, phenol red	14190	Invitrogen
100 × Pen/Strep	P0781	Sigma-Aldrich, UK
Fetal calf serum	F7524-500ml	Sigma-Aldrich, UK
Horse Serum	H1270-500ml	Sigma-Aldrich, UK
DMSO (molecular biology grade)	41639	Sigma-Aldrich, UK
1 × Trypsin/EDTA	T3924	Sigma-Aldrich, UK

Chapter 3:

Role of local over-expression of nerve growth factor on corneal allograft survival

3 Role of local over-expression of NGF on corneal allograft survival

3.1 Introduction

Neurotrophic factors are a broad family of proteins that are represented by nerve growth factor (NGF) (119), brain-derived neurotrophic factor (BDNF) (120), neurotrophin-3 (NT-3) (121) and neurotrophin-4/5 (NT-4/5) (122, 123). They are involved in a variety of pleiotropic biological functions such as development, maintenance and survival of most types of neurons and cells derived from neuronal crest. Their function is exerted by binding to two types of receptors, tyrosine kinase (Trk A-E) receptors and glycoprotein p75 receptor, with a different degree of affinity. A family of high-affinity Trk receptors is dominant and sufficient for activation of signal transduction. Co-expression of a low-affinity receptor p75 increases neurotrophin responsiveness, however, its role is more complex and less clearly defined (124, 125). There is evidence indicating that neurotrophins and their corresponding receptors are present in the cornea suggesting a physiological role in ocular surface mediating regulatory functions between cell layers of the cornea (126, 127). The best described and characterized neurotrophin that is involved in mediating physiological processes in the cornea is NGF. Moreover, corneal epithelial and endothelial cells are able to respond to NGF. Indeed, Lambiase et al showed that all three corneal layers synthesize, store and release NGF and additionally express TrkA (128). These findings suggest the presence of an auto/paracrine circuit and support of the pro-survival mechanisms mediated by NGF which has also been observed in neuronal and immune cells (129-131). Furthermore, *in vitro* experiments revealed that NGF modulates the proliferation and differentiation of rabbit corneal epithelial cells (132). The epithelial healing process is also considered to be dependent directly or indirectly on NGF activity. This is supported by *in vivo* studies and clinical observations. Antibody depletion of endogenous NGF significantly delayed the epithelial healing process in a rat model (128). In addition, it was suggested that corneal neurotrophic ulcers associated with dysfunction of sensory innervation may be a consequence of decreased concentration of local NGF

in a similar manner to skin ulcers caused by the impairment of sensor innervation (133). On the other hand, topical application of NGF to patients with corneal neurotrophic ulcers and also to rats with lesioned corneas resulted in accelerated healing of injured epithelium (128, 133).

Moreover, the presence of NGF in aqueous humor (134), whose concentration increases following ocular injuries, may also enhance maintenance and survival of the endothelium. This is supported by *in vitro* studies on immortalized human corneal endothelial cells (iHCEC) showing that these cells express and release NGF which enhances the expression of TrkA but not $p75^{NGFR}$ receptor (135). It was shown on cells of neural origin that the pro-survival signal depends on the balance between TrkA and $p75^{NGFR}$ where TrkA promotes cell survival and $p75^{NGFR}$ modulates the susceptibility to cell death in specific conditions (136). The effect of dose-dependent iHCEC survival in the presence of NGF may be regulated by an auto/paracrine mechanism followed by TrkA up-regulation that promote anti-apoptotic signals (135).

Apoptosis is a highly-regulated, evolutionary conserved form of programmed cell death that plays an important role in both physiological and pathological conditions (137, 138). In immune-mediated allograft rejection apoptosis is the frequent form of donor cell elimination. Moreover, apoptosis plays a crucial role in endothelial cell loss during storage and in graft failure during penetrating keratoplasty (107, 139). Several mechanisms that are able to induce apoptosis might be involved in endothelial cell loss during transplantation. Proinflammatory cytokines released by effector cells infiltrating the aqueous humor are considered to contribute to apoptosis induction of the corneal endothelium. Indeed, it was shown that a combination of cytokines (TNFα, IFNγ and IL-1) resulted in considerable apoptosis of mouse corneal endothelial cells 48 h after stimulation (140).

The anti-apoptotic effect of NGF was demonstrated during chronic hyperosmolar-stimulated human corneal epithelial cell (HCEpC) damage. Physical stress stimulated NF-κB-mediated NGF expression but also induced apoptosis (141). However, inhibition of NGF expression by specific siRNA or blocking TrkA receptor pathway resulted in increased activity of caspase-3 and epithelial cell apoptosis under

hyperosmolar conditions. Interestingly, inhibition of $p75^{NGFR}$ did not show protective effects which confirmed a primary role of TrkA in prevention of cell death (141). Similar protective mechanism of NGF from apoptosis might be involved during corneal endothelial cell loss.

Nonetheless, it was reported that adenovirus-mediated NGF gene transfer in the cornea significantly prolongs transplant survival in a rat model of keratoplasty, although, only 15% of grafts survived indefinitely. Additionally, NGF over-expression contributed to the survival of endothelium and preservation of its integrity after rat cornea transplantation. This result was supported by further data demonstrating up-regulation of anti-apoptotic molecule mRNA (Bag-1) and downregulation of proapoptotic molecule mRNA (Bax). The ratio Bag-1/Bax increased approximately 15 fold in comparison to the control cornea on day 12 after transplantation, however, protein level was not determined in this study (114). Due to the possibility of down-regulation of viral promoter activity, high immunogenicity of adenovirus vectors or immune-mediated elimination of transduced cells further improvements are needed. In this study the lentiviral vectors, as a less immunogenic tool for gene delivery, was investigated in the context of anti-apoptotic properties of NGF and prolongation of the corneal graft survival after transplantation. Also two different promoters, viral – CMV.IM and mammalian – EF-1α, were used for a transgene expression to evaluate their suitability for this study. The NGF-induced, anti-apoptotic mechanism, that protects endothelium from cell death, is also unknown and required additional studies. The apoptosis of the cells was determined on a morphological level, by flow cytometry based on the cells with hypodiploid DNA content and on a molecular level by assessing a cleaved caspase-3 level in the cells.

3.2 Results

3.2.1 Generation of lentiviral vectors encoding for nerve growth factor

3.2.1.1 Preparing plasmid constructs for lentiviral vector production

The first step for lentivirus (LV) generation was the preparation of the plasmid constructs containing the therapeutic gene such as the NGF gene. Two reporter plasmids, pWPT-EGFP and cPPT-EGFP, which carry two different promoters EF-1α and CMV, respectively, were used as backbones for the NGF fragment. As a template for the mouse NGF gene, an already existing plasmid pWPT-NGF, containing correct but inverted sequence of NGF was used (Fig. 3.1 A). To clone the NGF gene in the correct orientation into the destination plasmids the following cloning strategy was performed similar for both plasmids.

Primer design and PCR-amplification

Initially, specific primers were designed which flanked the NGF gene and contained restriction sites at the 5'-ends of primer sequences (Table 2.1 and Fig. 3.1 A). The restriction sites added to the NGF sequence enabled cloning of the NGF fragment into destination plasmids with correct orientation using specific restriction enzymes.

To achieve this, sequencing of pWPT-NGF plasmid with the reverse NGF fragment was performed. The primers for sequencing were designed according to the known sequence of pWPT backbone (Addgene plasmid 12255). The results revealed a correct sequence of NGF gene in the reverse orientation in comparison to the mouse NGF sequence (NCBI GeneBank; Ref. Seq. NM_013609.2) and evaluated the flanked sequences necessary to design primers for NGF gene amplification. Next, the flanking primers were designed with appropriate restriction sites necessary to clone NGF gene in the correct orientation into the destination plasmids. The reverse primer had the same sequence for both plasmids with BamHI restriction site at the 5'-end of the primer, however, the forward primer sequence differs between two

destination plasmids. For pWPT backbone a SalI restriction site was added at the 5'-end of the primer, whereas cPPT required the addition of XhoI restriction site. The primer sequences, which were used for cloning, are presented in table 2.1 (Methods section).

Then, pWPT-NGF plasmid with reversed orientation of NGF gene was used as a template for amplification. Two separate PCRs were performed to amplify NGF cDNA fragment which now contained the flanking regions with appropriate restriction sites. After the amplification procedure two NGF products were obtained, NGF/BamSal and NGF/BamXho, respectively, of the same size of 950 bp.

Ligation of amplified NGF product with an intermediate plasmid

Firstly, direct ligation of NGF fragment amplified by PCR into a destination plasmid was performed, however, this method was unsuccessful and hence indirect cloning strategy was utilized.

Therefore, both NGF products were separated after PCR amplification by electrophoresis in an agarose gel (Fig. 3.2 A). The bands were cut out from the gel and purified by spin columns. Then, samples were ligated with an intermediate plasmid pTZ57R/T. The amount of both PCR products used in ligation reaction was 100ng while the amount of an intermediate plasmid pTZ57R/T was 100ng.

After completion of the ligation reaction competent bacteria were transformed with the ligation mix and selected on antibiotic-containing agar plates. A few colonies were observed after overnight culture indicating successful ligation procedure. To verify the ligation process single colonies were picked and transferred to the LB medium and grown separately to amplify transformed bacteria from positive clones. pDNAs were isolated from the clones and correct size of the inserts were revealed by restriction enzyme analysis (Fig. 3.2 A). The restriction sites that flanked the insert were used to release the NGF fragment from pTZ/NGF vector. BamHI and SalI were used to verify the fragment which was cloned to the pWPT plasmid whereas BamHI and XhoI were chosen to release the insert destined for cPPT vector. Gel electrophoresis was used to separate two bands of the intermediate plasmid subsequent to restriction enzyme digestion. The 950 bp band

with the expected size indicating the NGF fragment and the other 2886 bp band representing linear sequence of pTZ57R/T (Fig. 3.2 B). The smaller bands were cut out from the gel and purified on the minicolumns as described above.

Cloning of NGF fragment into destination plasmid

The final step required preparing the appropriate destination vectors for inserting the NGF fragment. The pWPT-EGFP plasmid was digested with BamHI and SalI to remove the EGFP sequence and produce "sticky" ends which were compatible to the similar ends on the NGF/BamSal fragment. Likewise, the cPPT-EGFP vector was digested with BamHI and XhoI to remove the EGFP gene and to produce specific ends for NGF/BamXho insert (Fig. 3.2 B). Next, the vectors and inserts were ligated overnight and the reaction mixtures were used for bacteria transformation. The antibiotic selection was performed on the agar plates and up to three positive colonies were picked and amplified in LB medium. The plasmids were then isolated and the restriction analysis was performed.

3.2.2 Detection of NGF protein and functional activity assay

3.2.2.1 Confirmation the correct sequence of cloned NGF fragment

Thus far the mouse NGF gene was cloned into both LV plasmids, however, careful analysis of the nucleotide sequence was required to exclude mutations introduced by PCR or other problems, which might appear during a cloning process. Validating the sequence was essential prior to using these plasmids for further studies.

The enzymatic restriction analysis was performed with the destination plasmid to identify the correct size of restriction fragments and the orientation of NGF gene. Similarly to the intermediate plasmid, the restriction sites incorporated into the PCR primers in the PCR were chosen to evaluate the correct size of inserts. For pWPT-NGF construct BamHI and SalI enzymes were used to cut out the insert while restriction digestion of cPPT-NGF plasmid were carried out by BamHI and XhoI enzymes. The results of the analysis are presented in Fig. 3.2 C. As expected, the

950 bp bands represent the NGF fragment and the larger bands represent linear sequences of pWPT and cPPT plasmids, respectively.

Additionally, by using the restriction enzyme site ApaI it became possible to precisely determine the orientation of the insert. In the final construct, the first ApaI restriction site was located close to the 5'-end of the NGF gene while the second site was in the plasmid sequence. After enzymatic digestion the plasmids were cut in two fragments of different size. The fragment sizes differed depending on the NGF gene orientation and the Apa I restriction site location in the NGF sequence. Therefore, the electrophoretic separation would give a different fragment pattern in the agarose gel. The hypothetic enzymatic restriction analysis is presented in Fig. 3.3 A.

Indeed, the initial pWPT-NGF plasmid with reversed NGF sequence had different sizes of the fragments in comparison to the final pWPT-NGF construct when cut by ApaI and separated in the agarose gel (Fig. 3.2 C). Similarly, cPPT-NGF showed a correct size of the fragments according to the prediction (Fig. 3.2 C, 3.3 A and B).

No specific information about a sequence or any mutations were achieved by restriction enzyme analysis. The plasmid constructs, which showed the correct banding patterns, were sent for DNA sequencing. Not all the results confirmed a correct sequence of the NGF gene, however, all inserts had a correct orientation, which proved accuracy of restriction enzyme analysis. The lentiviral plasmids with a 100% identity of the insert sequence to the reference mouse NGF gene were kept at -20°C and used in further research. The bacteria colonies that contained the correct plasmids were stored at -80°C and used as a source of both verified plasmids pWPT-NGF or cPPT-NGF.

3.2.2.2 Verification of NGF expression after transfection with plasmid vectors

Hence, the NGF gene was cloned into pWPT and cPPT plasmids and its sequence and orientation were confirmed, however, the expression and activity of the encoded protein had still to be verified. The PCR with specific primers complementary to the NGF sequence was performed on both plasmids to verify the

presence of NGF fragments and to test PCR primers. The fragments visualized on the agarose gel had an expected size of 164 bp in length (Fig 3.4 A).

Before starting to generate LV vectors for cell trancduction experiments, NGF protein expression was analyzed by transfection of control cells. Using the polyethylenimine (PEI) protocol, 293T cells were transfected with 1 μg of each plasmid. pWPT-EGFP vector was used as a control. The NGF protein concentration was evaluated in the supernatants collected three days after transfection by specific ELISA. The results confirmed the expression of NGF protein from both plasmids demonstrating a high concentration of the protein with a mean value of 2.0±0.1 ng/ml for pWPT-NGF plasmid and 1,5±0.2 ng/ml for cPPT-NGF construct (Fig. 3.4 B). This demonstrated that the cloning procedure was correct and the plasmids were ready for further application.

3.2.2.3 Detection of biologically active NGF after transduction with LV vectors

As described above successful cloning resulted in NGF protein expression after transfection of HeLa cells with the plasmid vectors, however, it has not yet been shown whether the protein is active and fully able to modulate the signaling pathways. Moreover, recombinant lentiviral vectors have to be generated for *ex vivo* application. As described in Material and Methods section LV vectors were generated by co-transfection of 293T cells with 4 plasmids containing the following genes: a gene of interest, VSV-G envelope gene, gag-pol enzymes and helper rev sequence. The viral particles were harvested from the supernatants by an ultracentrifugation, resuspanded in 1% BSA in PBS solution, aliquoted and freezed at -80°C.

Furthermore, after the lentiviral vector production the expression of the transgene might be diminished by a low titer of the viral vectors or silencing of the promoter. Therefore, to clarify that the transduced cells express a therapeutic protein which is functionally active each lentivirus batch was routinely titered and expression of the therapeutic protein was monitored. The titration method was described in Material and Methods section and a concentration of LV vectors ranged between 3,4 x 10^7

and 1,0 x 10^9 TU/ml. The lower titer batches were used for *in vitro* studies while the cornea transductions were performed using the higher titer batches.

Finally, an activity assay was performed using the supernatants from transduced cells for PC12 cells (indicator cell line) culturing to reveal that the NGF protein is active. The expression of NGF protein was calculated by measuring concentration of NGF protein in the supernatants.

Two different promoters driving the transgenes expression were used in this study. The human cytomegalovirus immediate early promoter is thought to be a very strong promoter, however, as a viral-origin sequence it could be recognized and down-regulated by a cellular mechanism. On the other hand, mammalian elongation factor - 1α promoter is considered to provide a constitutive expression of a transgene but on a lower level in comparison to the CMV.IE promoter.

HeLa cells were transduced with 2.0 × 10^5 TU of LV.NGF and incubated overnight. 24 h after transduction medium was replaced. Supernatants were collected 24, 48 and 72 h after medium replacement and analyzed by specific ELISA. Supernatants from untransduced cells were used as a control. HeLa cells transduced with LV.NGF expressed high amounts of the protein 48 h after transduction (Fig. 3.5 A). This expression significantly increased over time when LV_{ef}NGF were used for transduction. Interestingly, transduction with LV_{cmv}NGF vectors resulted only in a mild increase of NGF concentration in the supernatant. Next, the secretion of NGF was quantified after transduction of the targeted tissue. NGF was not detected in the supernatant of untransduced rat corneas, whereas LV.NGF treated rat corneas expressed NGF as early as 24h after transduction. The concentration of NGF protein after 48h was 0.37±0.01 ng/ml for LV_{ef}NGF treated corneas and 0.28±0.04 ng/ml for LV_{cmv}NGF transduced corneas (Fig. 3.5 B). These data confirmed that lentivirus vectors encoding NGF efficiently transduced both HeLa cells and *ex vivo* cultured corneas resulting in substantial amounts of NGF protein.

Finally, it was important to determine whether secreted NGF was able to differentiate the NGF-responsive indicator rat PC12 cells into neuronal-like cells and induce neurite outgrowth. An immortalized Human Corneal Endothelial Cell line was used as *in vitro* model of corneal endothelium. PC12 cells were cultured in the

supernatants collected 72 h after transduction of HCEC cells with both LV.NGF or LV.EGFP vectors. Untreated cells and cells treated with 100 ng/ml of recombinant NGF (rNGF) served as negative and positive controls, respectively. Untreated cells as well as PC12 cells cultured in the supernatant from LV.EGFP-transduced cells did not change morphology and remained undifferentiated (Fig. 3.6 A, B). In contrast, an increase in the number of neurite-bearing cells was observed in PC12 cells cultured in the presence of rNGF or in the supernatants from LV.NGF transduced HCEC cells (Fig. 3.6 C, D, E). Taken together, these data suggest that LV-mediated gene transfer to the HCEC cells resulted in the secretion of functionally active NGF protein which was able to induce neurite outgrowth of PC12 cells. These results confirmed that biologically active NGF was successfully cloned in LV-vectors which will be used in all subsequent experiments.

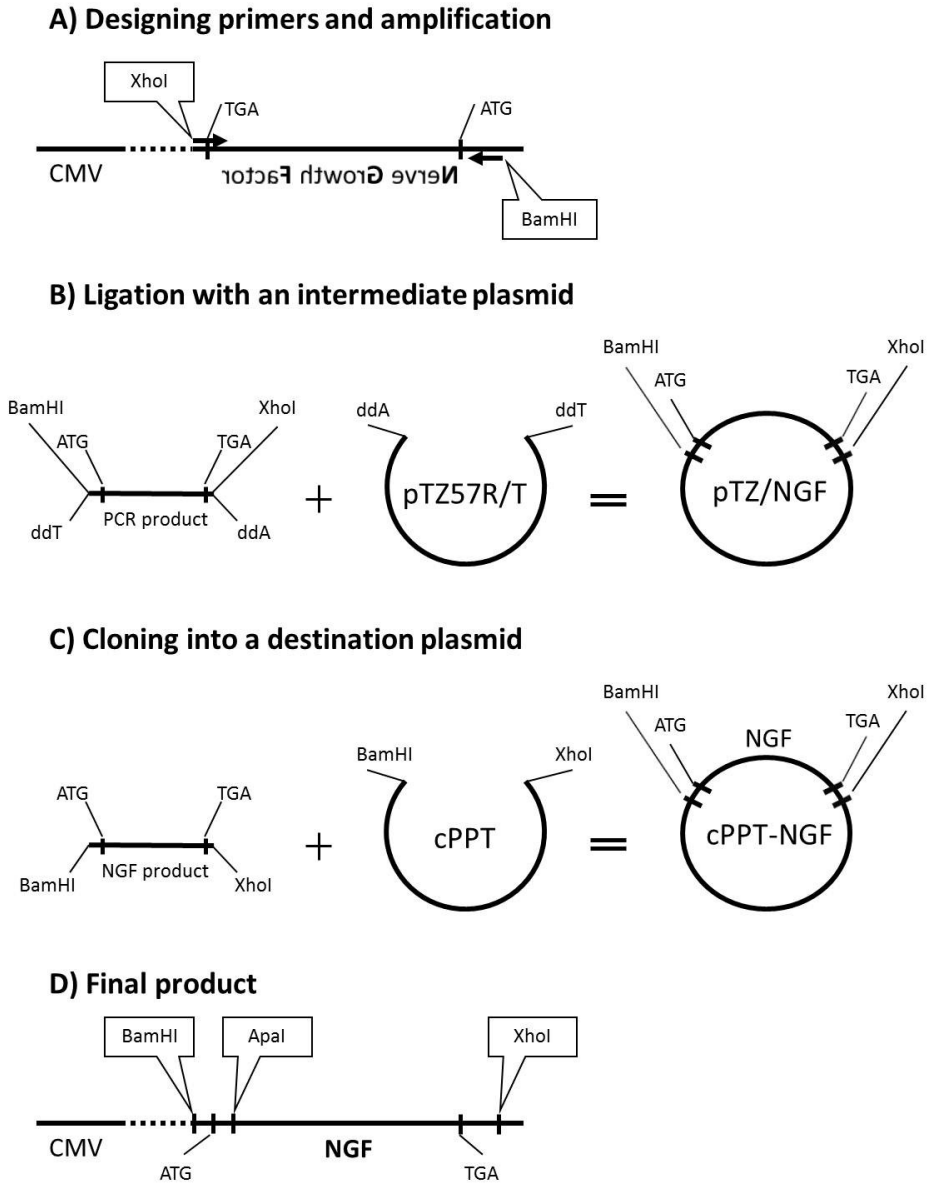

Fig. 3.1. Multiple steps in NGF gene cloning. A) amplification of NGF gene with specific, flanking primers with appropriate restriction sites required to clone NGF gene in the correct orientation into the destination plasmids **B)** ligation of PCR product with 3'-ddA overhangs with the linearized pTZ57R/T cloning vector tailing with 3'-ddT overhangs **C)** cutting the insert out with the specific restriction enzymes and cloning into a destination plasmid (pWPT of cPPT) linearizing with appropriate restriction enzymes **D)** the final product of the cloning process.

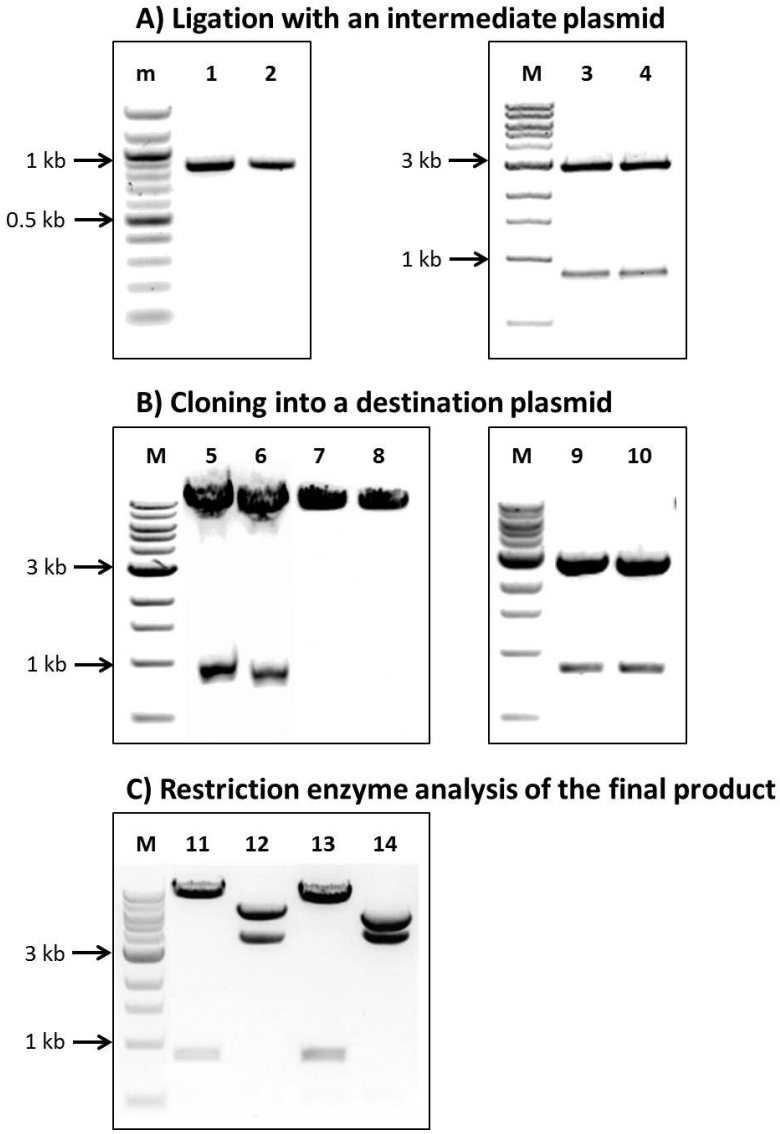

Fig. 3.2. The restriction enzyme analysis of the cloning products. A) left: amplified NGF products (950bp) with primer pairs containing either BamHI and SalI restriction sites (lane 1) or BamHI and XhoI (lane 2); right: intermediate plasmids after ligation with both PCR products digested with either BamHI and SalI restriction sites (lane 3) or BamHI and XhoI (lane 4) (the band sizes: 950 and 2886 bp) **B)** left: pWPT plasmid digested with BamHI and SalI before (lane 5; the band sizes: 950 and 8642 bp)) and after purification (lane 7); cPPT plasmid digested with BamHI and XhoI before (lane 6; the band sizes: 950 and 8642 bp) and after purification (lane 8); right: intermediate plasmids with NGF inserts digested with BamHI and SalI (lane 9) or BamHI and XhoI (lane 10) (the band sizes: 950 and 2886 bp) **C)** the final product analysis: pWPT-NGF plasmid digested with BamHI and SalI (lane 11) and with ApaI (lane 12; the band sizes: 3598 and 5994 bp); cPPT-NGF plasmid digested with BamHI and XhoI (lane 13) and with ApaI (lane 14; the band sizes: 3797 and 5703 bp). m – 100 bp DNA ladder; M – 1 kb DNA ladder (NEB).

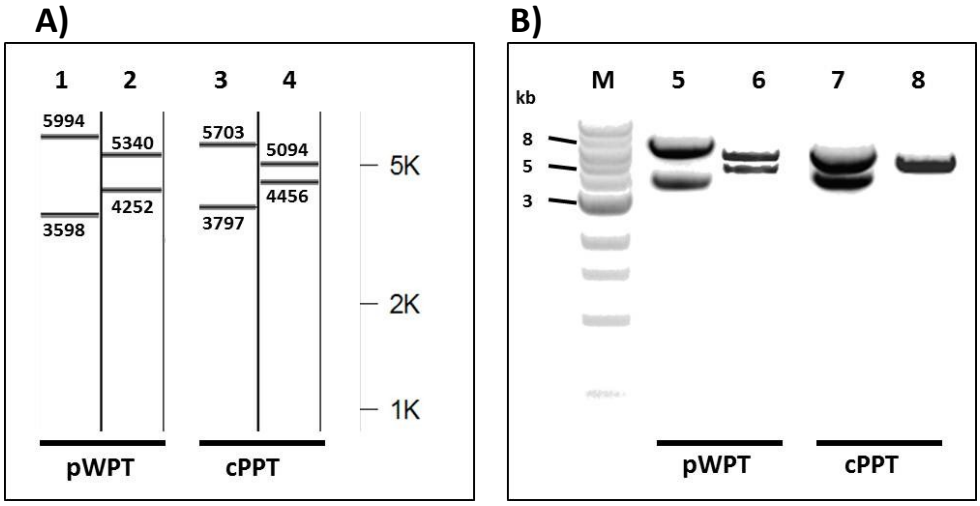

Fig. 3.3. The ApaI restriction enzyme analysis of the insert orientation. A) The theoretical electrophoretic gel visualization (NTI Vector software) of pWPT-NGF and cPPT-NGF vectors after ApaI hydrolysis: line 1 – the band pattern indicates a correct orientation of the NGF insert whereas in lane 2 – suggests inverted orientation of NGF fragment in pWPT-NGF plasmid; lane 3 and lane 4 show respectively, the correct and inverted NGF insert orientation in ApaI digested cPPT-NGF vector; **B)** The electrophoretic analysis of digested pWPT-NGF and cPPT-NGF vectors: lane 5 (the band sizes: 3598 and 5994 bp) and lane 7 (the band sizes: 3797 and 5703 bp) show the correct NGF insert orientation in ApaI digested pWPT-NGF or cPPT-NGF vectors, respectively; lane 6 (the band sizes: 4252 and 5340 bp) and lane 8 (the band sizes: 4456 and 5094 bp) exhibit the inverted orientation of NGF fragment in both plasmids. M - 1 kb DNA ladder (NEB).

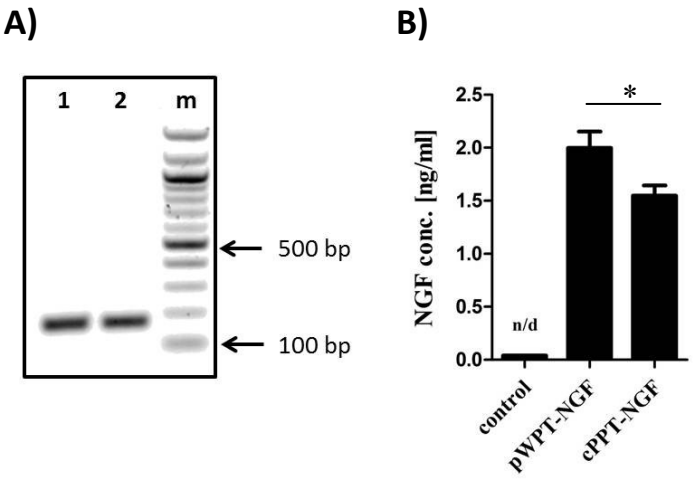

Fig. 3.4. Detection of NGF gene on destination plasmids and protein expression after transfection of HeLa cells with pWPT-NGF and cPPT-NGF plasmids. A) PCR with specific primers for NGF was performed on: lane 1 – pWPT-NGF and lane 2 – cPPT-NGF plasmid; M - marker **B)** culture supernatants were collected 72 h after transfection and the level of NGF protein was analyzed by ELISA. m – 100 bp DNA ladder (NEB). The average and error bars represent mean ± SD from two independent experiments performed in duplicates; * p≤0.01.

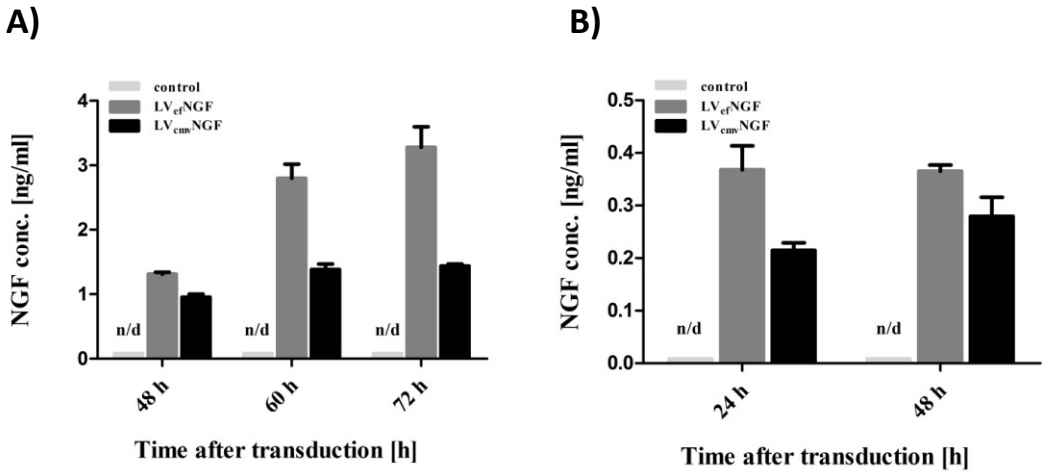

Fig. 3.5. Time-course of NGF expression in transduced HeLa cells and *ex vivo* cultured corneas. The total increase of NGF protein levels were analyzed by ELISA. Medium was replaced after transduction with LV vectors. **A)** HeLa cells were transduced with 2.0×10^5 TU of LV vectors. Culture supernatants from the cells were collected 48, 60 and 72 h after transduction with $LV_{ef}NGF$ and $LV_{cmv}NGF$. Untransduced cells supernatant sereved as a control. The average and error bars represent mean ± SEM from three independent experiments performed in duplicates. **B)** culture supernatants from *ex vivo* cultured corneas were collected 24 and 48 h after transduction with $LV_{ef}NGF$ and $LV_{cmv}NGF$. Untransduced corneas supernatant served as a control. The average and error bars represent mean ± SEM from three rat corneas.

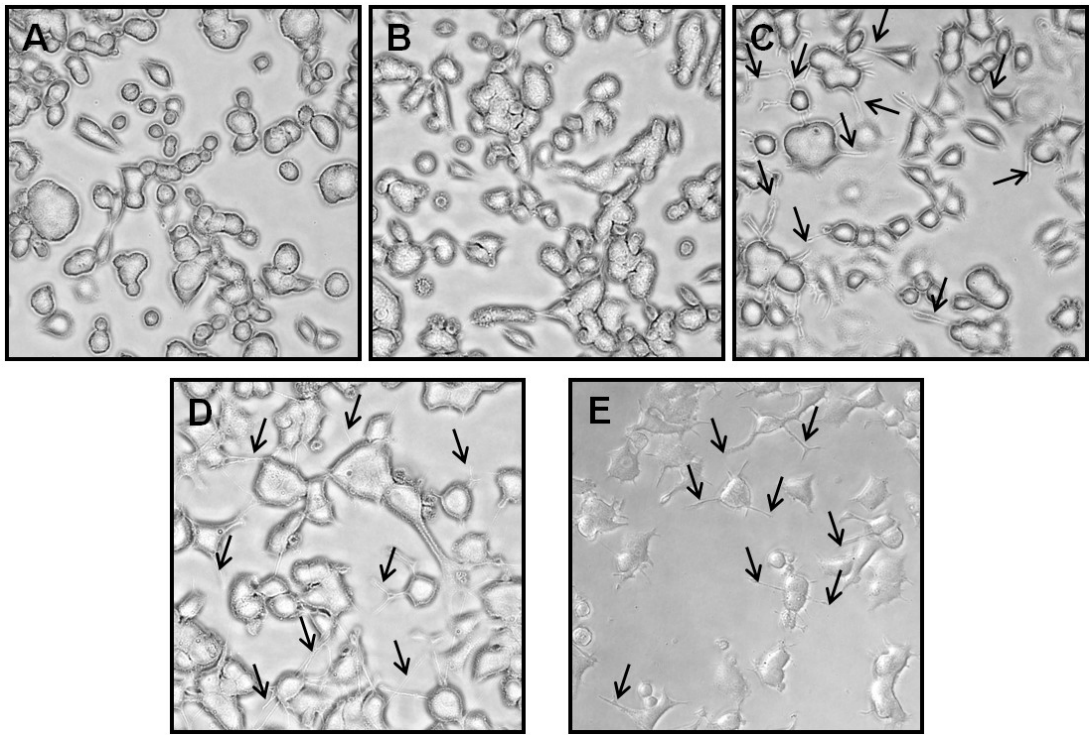

Fig. 3.6. Lentivirus mediated overexpression of NGF in HCEC cells leads to functionally active protein secretion and neurite outgrowth in PC12 cells. Microscopic examination of neurite outgrowth of PC12 cells cultured in: **A)** complete PC12 medium; **B)** supernatant from LV.EGFP transduced HCEC; **C)** complete PC12 medium with 100 ng·ml^{-1} rNGF; **D)** supernatant from LV_{ef}NGF transduced HCEC; **E)** supernatant from LV_{cmv}NGF transduced HCEC. The cells were monitored for 48 h. Black arrows indicate extending neurites. Representative microscopy images from three independent experiments are shown.

3.2.3 Role of NGF overexpression on corneal endothelial cell protection

3.2.3.1 Investigation of the anti-apoptotic effect of overexpressed NGF - in vitro model

Previously it has been reported that Ad-mediated NGF gene transfer to donor corneas protects the endothelial cells from apoptosis (114). To further characterize the anti-apoptotic effect of overexpressed NGF, immortalized HCECs were used as an *in vitro* model for these studies. A murine corneal endothelial cell line was not available, however, murine NGF is very homologous to human NGF (142) and it was demonstrated that ophthalmic administration of murine NGF produces no local or systemic side effects during human corneal ulcer treatment and restores corneal integrity in patients with corneal neurotrophic ulcers (133). These findings allowed us to investigate the anti-apoptotic effect of mNGF on HCEC. Rat PC12 cells were used as a reference cell line due to the large number of publications describing inhibition of the thapsigargin (TG)-induced apoptosis by NGF on these cells (143).

First, the experiments required to determine the concentration of TG to induce programmed cell death and the optimal time for HCEC harvesting were undertaken. Based on the well-known conditions required for apoptosis induction in PC12 cells (143), similar conditions were applied to HCECs. The caspase-3 activity assay, which detects the catalytic ability of caspase-3 to cleave fluorescently labeled DEVDase substrate (DEVD-MCA), was applied to evaluate the treatment protocols for activation of caspase-3 in HCECs. Cells were treated with three different concentrations of TG and harvested either 24 or 48 h after apoptosis induction. As shown in Fig. 3.7 A only cells harvested 48 h after TG treatment exhibited an increased level of active caspase-3. Interestingly, the activity of the enzyme was equal for all TG concentrations applied. Additionally, these results were confirmed by Western blot analysis of cleaved caspase-3 appearance in HCECs after stimulation with different concentrations of TG and time of treatment. HCECs treated with 1,5 µM TG for 48 h showed an increase of activated caspase-3 (17 and 19 kDa) in comparison to untreated control (Fig. 3.7 B). Unlike PC12 cells the protein could not be detected 24 h after treatment and required longer time of

incubation. More detailed time point analysis showed that a significant increase of caspase-3 level could be detected 36 h and 38 h after TG treatment (Fig. 3.7 C). The range between 36 and 40 h incubation with TG was chosen as the optimal time for HCEC harvesting.

In order to examine whether NGF gene delivery protects HCEC cells from endoplasmatic reticulum (ER) stress-induced apoptosis, a series of experiments was performed including the microscopic examination of both PC12 and HCEC cell line morphology, flow cytometric evaluation of apoptotic cells and the analysis of cleaved caspase-3 level by Western blotting. The experiment design was described in Material and Methods section.

Thus, the supernatants from either untransduced or transduced HCEC with LV_{ef}EGFP and both LV.NGF vectors were collected 72 h after transduction and stored at -80˚C. Then, collected supernatants were applied to the freshly-seeded PC12 or HCEC cells. rNGF was added to the medium as a positive control for apoptosis inhibition. Next, cells were cultured for 24h and then treated with 1.5 µM TG to induce apoptosis. PC12 cells were harvested 24 h after TG treatment whereas HCEC were kept in culture for 36 and 40 h after apoptosis induction according to optimized conditions. In some experiments 50 µM of pan-caspase inhibitor Z-VAD-fmk was added 30 min prior to the apoptosis induction.

First, microscopic examination of cell morphology was performed 24 or 48 h after apoptosis induction with TG, respectively for PC12 cells (Fig. 3.8) and HCEC (Fig. 3.9). Untreated cells served as controls (Fig. 3.8 A and 3.9 A). Apoptosis induction in PC12 cells was only observed when cells were treated with TG only or cultured in supernatants from untransduced HCEC or LV_{ef}EGFP transduced HCEC. Many cells were detached from the culture plate and showed apoptotic morphology which is indicated with white arrows (Fig. 3.8 B, E, F). In contrast, PC12 cells cultured in supernatants from either LV_{ef}NGF or LV_{cmv}NGF transduced HCEC as well as treated with rNGF remained adherent and only a small fraction of cells showed symptoms of programmed cell death (Fig. 3.8 D, G, H). Moreover, cells developed neuron-like morphology and induction of neurite outgrowth (black arrows) which confirms the presence of NGF in the supernatants. As expected, pre-treatment with a pan-

caspase inhibitor efficiently protected PC12 cells from cell death and from pathogenic morphological changes (Fig. 3.8 C). These results indicate that LV_{ef}NGF or LV_{cmv}NGF transduced HCECs produce functionally active NGF.

In contrast to our observed effects in PC12 cells, HCEC cultured in supernatants from untransduced HCEC or transduced with either LV_{ef}EGFP or both LV.NGF vectors showed detached cells with apoptotic morphology and decreased level of confluency in comparison to untreated control (Fig. 3.9 A, E, F, G, H). Furthermore, cells treated with TG in presence or absence of rNGF resulted in similar morphology phenotype and also showed increased numbers of apoptotic cells as indicated by white arrows (Fig. 3.9 B, D). Only cells treated with pan-caspase inhibitor prior to the apoptosis induction showed negligible number of detached cells. Although the total number of cells seemed to be lower than in the untreated control group, it could be due to the inhibition of cell proliferation after treatment with pan-caspase inhibitor (Fig. 3.9 C).

Next, flow cytometric analysis of apoptotic cell death by propidium iodide staining was performed according to Nicoletti protocol (116). Similar to the examination of PC12 cell morphology, flow cytometric analysis revealed the anti-apoptotic properties of both rNGF and secreted NGF present in supernatants from LV.NGF transduced HCEC (Fig. 3.10 A, B). The secreted NGF almost completely inhibited apoptosis in PC12 cells. In contrast, supernatants from untransduced or LV_{ef}EGFP transduced HCEC did not result in any protective effect to PC12 cells against TG-induced apoptosis (Fig. 3.10 A, B). HCEC treated with pan-caspase inhibitor showed a decrease (although not statistically significant) in apoptotic cell numbers in comparison to TG treated cells, however, no change in apoptosis level was observed when cells were cultured in presence of rNGF or in supernatants with secreted NGF (Fig. 3.10 C, D). Moreover, similar numbers of apoptotic cells were observed in HCEC treated with TG only or cultured in the supernatants from untransduced HCEC or LV_{ef}EGFP transduced HCEC. These data indicate that NGF was unable to prevent apoptosis after TG treatment in HCEC, nonetheless, the fold induction of apoptotic cells was lower compared to PC12 cells (Fig. 3.10 A, C). To examine whether a stronger induction of apoptosis will give a larger increase in apoptotic cells, HCEC

were cultured in the presence or absence of serum. In addition, different time points of incubation with rNGF were studied to determine the impact of incubation time on the protective effect of NGF against the ER stress-induced apoptosis. As shown in Fig. 3.11 A and B HCEC cultured without serum were more sensitive for TG induced apoptosis and resulted in higher fold changes compared to the cells cultured in the presence of serum. Furthermore, rNGF did not inhibit TG-induced apoptosis in HCEC of any fixed time point and even when rNGF was added to the medium twice before induction. These results indicated that HCEC cannot be protected from apoptosis by NGF independent from method of apoptosis induction. Finally, levels of cleaved caspase-3 was evaluated by Western blotting as a protein marker of ER stress-induced apoptosis. PC12 cells treated with thapsigargin and cultured either in complete medium or in supernatants from untreated HCEC showed high levels of cleaved caspase-3. In contrast, apoptosis was greatly reduced in presence of pan-caspase inhibitor or rNGF in the medium. Furthermore, reduction in activated caspase-3 was observed in cells cultured in supernatants from transduced HCEC with both LV.NGF vectors (Fig. 3.12 A). Similar experiments were performed on HCEC, however, only untreated cells did not show the cleaved caspase-3. Despite the presence of rNGF or apoptosis inhibitor in medium of TG-treated HCEC the level of caspase-3 remained at the same level in comparison to TG-treated cells. Although cells cultured in the supernatants from transduced HCEC with LV_{ef}NGF vectors showed reduced level of cleaved caspase-3, the other other results did not confirm this observation (Fig. 3.12. B), however, this experiment should have been repeated due to the imprecise results. Cells cultured in supernatants from transduced HCEC with LV_{cmv}NGF vectors did not demonstrate any reduction of ER stress-induced marker (Fig. 3.12. B). To verify it, even different batches of TG and rNGF were used for the experiment. None of the rNGF batches were able to prevent the expression of caspase-3 (Fig. 3.12 C). To summarize these experiment it was shown that LV.NGF transduced corneal endothelial cells secreted biologically active NGF. In addition, supernatants from LV.NGF transduced immortalized human corneal endothelial cells (HCEC) significantly reduced TG-induced apoptosis in control PC12 cells, however, no protective effect of either

rNGF or supernatant containing NGF could be observed in HCEC. Despite many repeats and different experimental settings it was not possible to confirm the hypothesis that NGF is able to protect human corneal endothelial cells from apoptosis in a similar manner like it protects PC12 cells.

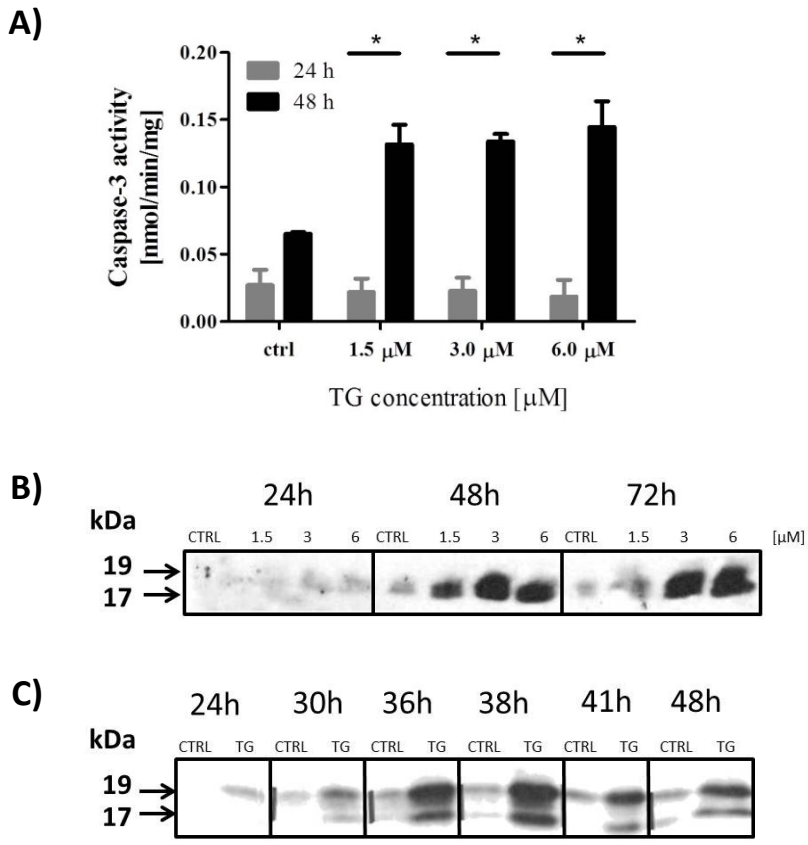

Fig. 3.7. Optimization of TG concentration and optimal time point required to induce programmed cell death in HCECs. A) The caspase-3 activity assay was performed to establish the treatment protocol for activation of caspase-3 in HCECs. The average and error bars represent mean ± SD from triplicates. **B)** Western blot of cleaved caspase-3 protein level after stimulation of HCECs with TG at different time points and increased concentration. **C)** Time-course of cleaved caspase-3 expression in HCECs after 1.5 µM TG stimulation.

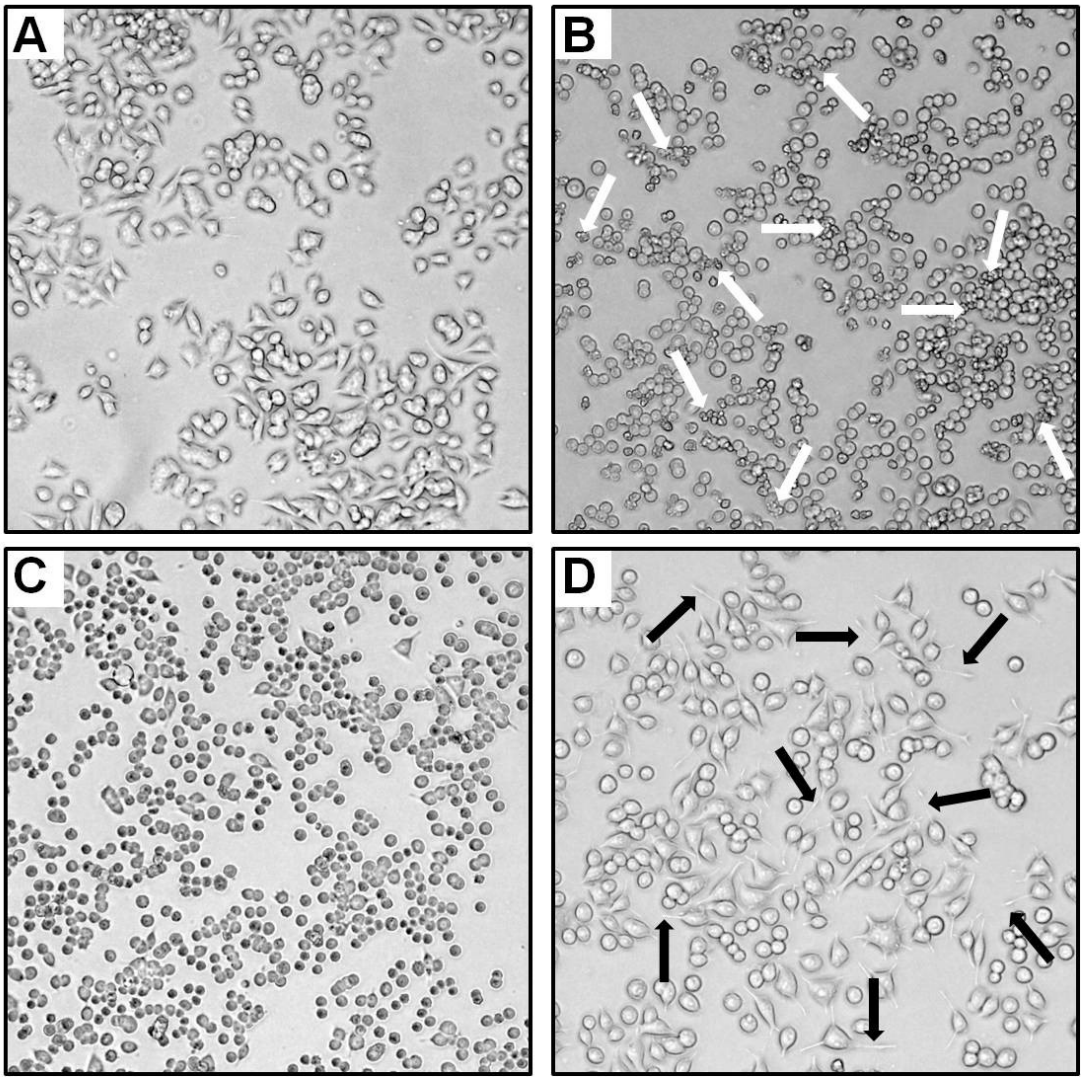
A
B
C
D

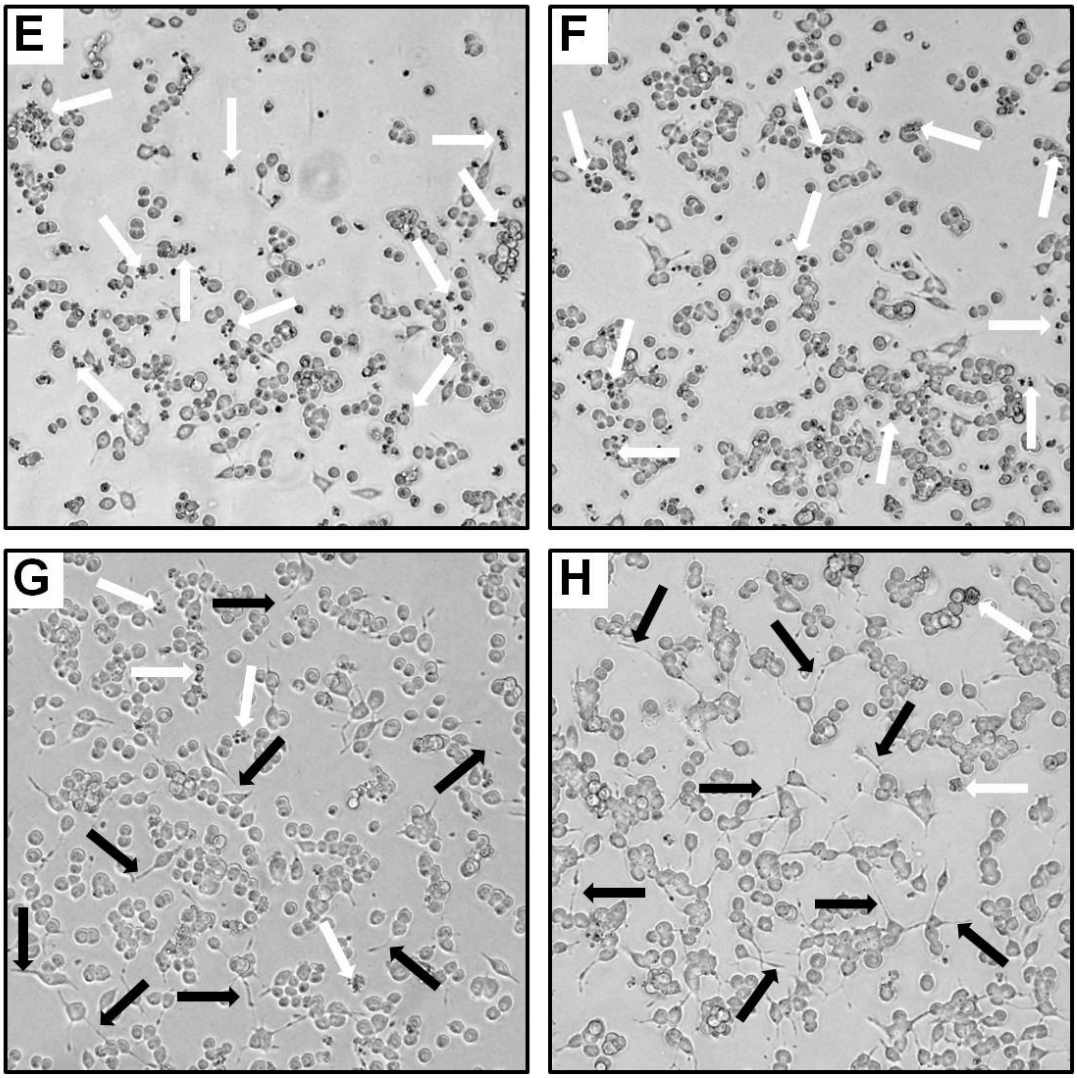

Fig. 3.8. PC12 cells cultured in the supernatants from LV.NGF transduced HCEC are protected against apoptotic changes in cell morphology induced by thapsigargin. PC12 cells were cultured in complete medium or in supernatants from HCECs 48 h prior to apoptosis induction and then treated with 1.5 µM thapsigargin for the following 24 h. Microscopic examination of apoptotic PC12 cells was evaluated. Complete medium: **A)** untreated cells; **B)** cells treated with TG only; **C)** cells cultured in presence of pan-caspase inhibitor Z-VAD-fmk; **D)** cells cultured in presence of 100 $ng \cdot ml^{-1}$ rNGF. HCECs supernatants from: **E)** untransduced cells; **F)** LV.EGFP transduced cells; **G)** LV_{ef}NGF transduced cells; **H)** LV_{cmv}NGF transduced cells. Apoptotic cells are indicated by white arrows and neurite outgrowth by black arrows. Figures are representative of 3 independent experiments.

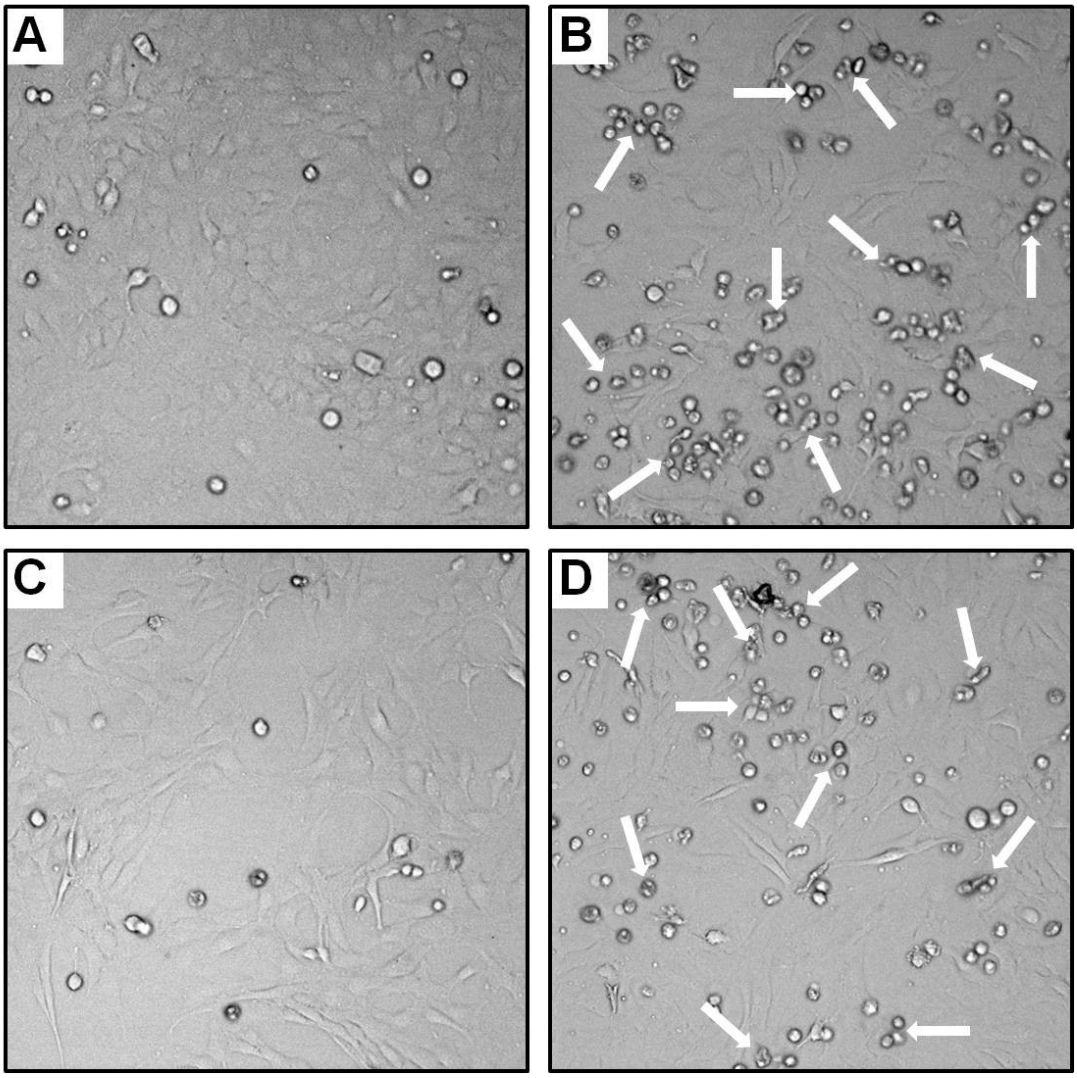
A
B
C
D

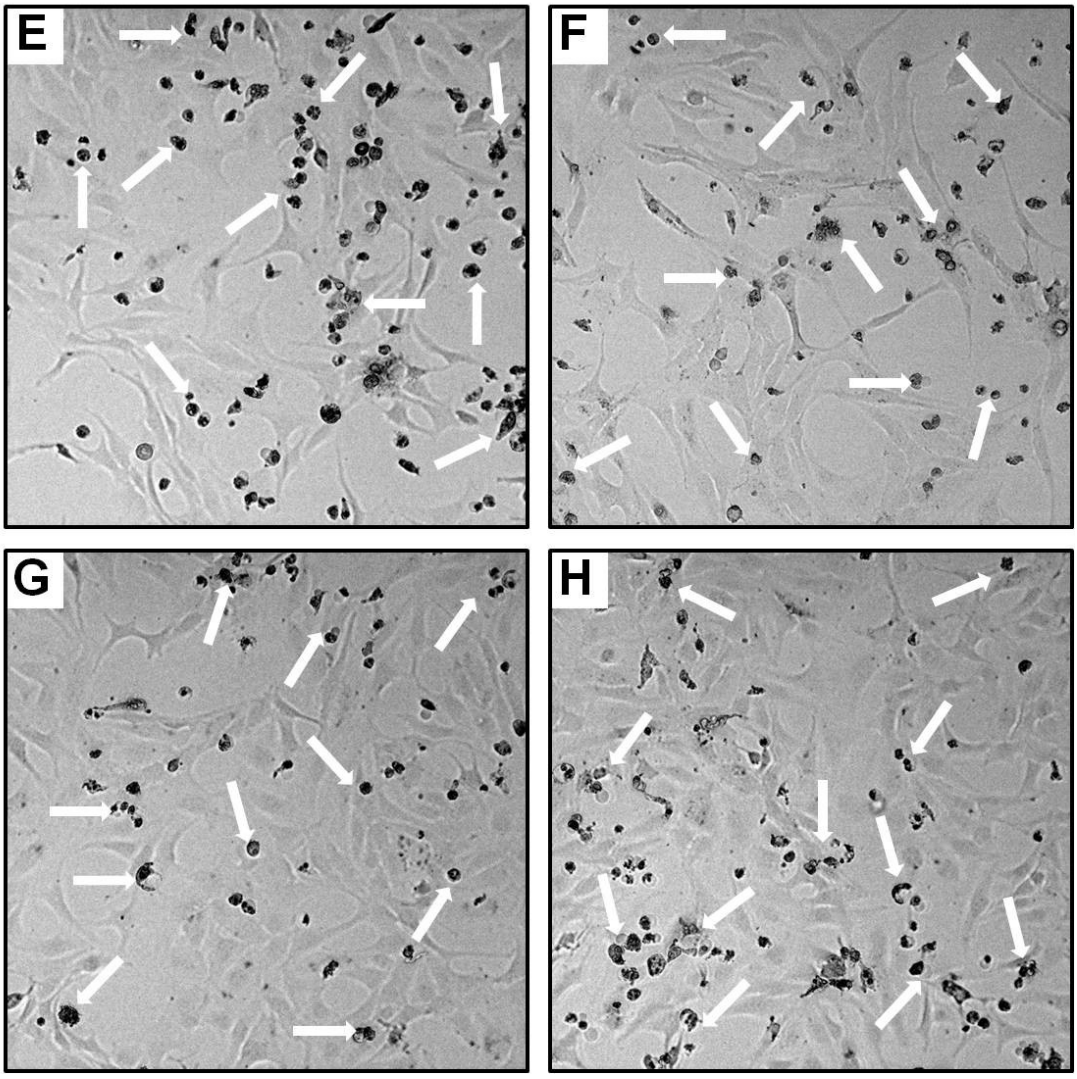

Fig. 3.9. HCECs cultured in supernatants from LV.NGF transduced HCECs are not protected against apoptosis induced by thapsigargin. HCECs were cultured in complete medium or in supernatants from HCECs 48 h prior to apoptosis induction and then treated with 1.5 µM thapsigargin for the following 24 h. Microscopic examination of apoptotic HCECs was evaluated. Complete medium: **A)** untreated cells; **B)** cells treated with TG only; **C)** cells cultured in presence of pan-caspase inhibitor Z-VAD-fmk; **D)** cells cultured in presence of 100 ng·ml^{-1} rNGF. HCECs supernatants from: **E)** untransduced cells; **F)** LV.EGFP transduced cells; **G)** LV_{ef}NGF transduced cells; **H)** LV_{cmv}NGF transduced cells. Apoptotic cells are indicated by white arrows. Figures are representative of 3 independent experiments.

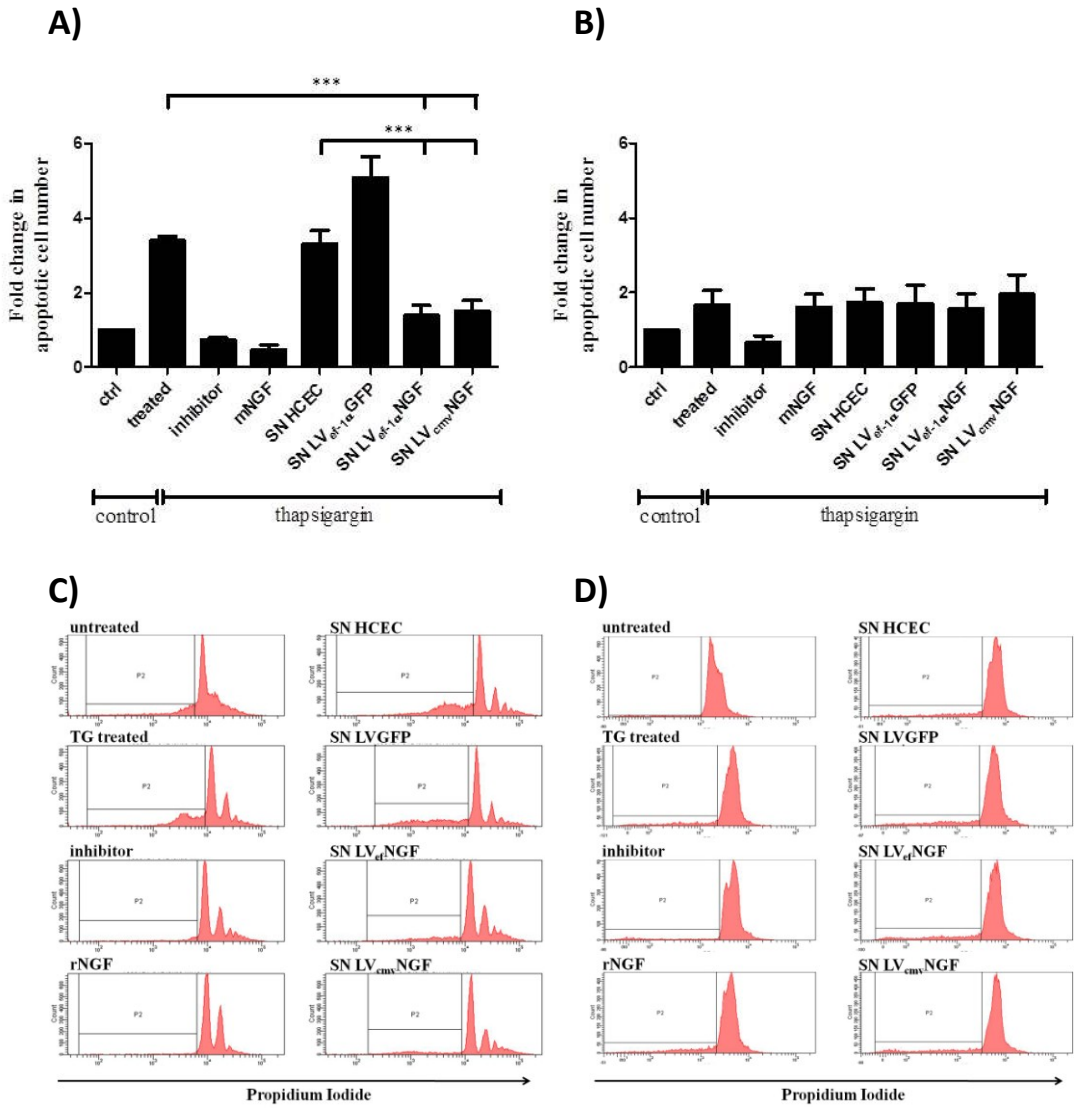

Fig. 3.10. Culture supernatants derived from LV.NGF transduced HCEC cells lead to significant reduction of apoptotic PC12 cells after TG treatment but not in HCECs. HCECs and PC12 cells were cultured 24 h before apoptosis induction in supernatants from transduced and control HCECs, complete medium pre-treated with rNGF (100 ng·ml^{-1}) or pan-caspase inhibitor (Z-VAD-fmk). Apoptosis was induced by treatment of cells with 1.5 µM TG. Treated PC12 cells were harvested 24 h while HCEC cells 48 h after apoptosis induction and analyzed for DNA content. The cells with hypodiploid DNA content were defined as apoptotic cells. Untreated cells served as a reference to estimate percentage of apoptotic cells. The average and error bars represent mean ± SD from three independent experiments performed in triplicates (*** $p<0.001$). **A)** Fold change of apoptotic PC12 cells; **B)** Fold change of apoptotic HCECs; **C)** Representative PI profiles of PC12 cells; **D)** Representative PI profiles of HCECs.

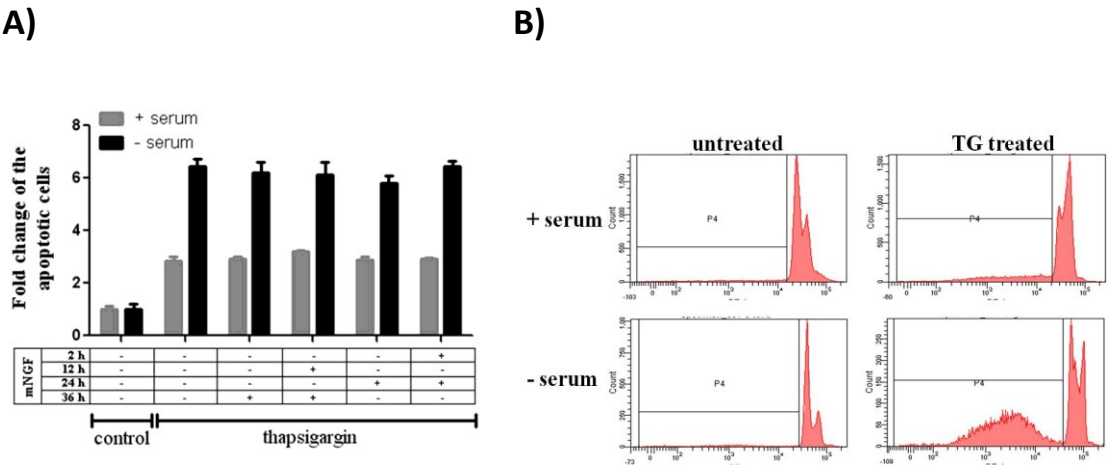

Fig. 3.11. Lack of serum results in increased number of apoptotic cells but exposition of cells to rNGF for various time periods does not lead to reduction of apoptotic cells. A) Fold change of apoptotic HCECs cultured in presence or absence of serum and exposed to rNGF for various time periods prior to TG induction. Treated cells were harvested 24h after apoptosis induction and analyzed for DNA content. The cells with hypodiploid DNA content were defined as apoptotic cells. Untreated cells served as a reference to estimate percentage of apoptotic cells. The average and error bars represent mean ± SD from one experiment repeated in triplicates. **B)** Representative PI profiles of HCECs cultured in presence or absence of serum.

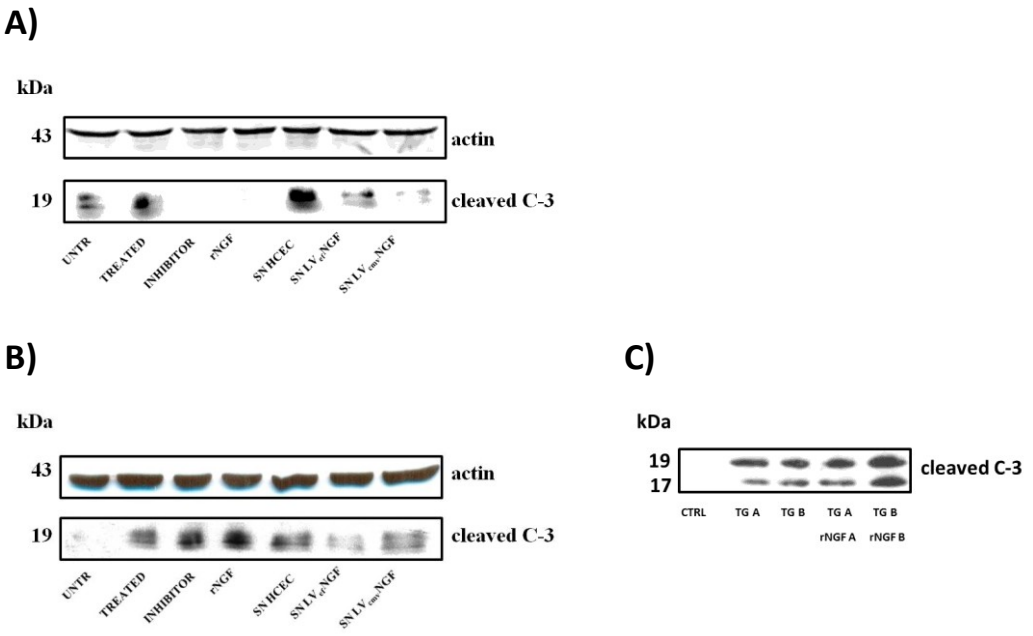

Fig. 3.12. Lentivirus mediated overexpression of NGF in HCECs leads to significant reduction of cleaved caspase-3 in PC12 cells after TG treatment but not in HCECs. HCECs and PC12 cells were cultured 48 h before apoptosis induction in the supernatants from transduced or untransduced HCECs or complete medium pre-treated with rNGF (100 ng·ml^{-1}) or pan-caspase inhibitor (Z-VAD-fmk). Apoptosis was induced by treatment of cells with 1.5 µM TG. Treated PC12 cells were harvested 24h after apoptosis induction whereas HCECs 48 h after TG treatment. The level of active caspase-3 was visualized by Western blot. Actin was used as a loading control. **A)** PC12 cells; **B)** HCECs; **C)** Western blot performed on HCECs treated with different rNGF and TG batches. HCECs were exposed on 100 ng·ml^{-1} rNGF for 48 h followed by 48 h TG treatment.

3.2.4 The effect of local lentiviral-mediated NGF gene transfer on corneal allograft survival

3.2.4.1 Optimization of ex vivo transduction of donor rat cornea by lentiviral vectors

As a first step towards optimizing the conditions for *ex vivo* gene transfer to the cornea by lentiviral vectors, the corneas explanted from donor animals were incubated with LV.EGFP viruses (1×10^5 TU/ml) for 24 h at 37˚C in 5% CO_2. The expression of EGFP protein was examined under fluorescent microscope 2 and 7 days after transduction and the images are presented in Fig 3.13. High expression levels of the EGFP protein was detected 2 days after transduction of *ex vivo* cultured corneas (n=2). The high level of EGFP expression remained up to day 7, however, significant disintegration of endothelium was noticed and the experiment was terminated at that point.

Next, to examine the optimal time window for corneal gene transfer, the corneas were incubated with LV.EGFP viruses (2×10^4 TU/cornea) for 1, 4 and 20 h followed by culture in fresh medium for further 48 h. In order to analyze the transduction efficiency more carefully, corneas were digested and single cell suspensions were analyzed by flow cytometry for GFP positive cells. As shown in fig. 3.14 expression of GFP protein depended on the time of incubation and showed almost 6% positive cells from total corneal cell suspension after 20 h of incubation. Although a higher percentage of transduction would be desirable it was noted that the graft quality was inadequate after 20 h of LV incubation (Mr. Maurice Morcos personal communication). The corneas remained floppy, the endothelial cell layer was disintegrated and unacceptable changes to the epithelium were reported. In contrast, 4 h of incubation had a minor impact on corneal rigidity and the transduction efficiency resulted in 3% of GFP positive cells (Fig. 3.14). Therefore, in all subsequent experiments a 4 h incubation time was utilized.

To verify whether the above-mentioned conditions could be applied for *in vivo* studies, the microscopic examination of GFP transduced corneas was performed

28 days after syngeneic keratoplasty. A corneal button was explanted from a Lewis rat, transduced with LV.EGFP (2×10^4 TU/cornea) for 4 h, washed 3 times in PBS and transplanted to a Lewis recipient. Additionally, the quality of endothelium was checked by 4',6-diamidino-2-phenylindole (DAPI) staining before cornea transplantation. The second corneal button was incubated for 4 h incubation in medium and then the cell nuclei were visualized by DAPI and examined by fluorescent microscope. The endothelium cell layer remained intact and no endothelial cell loss was observed during dissection and incubation of the cornea (Fig. 3.15). Furthermore, GFP protein expression could still be detected 28 days after syngeneic transplantation in transduced corneas. GFP positive cells were distributed equally on the surface of endothelium (Fig. 3.16). These results indicate that the protocol might be applicable for *in vivo* studies and used as a method for local gene transfer into the cornea. The experiment was performed only once prior to the *in vivo* studies to confirm a long term expression of a transgene delivered by LV vectors and reported by others (107) and also to verify the intact endothelial layer after a corneal button removal procedure performed by a surgeon. This experiment could serve as a quality control for the *in vivo* studies and should be performed routinely in the future experiments.

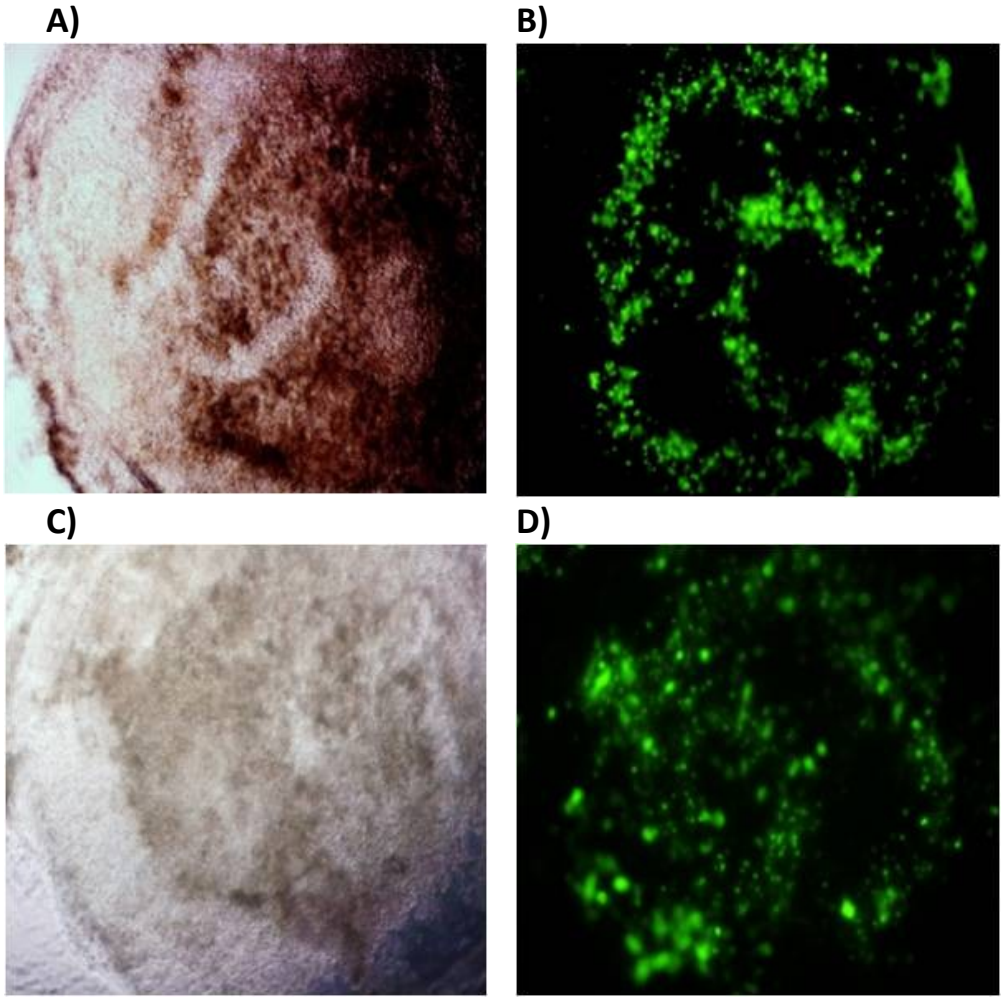

Fig. 3.13. *Ex vivo* cultured corneas transduced with LV.EGFP vector. The corneas were incubated with LV.EGFP viruses (1×10^5 TU/ml) for 24 h. The expression of EGFP protein was examined under fluorescent microscope. **A)** Light microscope image and **B)** Fluorescent image of the cornea 2 days after transduction; **C)** Light microscope image and **D)** Fluorescent image of the cornea 7 days after transduction. Representative images from at least 3 independent experimants are shown under 10x magnification.

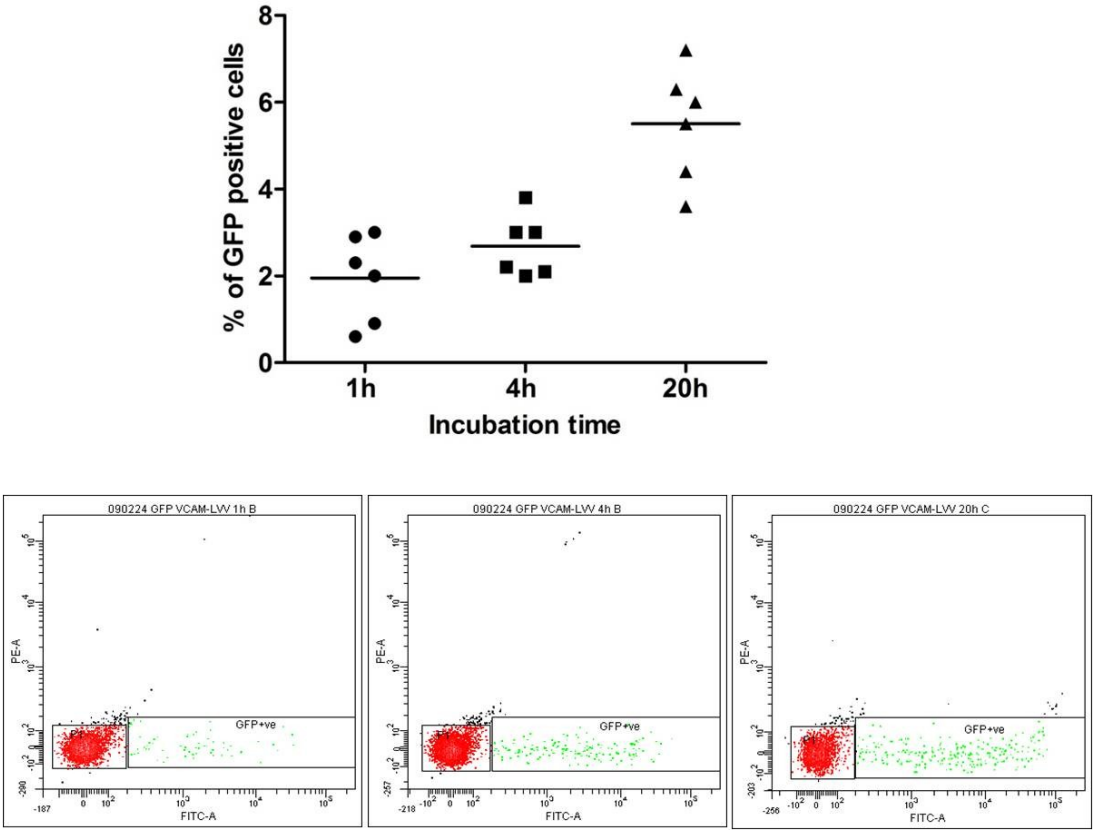

Fig. 3.14. Optimization of *ex-vivo* EGFP lentiviral transduction of donor corneas. A) Transduced corneas were digested after different time points and single cell suspensions were analyzed by flow cytometry for EGFP positive cells. Each data point represents one cornea. Untransduced corneas served as control and no EGFP positive cells were detected (data not shown). **B)** Representative flow cytometric profiles of EGFP positive cell analysis after 1, 4 and 20 h incubation of LV_{cmv}EGFP vectors with donor corneas.

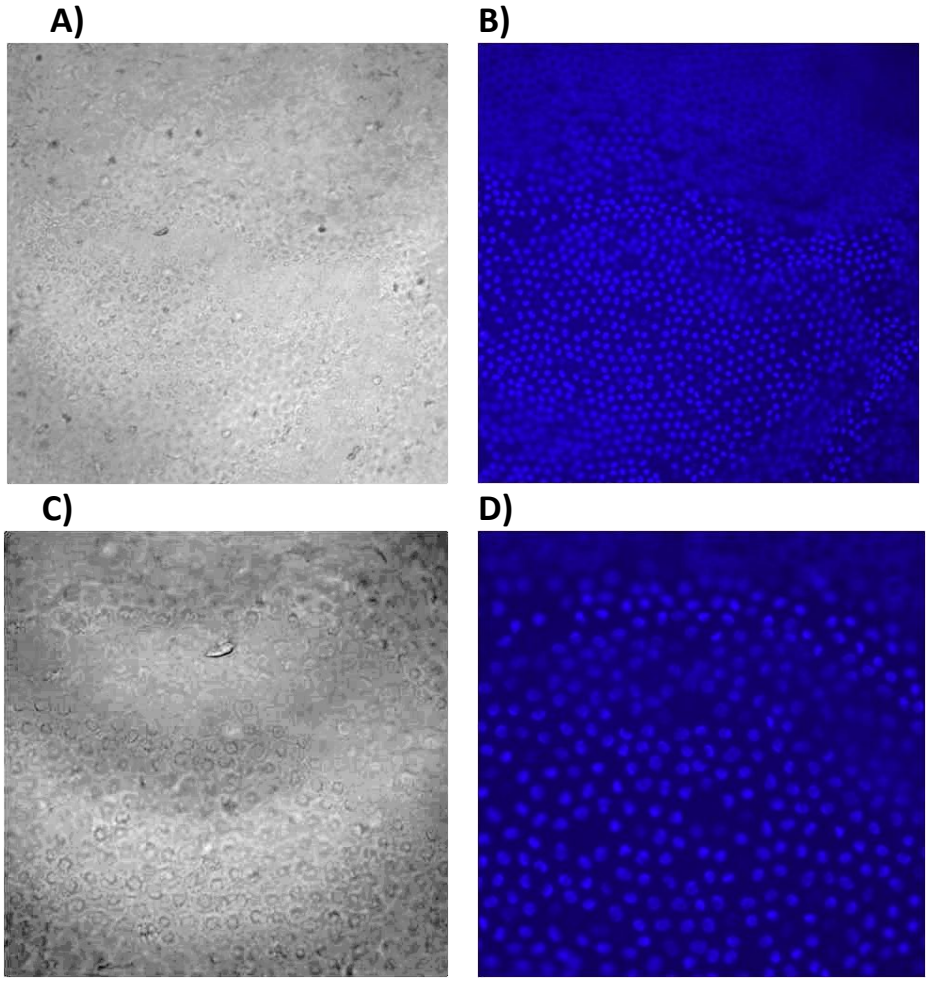

Fig. 3.15. Intact corneal endothelial layer after donor corneal button removal prior to transplantation. The cornea was stained *ex vivo* by DAPI to visualize the cell nuclei. Cells were distributed regularly. No cell loss was observed during preoperative cornea preparation. **A)** and **C)** Light microscope images of donor corneal endothelium under 20x and 40x magnification, respectively; **B)** and **D)** Fluorescent images of the same cornea under 20x and 40x magnification, respectively. (n=1)

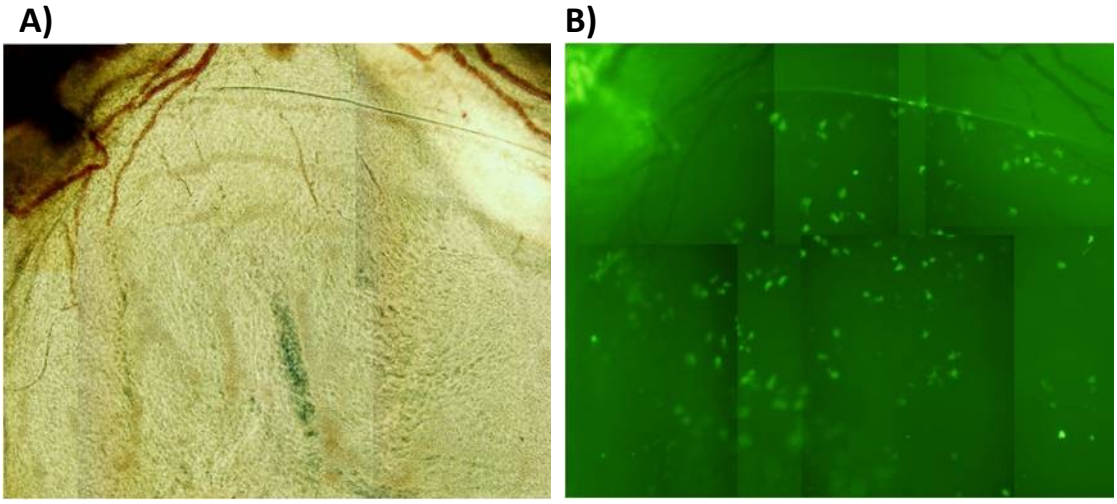

Fig. 3.16. Long-term expression of EGFP protein after syngeneic keratoplasty. Syngeneic cornea was transduced with LV.EGFP (2×10^4 TU/cornea) for 4 h, washed 3 times in PBS and transplanted. At 28 POD syngeneic graft was explanted and microscopic analysis was performed. **A)** Light microscopy image and **B)** fluorescent image of syngeneic graft is displayed (20x magnification). POD – post operative day.

3.2.5 *Ex vivo* LV-mediated gene transfer of NGF into the donor cornea

Although it was not possible to demonstrate that NGF protected HCECs from apoptosis in *in vitro* experiments, it was decided to proceed with *in vivo* studies. The rational for this was that HCEC, as an immortalized cell line, may have been resistant to the induction of programmed cell death. Furthermore, Ad-mediated NGF delivery to the cornea had previously been demonstrated to prolong allograft rejection (114).

The essential step towards determining a therapeutic effect of local NGF gene transfer was to analyze whether allograft rejection could be delayed by NGF overexpression. First, syngeneic keratoplasty (LEW to LEW, n=8) was performed which served as a control for the surgical procedure. As expected, there were no signs of rejection after syngeneic transplantation (Fig. 3. 17 A). Next, the time point of rejection and kinetics of untreated allografts were evaluated and monitored. The results revealed that the rejection process for corneal allografts in the Lewis-Dark Agouti (LEW-DA) model was rapid and occurred between 11 and 16 postoperative days (POD) with a median value of 14±1.3 (Fig. 3.17). Moreover, the rejection kinetics of the LV.EGFP treated controls were also included into the studies in order to analyze any vector-mediated adverse events. At first, syngeneic corneas were transduced with LV.EGFP vectors and transplanted into Lewis rats. Similarly to the control syngeneic group 100% of grafts survived (Fig. 3. 17 A). In contrast, the LV.EGFP-treated allografts rejected rapidly between day 11 and 14 with a median value of POD 11.5±1.4. Finally, LV_{ef}NGF vector was used to transduce donor corneas followed by keratoplasty. Corneal allograft rejection was detected at a median value of 15.0±2.0 days after surgery (range 12-21 days). The difference between untreated allogeneic controls and the LV.NGF treated group survival curves was not statistically significant (log-rank test: χ^2=2.0, p=0.15; Wilcoxon test: χ^2=1.4, p=0.23; excluding long term survivors), however, in comparison to LV.EGFP-treated animals there was a significant difference confirmed by two statistical tests (log-rank test: χ^2=4.0, p=0.045; Wilcoxon test: χ^2=4.9, p=0.027;).

Representative photographic images of transplanted corneas from all groups are shown in Fig. 3.18. Panel A and C show syngeneically transplanted corneas either untransduced or transduced with LV.EGFP, respectively. Both corneas did not display any sign of rejection throughout the observation period. In contrast, symptoms of rejection were observed between POD 11 and 16 in untreated allografts or LV.EGFP transduced corneas (Fig. 3.18 B, D). Both images demonstrate accelerated rejection of the transplanted corneas with no visibility of the anterior chamber. Similarly, LV.NGF transduced allografts are rejected with high opacity score 14 days postoperative (Fig. 3.18 E). The cornea was also highly neovascularised. Based on these results the experiments using NGF gene transfer to prolong corneal allograft survival were abandoned.

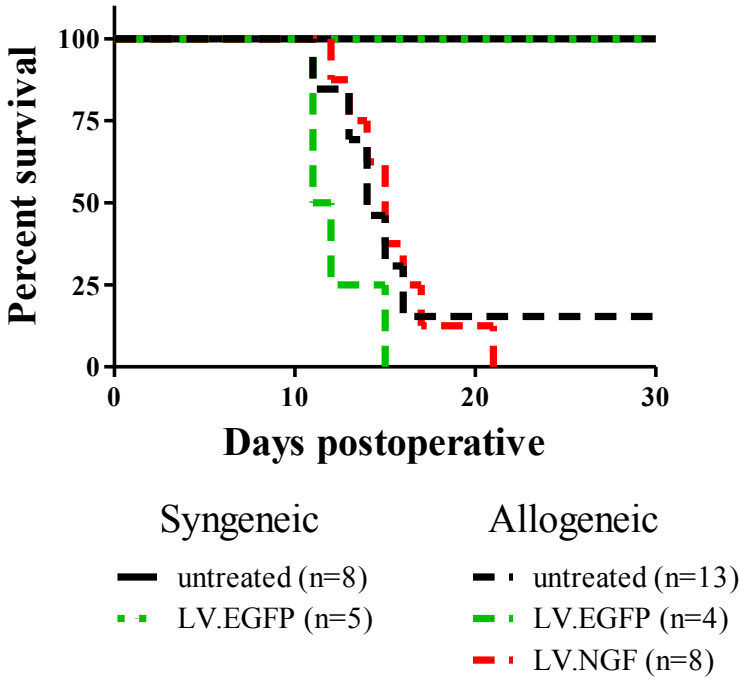

Fig. 3.17. The rejection kinetics of allografted corneas and syngeneic controls. The data presents the survival curves censored at day 30 (the end of the observation period) of untreated syngeneic (n=8) and allogeneic (n=13) controls. Additionally, the survival rates for LV.EGFP-treated syngeneic corneas (n=5), LV.EGFP-transduced allografts (n=4) and corneas transduced with LV.NGF vectors (n=8) are shown. There are no statistical difference between the untreated allogeneic control and LV.NGF-treated group survival curves (log-rank test: χ^2=2.0; p=0.15), however, the difference between the corneas transduced with LV.NGF vectors and LV.EGFP-transduced allografts is statistically significant (log-rank test: χ^2=4.0; p=0.045).

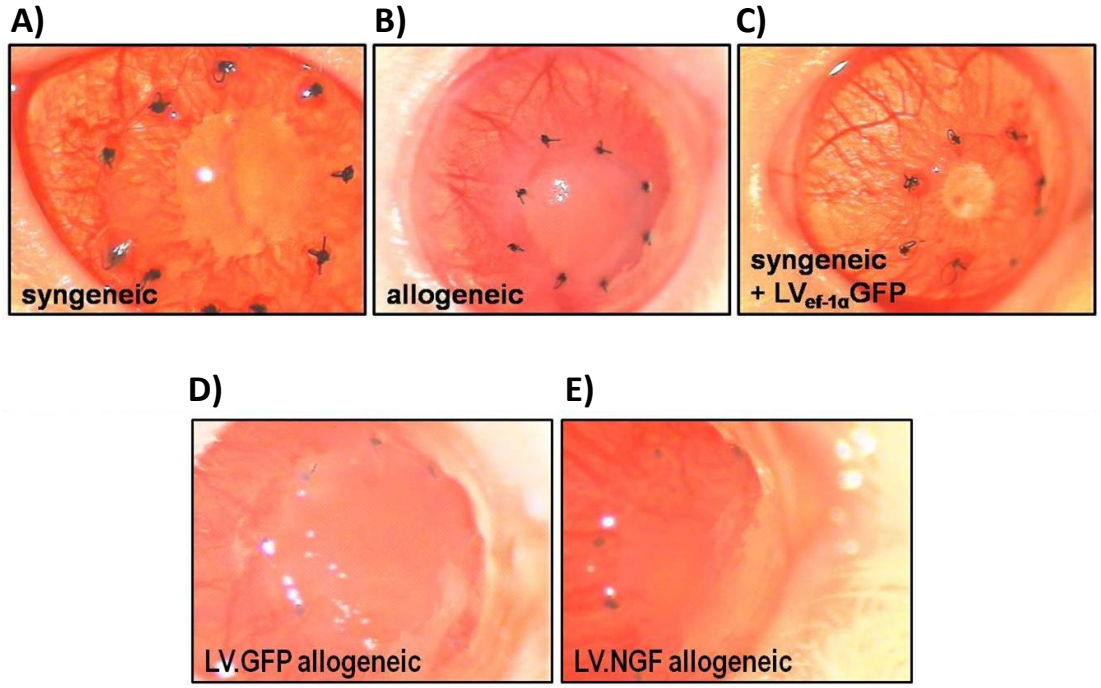

Fig. 3.18. Representative photographic images of transplanted corneas taken on day of rejection for allografts or on day 30 for syngeneic groups. A) syngeneic control (OP=0, NV=0); **B)** allogeneic control (OP=2.5, NV=2); **C)** syngeneic treated with LV.EGFP vectors (OP=0, NV=1); **D)** LV.EGFP-treated allograft (OP=3, NV=2); **E)** LV.NGF-transduced corneas (OP=3, NV=1). OP – opacity score, NV – neovascularization.

3.3 Discussion

In the first part of this chapter efficient cloning, expression and physiological activity of secreted nerve growth factor (NGF) after gene transfer both in target cells and corneal tissue was demonstrated. NGF gene expression was driven by two different promoters: human polypeptide chain the elongation factor - 1α (EF-1α) that drives ubiquitous expression of a constitutive gene responsible for the elongation of mRNA during translation and the human cytomegalovirus immediate early (CMV.IE) promoter that has been widely used as a standard promoter for many gene vector systems.

The choice of the transgene promoter determines the strength of transgene expression after gene delivery into target cells. There are several parameters that have to be considered during these experiments. The strength of gene expression may be a key factor to achieve a therapeutic outcome because many effects are dose dependent. It may also be necessary to tightly control the expression in some circumstances. For transplantation procedures it might be preferable to utilize inducible promoters that can be fully controlled and can activate gene expression only under specific time frame or conditions (e.g. rejection episode). In other conditions, however, such a constantly inflamed and vascularized corneal bed environment, constitutive expression may be desirable. It is believed that host-derived promoters may be less harmful and interfering to the cell machinery and, in contrast to promoter elements acquired originally from viruses, are not down-regulated *in vivo* (144). Additionally, tissue specific promoters restrict therapeutic gene expression to target sites and can further improve the safety and controllability of the delivered insert. The main risk factor which has to be assessed is the potential of promoter elements in integrative viral vector systems (e.g. lentiviral vectors) to trans-activate host neighboring genes. Indeed, it was shown in three different human cell lines that the gene expression driven by commonly used promoters EF-1α, CMV, SV40 and PGK located internally within integrative vectors may trans-activate host genes (145). Notwithstanding, the transcriptional strength of a promoter was correlated with its possibility to trans-activate neighboring

elements that may carry a significant risk of oncogenic events (145). Overall, it is very difficult to select a relatively safe promoter for an integrating vector with a universally good expression profile, which could be expected to minimize the risk of trans-activation and support adequate level of transgene expression.

Several promoters were tested for gene over-expression in the cornea, however, the most frequent promoter used in these studies and demonstrating the strongest transgene expression was the CMV immediate early promoter. Despite efficient Ad-mediated gene delivery to the corneal tissue and high level of transgene expression driven by CMV promoter, the reporter gene activity was transient and decreased after transduction (146, 147). The short-term expression may be explained by the observation that the CMV promoter transferred to the muscle tissues by Ad vector were transcriptional silenced by extensive methylation (148). However, stable transgene expression was reported in human corneal tissue for up to 60 days after transduction with a LV containing CMV promoter (1). The long-term expression of the GFP gene under the CMV promoter was also demonstrated after lentiviral-mediated delivery to the rat *ex vivo* cultured corneas (107). These results suggest that the CMV promoter element can be used for long-term and stable expression of the therapeutic gene in combination with integrative vector such as SIN HIV-1-based lentiviral vector. In contrary to the CMV promoter, the expression driven by the EF-1α promoter is consistent over time and is relatively independent from any physiological changes of the cell. As a housekeeping gene promoter in most cell types, it has high levels of activity and is not silenced during transcriptional process (149). The strong expression of GFP driven by the EF-1α promoter in the corneal endothelium was described after intracameral injection of the LV, however, the length and stability of expression was not determined (150). We have chosen to test both endogenous and viral promoters for LV-mediated gene transfer.

In this project expression of NGF after transfection or transduction with both vectors containing EF-1α or CMV promoters was confirmed in two different human cell lines and also in *ex vivo* cultured rat corneas. Transfected HeLa cells secreted significant and comparable amounts of NGF revealing that both constructs carry the insert under the functional promoter. This suggests that other gene regulatory

elements were not modified during the cloning procedure (Fig. 3.4). Furthermore, the fully functional LV_{ef}NGF and LV_{cmv}NGF vectors were generated and tested on HeLa cells (Material and Methods; section 2.2.3). Supernatants were collected after 48, 60 and 72 hours following 24h of transduction. Both vectors showed relatively high transgene expression. Interestingly, NGF expression driven by EF-1α promoter constantly increased over time, in contrast to CMV-controlled expression which increased only in the first 48 h and then remained unchanged (Fig. 3.5 A). In addition, other studies demonstrated a significant increase of protein product in time up to 72 h after Ad-mediated anti-apoptotic genes transfer whose expression was driven by CMV promoter (151). It has to be considered that different viral vectors are varying in transduction potential, tropism to broad range of cell types, utilization of cell machinery to replicate and as a consequence differ in doses used for the same experimental procedure which provides difficulties to compare the results.

NGF concentration was also determined after LV-mediated gene delivery to *ex vivo* cultured rat corneas as an *in vitro* organ culture model. A significant amount of NGF could be detected after treatment with both LV vectors 24 h after transduction and the concentration remained unchanged for the next 24 h (Fig. 3.5 B). However, NGF concentration was relatively low in comparison to previous results after Ad-mediated NGF delivery to rat cultured corneas (114). It is necessary to point out that the experimental conditions differ between these studies and a direct comparison is not adequate. The concentration of secreted NGF in culture supernatants was 6.88 ng/ml 3 days after Ad.NGF gene therapy and only 0.37 ng/ml 2 days after LV_{ef}NGF delivery (Fig. 3.5 B). Adenovirus vectors, as non-integrative vectors, are known to rapidly induce high level of transgene expression in corneal endothelium with peak expression already at day 3 in *in vivo* syngeneic murine corneal grafts (91). In contrast, LV-mediated transgene expression is delayed due to the time necessary for the integration process into the host genome (152). The maximum expression of enhanced yellow fluorescent protein (EYFP) in ovine corneas was reached by day 14 after LV-based gene delivery, however, this process may be species dependent (153). In addition, direct comparison of IL-10 mRNA level

in Ad-CMV-IL10 and LV-SV40-IL10 transduced ovine corneas following 4 days *ex vivo* culture revealed 10^3-fold higher expression of IL-10 mRNA in Ad-CMV-IL10 transduced corneas. Similarly, the IL-10 protein levels increased rapidly over the first 6 days after Ad-mediated gene delivery up to approximately 40-fold compared with the control corneas at day 15. In contrast, it was shown that there is a steady increase in IL-10 expression over the period of cornea culture after LV-SV40-IL10 transduction ending up in only 10-fold increase over the control cornea at day 15 (154). Overall, these results suggest that only a lower level of secreted therapeutic protein can be achieved after LV gene transfer to the cornea in comparison to Ad vectors and the transgene expression is delayed, however, stably increases over time. It should be also indicated that, despite a potential value of these studies, the different promoters were used (SV40 vs. CMV in previous study) and different viral vectors which makes the results difficult to compare. As it is known concentration of a therapeutic protein is of high relevance this could be a reason why prolongation of corneal allograft survival was not achieved after LV-mediated gene transfer.

Lastly, culture supernatants from transduced human corneal endothelial cells (HCEC) with LV.GFP and both LV.NGF vectors were collected to confirm physiological activity of secreted NGF protein. The functional assay is based on the unique ability of PC12 cells to differentiate into neuron-like cells in the presence of NGF. As expected, neurite outgrowth was observed in cells which were cultured in the supernatants from LV.NGF transduced HCEC but not from LV.GFP transduced endothelial cells. PC12 cells also differentiated into neuron-like cells when rNGF was added to the complete medium as a positive control (Fig. 3.6). These findings suggest that NGF secreted by transduced corneal endothelial cells with both LV vectors is physiologically active and may serve as the anti-apoptotic factor during immune-mediated endothelial cell loss. Indeed, the therapeutic potential of NGF is widely described in the literature (155) and PC12 cells act as well established model for investigating pro-survival mechanisms on neuronal-origin cells in response to NGF (143). To characterize the anti-apoptotic role of induced NGF on endothelial cells the immortalized HCECs were used as an *in vitro* model. PC12 cells served as

a reference cell line due to the large number of publications describing the inhibition of thapsigargin (TG)-induced apoptosis by NGF on these cells (143). In contrast to PC12 cells where the apoptotic manifestation including morphological changes, presence of sub-G1 population or active form of caspase-3 was detected already 24 h after TG treatment, HCEC cells showed delayed signs of apoptosis (Fig. 3.7). We could show that detection of endothelial apoptotic cells was possible after 48 h incubation with TG. However, HCEC cells cultured without serum were more predisposed to apoptosis and resulted in 6-fold increase in the number of cells with hypodiploid DNA content in comparison to untreated cells (Fig. 3.11). Despite the neuronal origin and presence of both surface NGF receptors neither recombinant NGF nor overexpressed NGF did protect HCECs from TG-induced apoptosis (Fig. 3.9-12). It is also possible that the level of NGF receptors expression on a surface of HCECs is not sufficient to initiate a signal transduction or this signal is blocked or modified downstream. To elucidate this problem it would be necessary to determine the comparative level of expression of NGF receptors in both PC12 and HCEC cell lines and also to investigate the signal transduction pathway downstream from NGF receptors. Exposure of HCECs to rNGF for various time periods and even additional doses of growth factor also did not reduce the number of apoptotic cells (Fig. 3.11). There are significant differences between immortalized HCEC and primary endothelial cells which were described elsewhere (111, 156). In primary human ECs, the percentage of apoptotic cells continuously increased over time in contrast to iHCEC which showed several spikes of enhanced apoptosis creating a wave-like pattern (111). Moreover, pHCEC showed a significant reduction of apoptosis from 63 to 24% when transduced with LV.Bcl-X_L. In iHCEC low level of apoptosis was achieved (15-20% of apoptotic cells) and no protective effect of anti-apoptotic protein Bcl-X_L was observed (156). This suggests that immortalized HCECs have strong inner pro-survival mechanisms and deregulated cell cycle which may mask the anti-apoptotic effects. Future work may analyze NGF effects on primary HCEC.

Despite the fact that supernatant with secreted NGF did not protect iHCECs from apoptosis, it showed considerable anti-apoptotic effects on PC12 cells significantly

reducing the number of sub-G1 (apoptotic) cells (Fig. 3.10 A and C) as well as markedly inhibiting caspase-3 activation (Fig. 3.12 A) and preserving the healthy cell morphology (Fig. 3.8). This neuroprotective effect of LV-mediated NGF gene delivery might be a potential therapy for many neurodegenerative diseases as PC12 cells are frequently used as a model for studies on the action of NGF on apoptotic mechanisms in neuronal cells (157). Indeed, there are already several clinical trials on different neurodegenerative diseases that utilize viral vector-mediated NGF delivery as a potential therapeutic strategy (158, 159). It was reported that LV.NGF delivery to the basal forebrain of aged primate significantly restored cholinergic neuronal markers to levels of young monkeys. These findings can be used as a potential treatment to protect degenerating cholinergic neurons in Alzheimer's disease (160). A phase 1 clinical trial of NGF therapy on Alzheimer's disease also suggested an improvement in the rate of cognitive decline after implantation of autologous fibroblasts genetically modified to express NGF into a forebrain of 8 individuals with mild Alzheimer's disease (161).

As described before integrity of corneal endothelial layer was better preserved in Ad.NGF transduced rat corneas in comparison to control grafts 12 days after transplantation. In addition, Ad-mediated NGF gene transfer resulted in significant prolongation of allograft survival (114).

In order to investigate whether LV-mediated NGF gene therapy may achieve similar therapeutic outcome, but without known adverse effects of Ad gene transfer, optimization of gene delivery with LV was performed. Similarly to other reports, LV vector transduction of *ex vivo* cultured corneas resulted in strong expression of the reporter gene which was equally distributed among endothelium and maintained at least 7 days after gene delivery (Fig. 3.13). Furthermore, the optimal time of virus transduction of *ex vivo* cultured corneas was obtained. Although, corneal buttons can be stored for extended periods of time compared to other organs, the quality and viability of endothelial cells decrease over time which may result in graft failure (110). For the first time the kinetics of reporter GFP gene expression in *ex vivo* cultured corneas was assessed by whole graft flow cytometry analysis for GFP positive cells. The most often selected incubation times for murine corneal

transduction with LV vectors are: either short transduction time (between 3 and 6 h) (153) or long incubation time (over-night up to 24 hours) (107). Our study show that there is a time-dependent increase in GFP-positive cells (Fig. 3.14), however, the corneas remained floppy, endothelial cell layer was disintegrated and unacceptable changes to the epithelium were reported after 20 h of incubation. The 4 h incubation time point had only a minor impact on corneal rigidity and was therefore chosen for further studies. This observation is in agreement with results published by Fuchsluger *et al.* where a significant increase of apoptotic endothelial cells over time of transduction was reported (110).

To avoid graft failure incidents due to inadequate endothelial quality after pre-operative manipulation the integrity of the endothelial layer was assessed under the fluorescent microscope by cell nuclei visualization. The results revealed that the 4 h incubation period had no impact on endothelial cell number or their morphology (Fig. 3.15). In addition, syngeneic grafts transduced with LV.GFP survived without any rejection episode and were similar to untreated control grafts. The graft transparency and lack of corneal edema suggests that the endothelium was fully preserved during *ex vivo* manipulation and after transplantation (Fig. 3.17 and 3.18). Moreover, strong GFP expression was still detectable in syngeneic grafts 28 days after keratoplasty (Fig. 3.16). It has previously been reported that syngeneically grafted corneas are able to express EGFP protein up to 8 weeks after transduction with LV vectors (107).

There are few studies showing successful gene transfer to the corneal endothelium mediated by LV vectors, however, the conditions and efficacy of transduction as well as the species used, differ between experimental settings. Using the EIAV.IDO vector, Beutelspacher and colleagues demonstrated significant prolongation of murine corneal allograft survival after 1 h *ex vivo* incubation in 250 µl of the virus vectors at an MOI of 100 (102). Despite prolonged graft survival the transduction efficiency was not assessed. Over-expression of IDO after transplantation was quantified by real-time PCR in both syngeneic and allogeneic grafts. In the other studies *ex vivo* cultured corneas were incubated overnight in optisol-GS containing 6 µg/ml of polybrene and 1×10^7 IU/ml of lenti-IZsGreen or lenti-IZsGreen-xL or

5.5×10^6 IU/ml lenti-EGFP (107). The transduction efficiency of the vector was determined for syngeneically transplanted murine corneas at week 1 and 8 showing 15% of infected cells for both observation periods. Kinetics of transgene expression and efficiency of transduction after LV-mediated gene transfer was investigated using human corneas (110). It was demonstrated that the transgene expression was detected 48 h after cornea transduction. Only 1 h incubation resulted in more than 80% of reporter gene positive cells, however, longer exposure to the virus only modestly increased the transduction efficiency and led to endothelial cell apoptosis. The corneal transduction was conducted at 37˚C with 3×10^5 IU/ml of lenti-CMV-MCS-IZsGreenW in Biochrome Cornea Medium I in the presence of 8 mg/ml polybrene. The authors also assessed transgene expression under hypothermic (4˚C) conditions demonstrating no major differences between corneal donor-tissue storage conditions. Interestingly, the hypothermic conditions were indicated as more applicable for Ad-mediated gene transfer to the murine cornea. The *in vivo* GFP expression in murine corneal grafts transduced at 4˚C resulted in much stronger expression compared to those grafts transduced at 37˚C (91). Taken together and in agreement with other observations the *ex vivo* cornea transduction protocol established during these studies may be a suitable method for local gene transfer into the rat cornea, however, due to the differences between experimental set-ups and protocols that are used by scientists and also different methods of determining efficiency of transduction, it is difficult to compare the results of individual studies.

In order to test the main hypothesis of this chapter the effect of local NGF over-expression on corneal allograft survival was examined. As shown in Fig. 3.17 local LV.NGF gene transfer did not prolong corneal allograft survival *in vivo*. This is in contrast to previous reported work showing that Ad-mediated NGF gene transfer resulted in a delayed rejection process (Ad.NGF MST 16.8 ± 1.4 vs. Ad.β-Gal MST 13.3 ± 0.3) and showed a protective effect on corneal endothelium (114). As stated before single NGF treatment could be applied as a supplementary therapy for other immunomodulatory therapies such as CTLA4.Ig to improve endothelium integrity and overall add benefits to the cornea transplantation (114). In contrast to Ad.NGF

gene transfer, transduction of the cornea with LV vectors resulted in much lower concentrations of secreted NGF which may be a key factor for therapeutic success. Interestingly, it was shown that either the level of IL-10 mRNA or secreted IL-10 protein after LV.IL-10 corneal transduction was greatly less than expression driven by an analogous adenoviral vector. As a consequence, median graft survival was prolonged by only 7 days after LV.IL-10 transduction versus a median prolongation of 35 days when Ad-CMV-IL10 was used to transduce ovine donor corneas (154). Additionally, the kinetics of gene expression driven by LV vectors was delayed which might decrease a potential therapeutic effect of overexpressed transgene by skipping the important time point in rejection process. Similarly, too little NGF concentration, too late after transplantation might diminish the protective role of NGF on the corneal endothelium.

To fully understand the potential anti-apoptotic properties of NGF on corneal endothelial cells it would be necessary to perform the experiments on the primary corneal endothelial cells. These cells are more vulnerable to stress condition such as induced apoptosis (156) and the cytoprotective effect of NGF could be detectable. Also the expression level of NGF receptors and the signal transduction pathway would be more similar to physiological conditions and the potential anti-apoptotic effect could be evaluated at the molecular level.

The efficiency of LV production or level of NGF expression can be improved by optimization of both protocols. As mentioned before corneal transduction conducted in Biochrome Cornea Medium I in the presence of 8 mg/ml polybrene for only 1h resulted in more than 80% of transduced cells. Currently, to my knowledge it is the most efficient protocol for the *ex vivo* cornea transduction.

It was reported that NGF together with other neurotrophins are present in the aqueous humor. However, in this study the NGF concentration after LV-mediated gene delivery was not determined. To better control the *in vivo* experiment it would be necessary to evaluate the NGF concentration after gene delivery and to determine a kinetics of NGF expression postoperatively.

Finally, investigation of a low risk (uninflamed) model of cornea transplantation and a low-responder characteristics of the strain combination (78, 162) could be

beneficial to study prolongation of the cornea allograft survival and the anti-apoptotic properties of NGF. It is possible that a rapid rejection and infiltration of the lymphocytes to the graft could mask an anti-apoptotic effect of NGF. On the other hand, a moderate rate of rejection may cause less damage to the corneal endothelium and reveal cytoprotective effect of NGF.

Taken together, the receptors for NGF were detected in all corneal cell layers (epithelium, stroma and endothelium) in both human and rat corneas as well as in immortalized corneal cell lines (127, 128, 141). It is well documented that NGF can be used as a therapeutic agent for accelerating corneal epithelial healing process (128). In addition, NGF can act as an anti-apoptotic agent promoting human corneal epithelial cell survival from hyperosmolar-stress induced apoptosis (141). Moreover, Ad-mediated NGF delivered to the cornea improves corneal graft survival and demonstrates cytoprotective properties (114). All these findings support the hypothesis that LV.NGF treatment could have a beneficial effect on corneal healing and maintenance of endothelium integrity after keratoplasty, however, further studies are required.

Chapter 4:

Role of lentivirus-mediated overexpression of programmed death-ligand 1 on corneal allograft survival

4 Role of lentivirus-mediated overexpression of PD-L1 on corneal allograft survival

4.1 Introduction

The T-cell co-stimulatory pathways are important therapeutic targets for tolerance induction and allogeneic graft survival. It was shown that rejection of transplanted allogeneic tissues can be mediated by negative co-stimulatory pathways (163, 164). Currently, the best described inhibitory receptors that critically regulate peripheral T-lymphocyte activity are: cytotoxic T lymphocyte antigen 4 (CTLA-4) (165) and programmed death 1 (PD-1; CD279) (166). Despite the fact that both receptors limit T-cell functions, their roles are not overlapping. CTLA-4 attenuates T cells in lymphoid structures early during T cell development, while PD-1 acts later, within tissue-specific sites for maintaining long-term tolerance (167).

The relevance of PD-1 signaling for lymphocyte inactivation and tolerance induction was shown by development of lymphoproliferative and autoimmune disease in PD-1 deficient mice (168-170). PD-1 is described as an inhibitory receptor found on the surface of activated B and T cells, thymocytes and myeloid cells (166, 170). Programmed death-ligand 1 and programmed death-ligand 2 (PD-L1 and PD-L2) are known ligands for PD-1. Both are type 1 transmembrane proteins belonging to the B7 family (171, 172). PD-L1 has been detected on lymphoid cells including monocytes, antigen presenting cells and B cells, as well as in non-lymphoid tissues such as the heart, lung, placenta, kidney, liver and cornea (173, 174). In contrast, PD-L2 is expressed exclusively on dendritic cells and monocytes (172, 173). The negative co-stimulatory pathway PD-1/PD-L1 (and/or PD-L2) has been considered as a potential target for therapeutic intervention in organ transplantation due to its role in T-cell inhibition and induction of long-term peripheral tolerance. Although systemic application of a chimeric PD-L1.Ig and PD-L2.Ig fusion protein did not induce significant prolongation of mouse cardiac allograft survival, injection of PD-L1.Ig in combination with immunosuppressants (cyclosporin A or rapamycin) led to enhanced survival of the graft (175). Interestingly, Watson et al. demonstrated that

systemic PD-L1.Ig treatment of mice receiving fully MHC-mismatched corneal allografts prolonged transplant survival (176). The expression of endogenous PD-L1 plays an important role in the regulation of T cells, which home to the cornea by modulation of specific chemokines and chemokine receptors, as shown by using PD-L1 deficient mice or PD-L1 blocking antibody in a model of dry eye syndrome (177). Human corneal endothelial cells can negatively regulate CD4+ T-cell proliferation by a cell contact mechanism that is dependent on PD-L1 and PD-1 interaction (178). Moreover, a recent study illustrated that expression of PD-L1 on multiple myeloma cells attenuated therapeutic efficacy with specific cytotoxic natural killer (NK) cells (179). It has to be considered that for potentially immunogenic tumors the stable expression of PD-L1 can serve as a mechanism to escape from host immune response (180). It is known that expression of PD-L1 is transiently induced by inflammatory stimuli by various of cells including corneal endothelium, however, in a chronic inflammation environment a continuous expression of PD-L1 might promote carcinogenesis (181, 182).

In summary, previous observations led us to investigate the role of PD-L1 overexpression in corneal cells to prolong corneal allograft survival, without the need for general immunosuppression.

4.2 Results

4.2.1 Local overexpression of PD-L1 leads to prolongation of corneal allograft survival

A lentiviral vector encoding for rat PD-L1 (LV.PD-L1) under the control of the ubiquitin-promoter was generated from mRNA isolated from rat heart tissue by Dr. Mikhail Nosov. LV.EGFP served as vector control. First, we wanted to answer the question whether LV vector would lead to an overexpression of the therapeutic construct in our target tissue. For this, rat donor corneas were collected, transduced *ex vivo* with either LV.EGFP or LV.PD-L1 and transplanted into syngeneic recipients. We could show by real-time RT-PCR analysis that high levels of either EGFP or PD-L1 mRNA was expressed in donor corneas on day 7 after transplantation (Fig. 4.1 A). To confirm that elevated levels of PD-L1 expression was due to LV-transduction and not as a result of endogenous up-regulation of PD-L1 expression on ocular cells under inflammatory conditions (115), RT-PCR with LV.PD-L1-specific primers was performed. Up-regulation of PD-L1 mRNA was only observed in LV.PD-L1 transduced corneas and not in LV.EGFP transduced corneas indicating the specificity of the approach (Fig. 4.1 B). These results confirmed successful process and generation of LV.PD-L1 vectors. As expected, LV.PD-L1 effectively transduced donor corneas thereby demonstrating that they can be used for further experiments. To confirm the PD-L1 expression on the cell surface flow cytometry was performed, however, due to the lack of specific rat anti-PD-L1 antibodies and a low cross-reactivity of rat PD-L1 with mouse anti-PD-L1 antibodies the results were ambiguous.

In order to determine the influence of PD-L1 overexpression on allogeneic corneal graft survival the survival rates of grafts were evaluated and presented as Kaplan-Meier survival plots (Fig. 4.2 A). Corneal opacification was assessed and recorded every second day until either the graft rejected or until the end of the observation period (POD 30). Both untreated syngeneic grafts or syngeneic grafts transduced with LV.EGFP survived until POD 30. In contrast, both corresponding allogeneic groups (i.e. untreated and LV.EGFP transduced) were rapidly and uniformly

rejected. Importantly, 5 out of 6 LEW animals (83%) that received the LV.PD-L1 transduced DA corneas did not reject their allografts and this remained the case until the end of the observation period (up to POD 30). Moreover, the mean value of opacity decreased gradually from 2.7 on day 21 to 1.3 at POD 30 (Fig. 4.2. B). In comparison, both allogeneic control groups reached the highest opacity score on the day of rejection, whereas syngeneic control grafts were transparent and only showed minimal levels of post-op opacity. These data were confirmed by histological analysis of corneal grafts which were harvested on POD 14 and 30. Untreated allogeneic control corneas showed a high number of infiltrated cells on day 14, however, inflammatory cell infiltration into LV.PD-L1-treated corneas (Fig. 4.3 C) was substantially lower compared to both untreated corneas (Fig. 4.3 A) and LV.EGFP-transduced grafts (Fig. 4.3. B). Moreover, the number of inflammatory cells in the stroma of LV.PD-L1-transduced corneas was reduced at POD 30 (Fig. 4.3 E). The untreated, transparent syngeneic graft served as a control (Fig. 4.3 D). Additionally, the thickness of the allogeneic corneas on POD 14 was compared between the groups. Histological analysis revealed significantly reduced edema development and corneal thickness in the LV.PD-L1 treated group in comparison to untreated or EGFP transduced corneal grafts (Fig. 4.4). Overall, these results strongly suggest that local overexpression of PD-L1 attenuates rejection and prolongs graft survival, without fully protecting the allogeneic cornea from cell infiltration and opacity development.

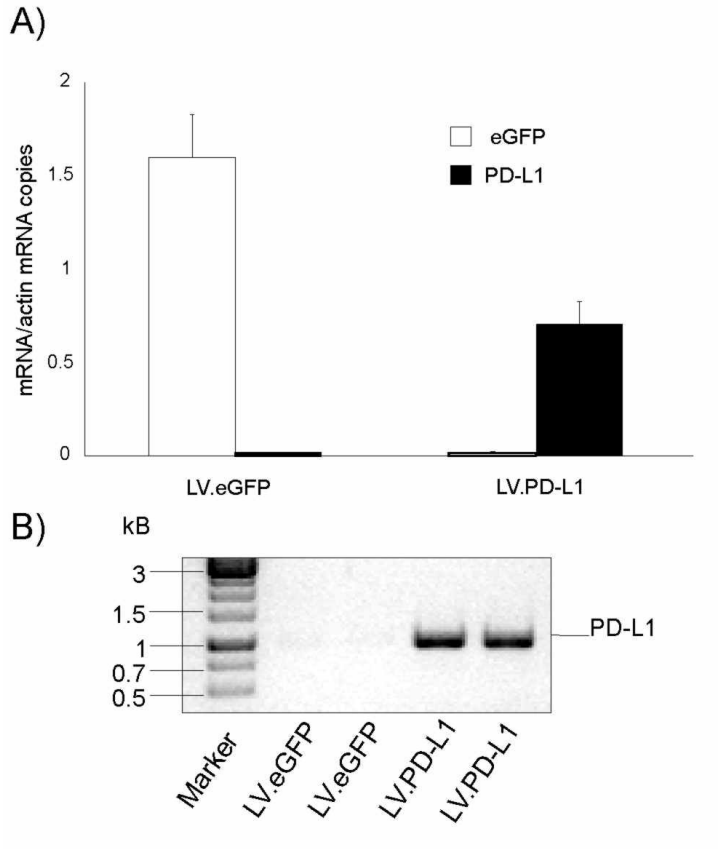

Fig. 4.1. Detection of lentivirus-mediated overexpression of PD-L1 in syngeneic transplanted corneas. A) mRNA expression levels of EGFP and PD-L1 in corneas transduced by LV.EGFP or LV.PD-L1 7 days post transplantation as measured by real-time RT-PCR. **B)** Conventional PCR for the detection of lentivirally transferred PD-L1 in transduced corneas with specific primers for LV-mediated PD-L1 expression.

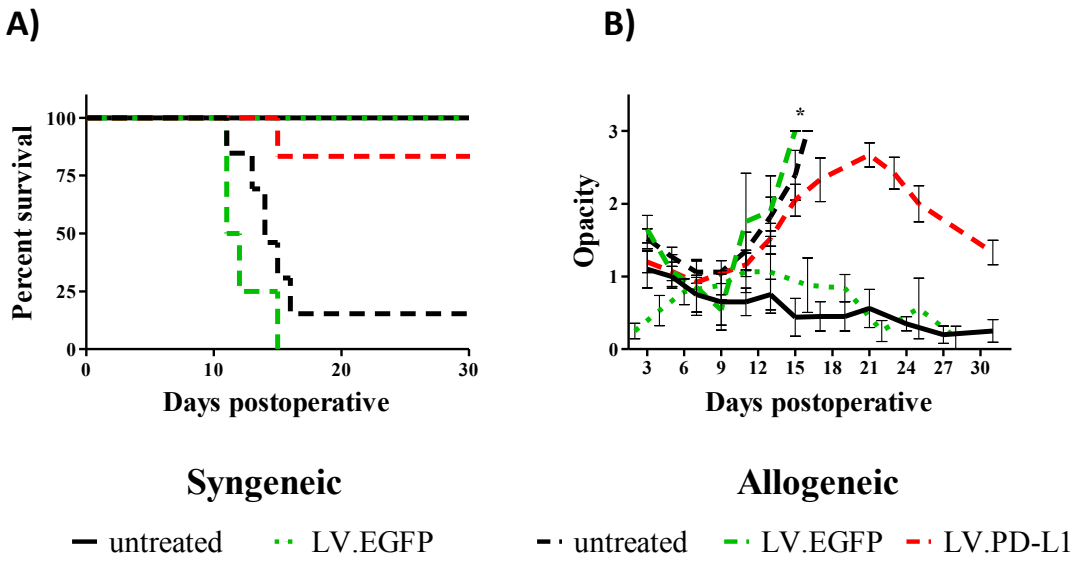

Fig. 4.2. Lentivirus-mediated overexpression of PD-L1 in cultured corneas led to prolongation of corneal allograft survival. A) Graft survival curves of syngeneic control (n=8) or LV.EGFP transduced corneas (n=5), allogeneic control (n=11), LV.EGFP (n=4) and LV.PD-L1 (n=6) transduced corneas up to day 30 after transplantation. **B)** Opacity score of the same allografts transplanted with syngeneic control, LV.EGFP transduced corneas and allogeneic control, LV.EGFP and LV.PD-L1 transduced corneas. *p≤0.05

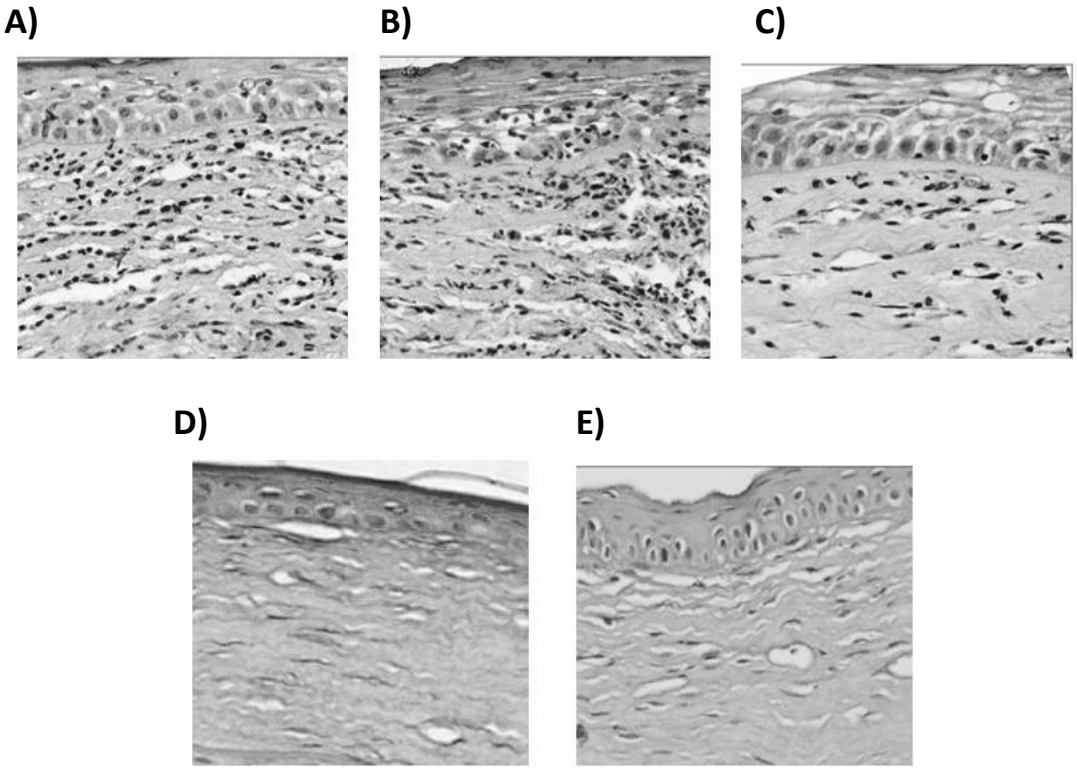

Fig. 4.3. Haematoxylin-Eosin staining of corneal tissue sections showing cell infiltration.
A) allogeneic control; **B)** LV.EGFP; **C)** LV.PD-L1 – transduced corneas on day 14 and **D)** syngeneic control; **E)** allogeneic LV.PD-L1 transduced corneas on day 30 after transplantation. Allogeneic control corneas showed a high number of infiltrated cells on POD 14, however, the infiltration into LV.PD-L1-treated corneas was substantially lower than into untreated corneas or LV.EGFP-transduced grafts. Also the number of infiltrating cells in the stroma of LV.PD-L1-transduced corneas was decreased at POD 30. Representative images from at least 3 animals per group are shown.

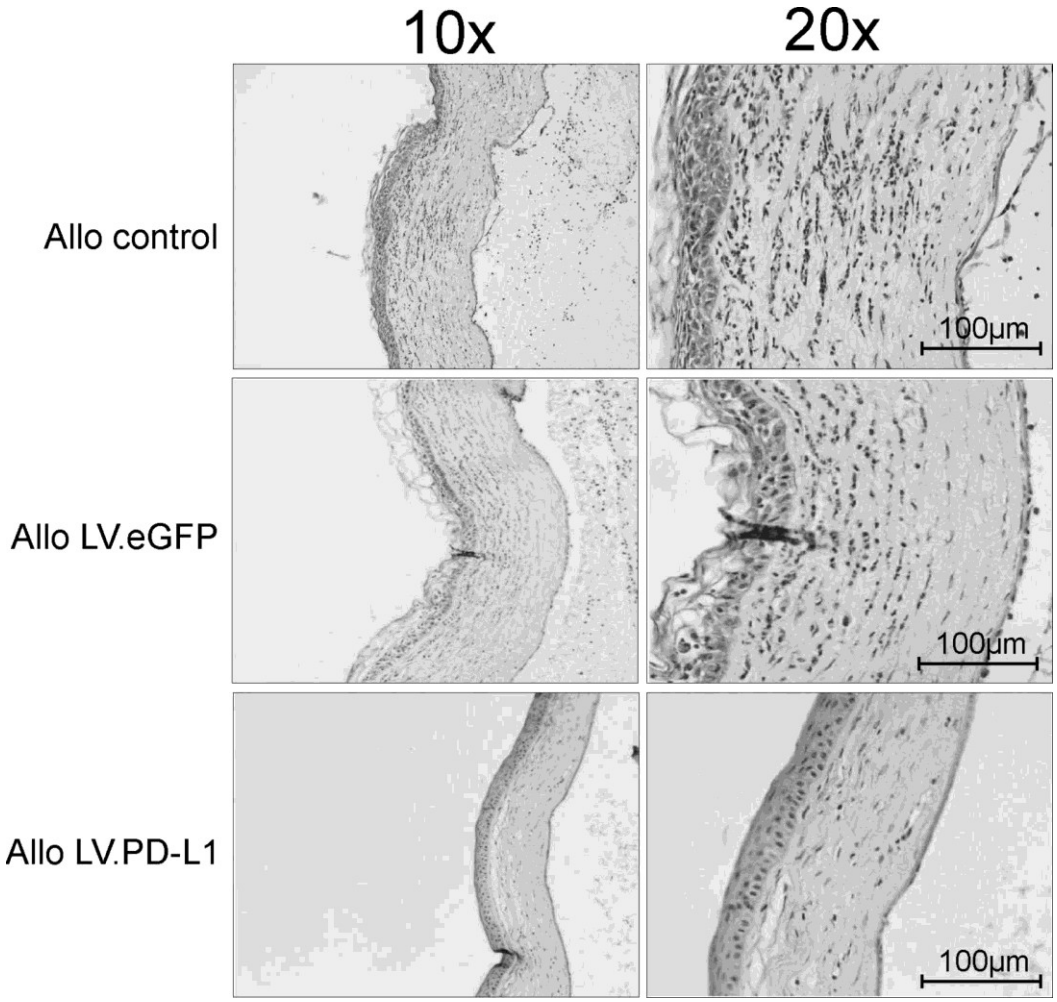

Fig. 4.4. Haematoxylin-Eosin staining of corneal tissue sections showing edema development. Haematoxylin-Eosin staining of tissue sections of allogeneic control, LV.EGFP or LV.PD-L1 transduced corneas on day 14 after transplantation. Representative images in 2 magnifications (10x and 20x) are shown. Histological analysis revealed significantly reduced edema development and corneal thickness in the LV.PD-L1 treated group in comparison to untreated or EGFP transduced corneas. Representative images from at least 3 animals per group are shown.

4.2.2 Flow cytometric characterization of immune cells from transplanted animals

In order to study the influence of PD-L1 overexpression on inflammatory cell populations within the allografts, allogeneic transplants were collected from three experimental groups at a time-point corresponding to the average day of rejection of the control group (between day 13 and 14). Inflammatory cells were isolated from explanted corneas by collagenase digestion and analyzed by flow cytometry as described previously (78). Moreover, cells from ipsi-lateral and contra-lateral submandibular and superficial cervical LNs and PBMCs were collected from the same animals and subjected to flow cytometric analysis. Several different populations that may participate in cornea allograft survival after *ex vivo* LV.PD-L1 treatment were analyzed.

4.2.2.1 Role of local overexpression of PD-L1 on NK/NKT cell population

As mentioned previously not only are $CD8^+$ T cells, NK and NKT cells present in the aqueous humor two days post-op, but their numbers continue to increase until rejection occurs. Several studies have shown that each of these cell populations might be involved in corneal graft rejection (76, 77).

Firstly, CD8+ T cell subsets were evaluated based on the expression of CD161 (NKRP1 in rodents). The analysis was performed on cells from rejecting graft recipients and the staining strategy is presented in Fig. 4.5. Lymphocytes from analyzed tissues were discriminated for CD3+ and CD3- populations (Fig. 4.5 B, C upper panels). Further gating within CD3+ group of CD8 vs. CD161 scattered three subtypes of CD8+ populations based on the CD161 staining intensity: CD8+CD161- subpopulation, CD8+CD161+ cells and a minor subtype of CD161++ T cells (Fig. 4.5 B lower panel). These CD8+ T cell subpopulations were also described elsewhere (183, 184). Flow cytometric analysis of CD161 expression on CD3-CD8+ population defined two distinguishable subsets which were mostly present in rejecting corneas: a major subset of CD3-CD8+CD161+ and a minor subset of CD3-CD8+CD161++ (Fig. 4.5 C lower panel). The latter population was also observed in PBMCs with relatively

high frequency (~7%) and in ipsi-lateral and contra-lateral LNs with less than 1% of CD3-CD8+ population. Overall, a significantly higher frequency of CD3+CD8+CD161+, CD3-CD8+CD161+ and CD3-CD8+CD161++ cells which correspond to NKT, NK and activated NK cells, respectively, were observed in rejecting control corneas when compared to their presence in the LNs and PBMCs (Fig. 4.6 and 4.7).

Further analysis of CD8+ subpopulations between experimental groups indicated that the frequency of CD3+CD8+CD161+ cells was significantly reduced from 18.7±5.8% in control or 15.5±2.0% in LV.EGFP transduced allografts to 10.4±1.7% in LV.PD-L1 transduced corneas (Fig. 4.6 upper panel). This reflects an overall reduction of 44% in graft infiltration by this particular cell population. A significant reduction of infiltrating cells in LV.PD-L1 transduced corneas was also found in the CD3+CD8+CD161- (cytotoxic T cells) compartment. The frequency of cells was reduced from 5.9±2.1% in control and 6.5±1.2% in LV.EGFP transduced allografts to 2.9±0.9% in LV.PD-L1 transduced corneas (Fig. 4.6 upper panel). Finally a profound, albeit not significant, reduction in CD3-CD8+CD161+ (NK cells) cells was observed in LV.PD-L1 transduced corneas compared to untreated and LV.EGFP transduced corneas. In addition, activated NK cell (CD3-CD8+CD161++) frequency was elevated in allogeneic control and LV.EGFP treated corneas but not in LV.PD-L1 transduced grafts (Fig. 4.7 upper panel).

No significant differences in cellular distribution were observed in our analysis of LNs and PBMCs (Fig. 4.6 and 4.7 lower panels) which was not unexpected due to the nature of the local gene therapeutic application.

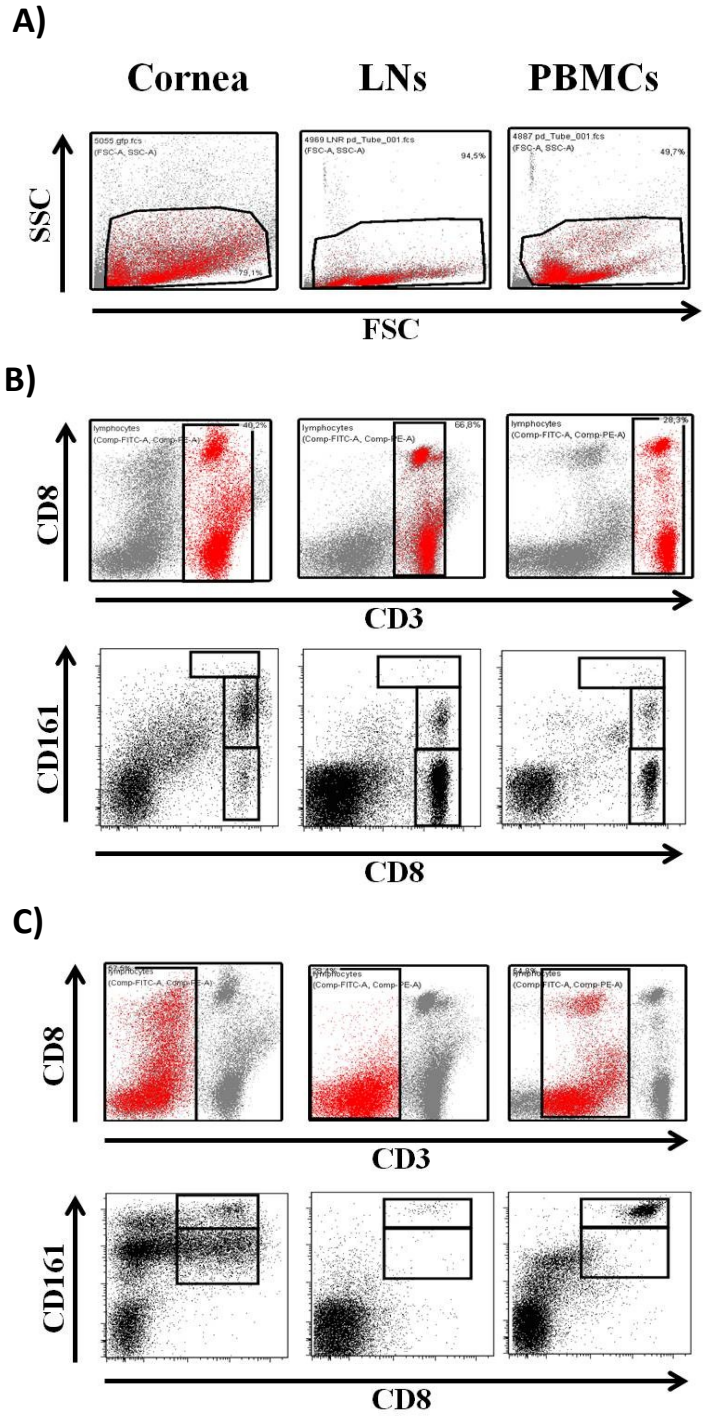

Fig. 4.5. Gating strategy of NK/NKT cell subpopulations. The cell subpopulations were analyzed on POD 14 in allografts, ipsi- and contralateral lymph nodes and PBMCs. **A)** FSC vs. SSC gate distinguish lymphocytes; B) Upper panel: CD3+ subpopulation of cells; Lower panel: analysis of CD161 expression on CD8+ T subpopulation; C) Upper panel: CD3- subpopulation of cells; Lower panel: two different subtypes of CD3-CD8+ subpopulation.

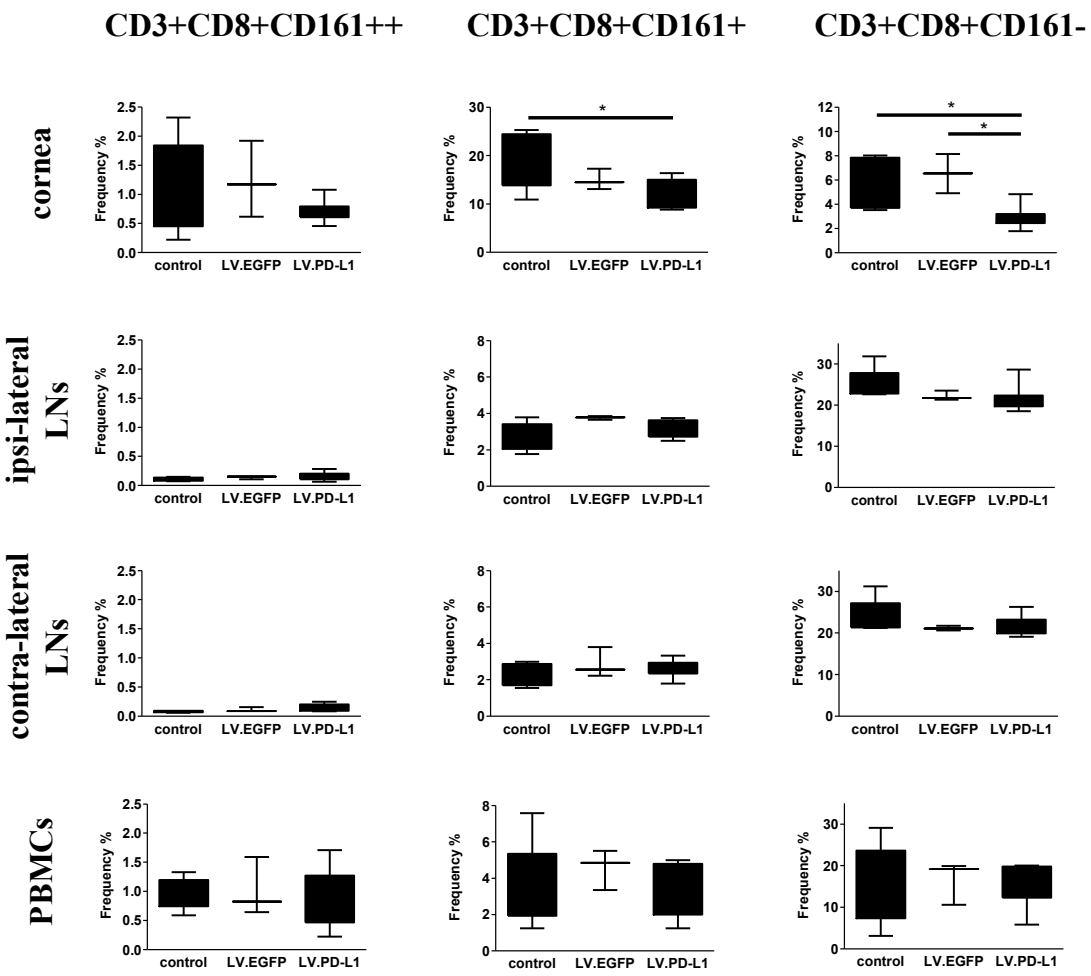

Fig. 4.6. Analysis of CD161 expression on CD8+ T cells. Frequency of different subpopulations of CD8+ T cells in transplanted corneas, both LNs and PBMCs from allogeneic control (n=5), LV.EGFP (n=3) and LV.PD-L1 (n=7) groups as shown as the percentage from CD3+ cells; * p≤0.05.

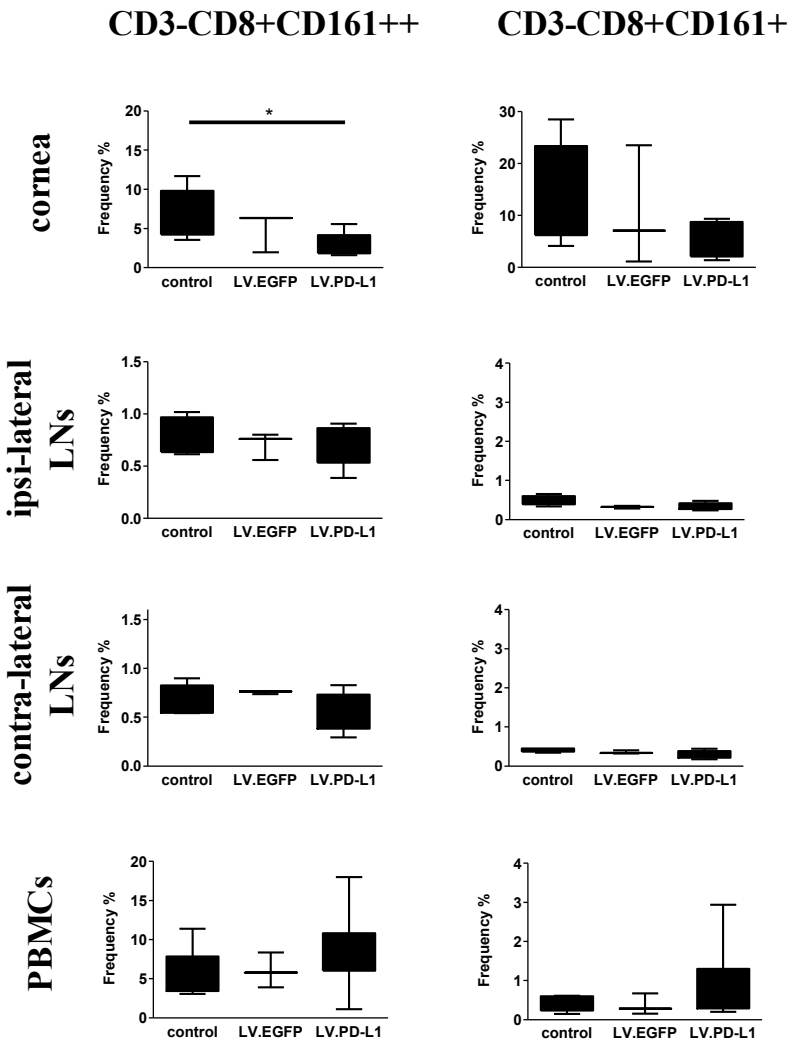

Fig. 4.7. Analysis of CD161 expression on CD3-CD8+ subset of lymphocytes. Frequency of different subpopulations of CD3-CD8+ cells in transplanted corneas, both LNs and PBMCs from allogeneic control (n=5), LV.EGFP (n=3) and LV.PD-L1 (n=7) groups as shown as the percentage from CD3- subset; * p≤0.05.

4.2.2.2 Role of local overexpression of PD-L1 on CD4+ T cell population

Several studies have shown that rejecting corneal grafts are infiltrated by many cell types including neutrophils, macrophages and lymphocytes, within which CD4+ T cells play a major role in mediating corneal graft rejection (62, 63, 72).

In order to delineate the impact of PD-L1 overexpression on CD4+ T cells, the changes in this subpopulation were analyzed in corneal grafts, LNs and PBMCs. The frequency of CD4+ T cells was compared between the experimental groups. As before, the gating strategy used for analyzing CD4+ T subsets is presented in Fig. 4.8. Interestingly, there were no significant changes between allogeneic controls and the PD-L1 transduced group in all analyzed organs. Moreover, the frequency of CD4+ T cells remained similar, approximately 40% of leukocytes being present in donor corneas, lymph nodes and PBMCs (Fig. 4.9 left panel). Similarly, the percentage of CD4+CD134+ cells, which refers to an activated CD4+ T cell population, was also quantified and no significant changes were observed between all allogeneic groups. Despite similar frequency of $CD4^+$ T cells in donor corneas, LNs and PBMCs, the frequency of activated $CD4^+$ T cells in the corneas in all allogeneic groups was profoundly higher compared to LNs and PBMCs (39,5±2,5% vs. 16,9±2,1% and 8,8±2,3%, respectively) (Fig. 4.9 right panel). Although PD-L1 treatment did not affect the frequency of activated T cells ($CD4^+CD134^+$), the increased level of this cell subset in rejected corneas suggests an important role in the allograft rejection process.

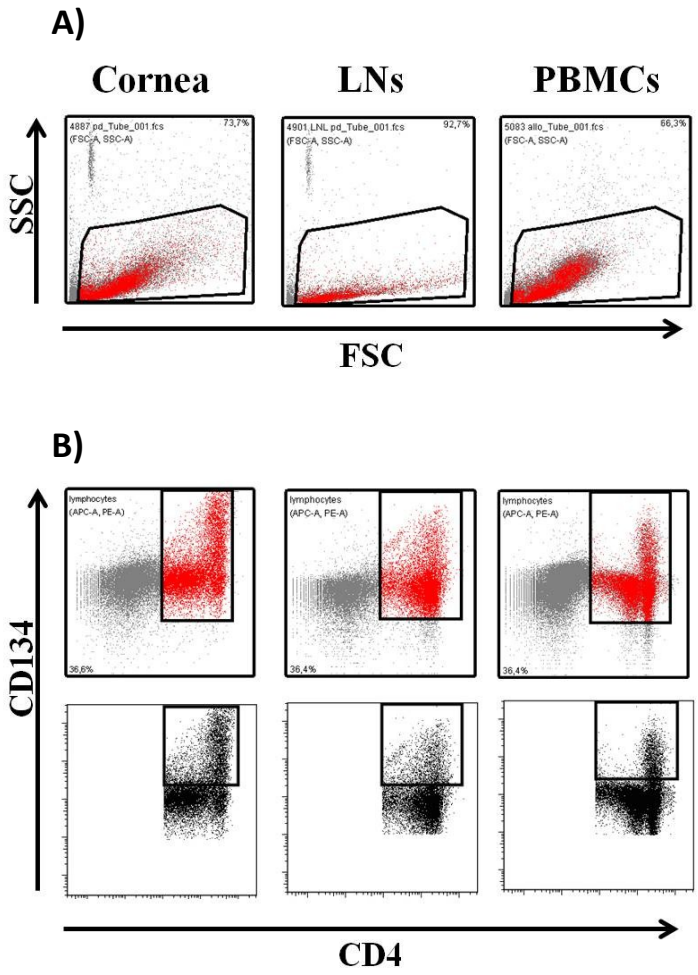

Fig. 4.8. Gating strategy of activated CD4+ cell subpopulation. The cell subpopulations were analyzed on POD 14 in the allografts, ipsi- and contralateral LNs and PBMCs. **A)** FSC vs. SSC gate distinguish lymphocytes; B) Upper panel: CD4+ subpopulation of cells; Lower panel: analysis of CD134 expression on CD4+ cell subset.

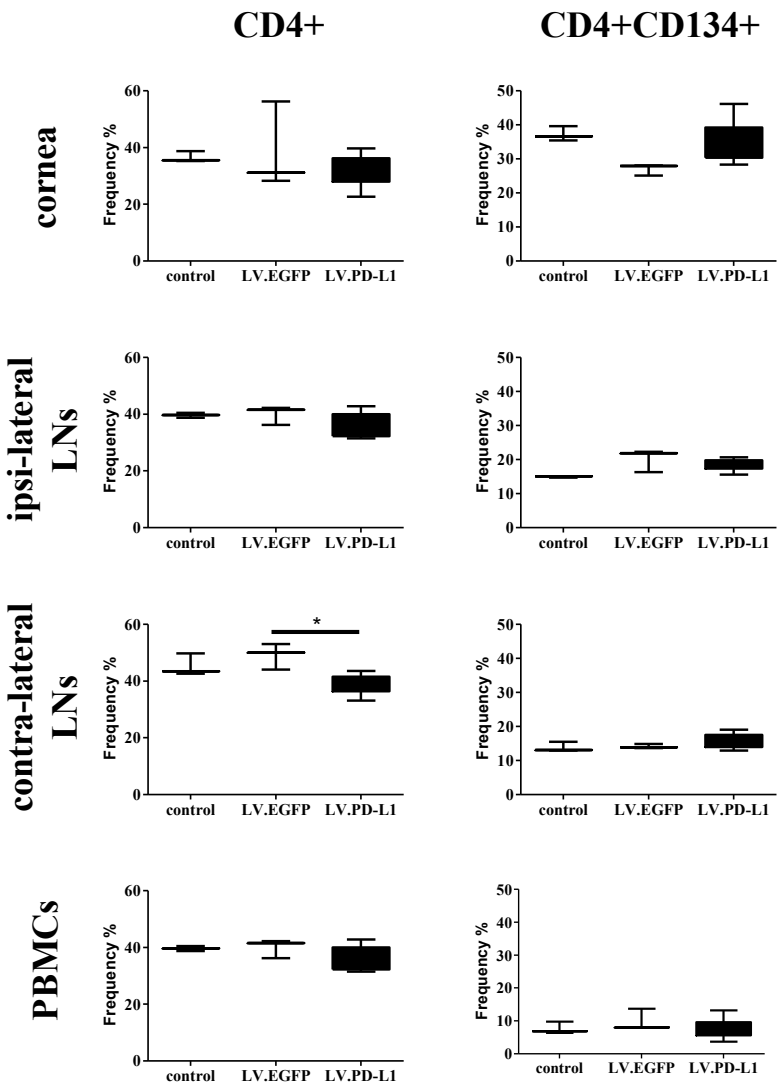

Fig. 4.9. Analysis of CD4+ subset and activated CD4+ lymphocytes. Frequency of CD4+ cell subpopulation and CD4+CD134+ subset in transplanted corneas, both LNs and PBMCs from allogeneic control (n=3), LV.EGFP (n=3) and LV.PD-L1 (n=7) groups as shown as the percentage from CD4+ subset or lymphocytes fraction; * p≤0.05.

4.2.2.3 Role of local overexpression of PD-L1 on B-cells

Lastly, the frequency of B-cells was analyzed in ipsi-lateral and contra-lateral lymph nodes and PBMC (Fig. 4.10). As described elsewhere (80) neither antibodies nor complement are necessary to mediate rejection of allogeneic corneas in mice. This conclusion is based on studies showing that B-cell and C3 deficient animals rejected corneal grafts with the same incidence as wild-type control subjects. However, only a low-risk model of corneal transplantation was assessed in this study. Others showed that the role of B cells is masked by robust T-cell-mediated effector mechanisms (81) and might be important in specific conditions such as keratoplasties performed in high-risk human eyes which have been reported to elicit donor-specific antibody response associated with graft rejection (82). Moreover, it was described that B cells are important during the establishment of peripheral tolerance and maintaining the ocular immune privilege (83, 84).

B-cells were characterized as CD45R-bearing cells and were gated on cells from LNs and PBMCs as presented in Fig. 4.10 A and B. The frequency of CD45R+ cells in allogeneic controls, LV.EGFP and LV.PD-L1 treated animals was not significantly different in any of the analyzed LNs. CD45R+ cells comprised 35.4±3.8, 33.8±11.2 and 44.4±9.8% of lymphocytes in ipsi-lateral LNs of all three treated groups, respectively. There was also no significant difference in B-cells between the groups in PBMCs, however, the frequency was of a lower level in comparison to LNs and ranged between 3.4 and 12.1% of PBMCs.

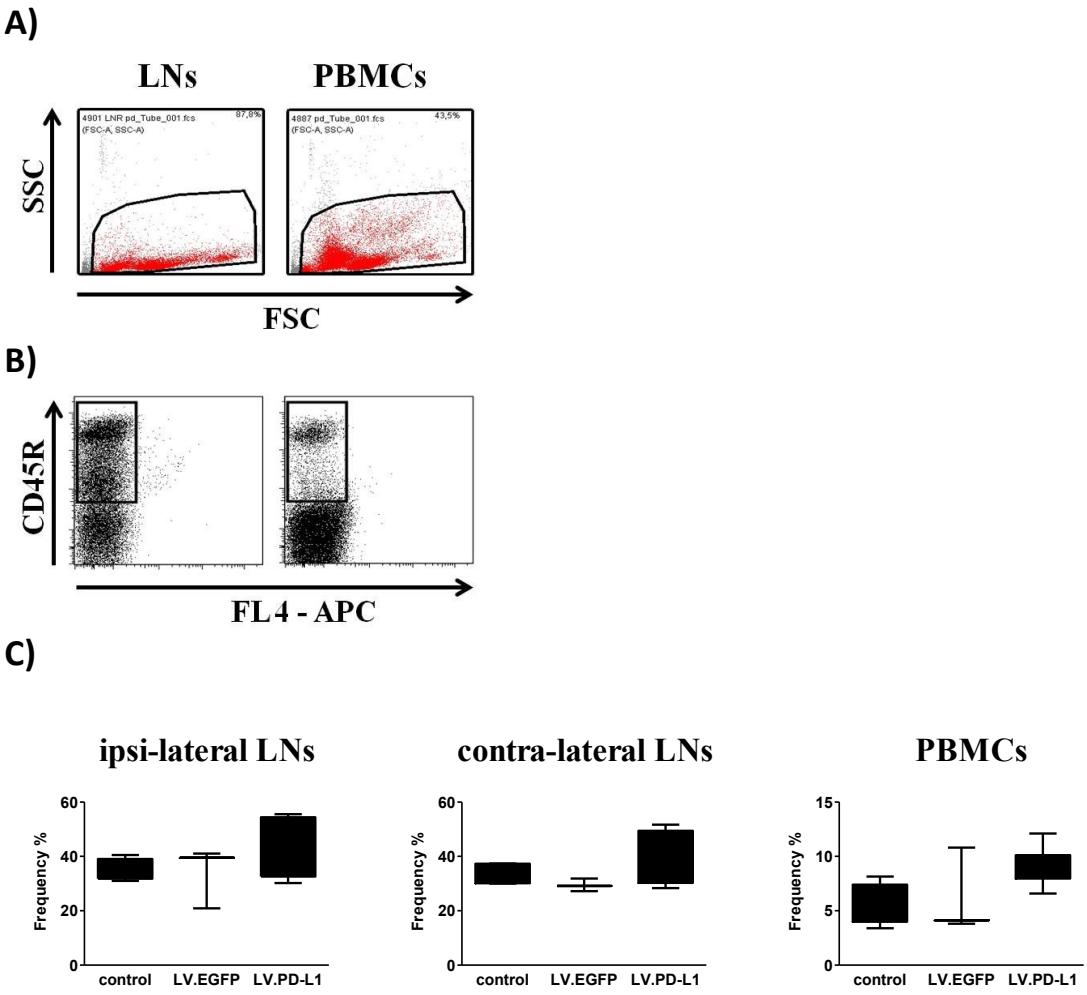

Fig. 4.10. Gating strategy and analysis of B cells. B cells were analyzed on POD 14 in the ipsi- and contralateral LNs and PBMCs. **A)** FSC vs. SSC gate distinguish lymphocytes; **B)** CD45R+ subpopulation of cells define B cells; **C)** Frequency of B cells in both LNs and PBMCs from allogeneic control (n=5), LV.EGFP (n=3) and LV.PD-L1 (n=7) groups is shown as the percentage from lymphocyte fraction.

4.3 Discussion

There are several studies reporting that PD-L1 plays a crucial role in inhibiting immune responses and promoting peripheral tolerance. Furthermore, the PD-1/PD-L1 pathway was suggested to be essential for the maintenance of cardiac allograft tolerance and to be involved in controlling effector T cell proliferation as well as induction of T cell anergy (185). Indeed, systemic application of a chimeric PD-L1.Ig in combination with cyclosporin A or rapamycin led to enhanced survival of mouse cardiac allografts (175). On the other hand, heart allografts in both PD-L1 deficient donors and recipients were rejected at a higher tempo and promoted Th1- or Th2-type immune responses in heart allograft recipients (186). Additionally, it was demonstrated that the PD-1/PD-L1 pathway is also involved in tolerance induction of other allogeneic graft. Combined, but not single, treatment of recipient mice with PD-L1.Ig and anti-CD154 resulted in long-term islet allograft survival (187). Interestingly, an autologous hematopoietic stem cell (HSC) – based protocol to improve the outcome of islet transplantation revealed the involvement of PD-L1 in promoting long-term survival of the allograft. It was shown that mobilized HSCs expressed the PD-L1 molecule at substantial levels and that this played a role in alloimmune response inhibition in a mixed lymphocyte reaction (MLR) assay which was in contrast to HSCs extracted from the PD-L1 knock-out mice (188). These results indicate that the PD-L1 signaling pathway is required for allograft tolerance.

Other studies have demonstrated a key function of PD-L1 in maintaining immune privilege in different tissues. It was shown that islet transplantation in the testis resulted in islet allograft survival, however, blocking PD-L1 or PD-1 abrogated allograft survival and abolished the suppression of T-cell proliferation and acceleration of T-cell apoptosis (189). It is also well documented that eye tissues constitutively express PD-L1 resulting in apoptosis induction of effector T cells via a cell contact-dependent mechanism. This feature of PD-L1 is thought to contribute to the immune privileged status of the eye (41, 178). PD-L1 is constitutively expressed by corneal epithelium, endothelium, iris/ciliary body and retinal pigment epithelium in the normal eye. In addition, IFN-γ upregulates PD-L1 expression in all

ocular cells including stromal cells. Similarly, higher levels of PD-L1 expression were observed in inflamed ocular tissues suggesting that this molecule might be involved in reestablishing *in situ* immune homeostasis by compensatory response to inflammation and suppression of IFN-γ and TNF-α. The ocular tissues that express PD-L1 are located near strategic areas which are engaged in the interaction between inflammatory cells and ocular tissues (115). Indeed, corneal allografts from PD-L1-deficient mice underwent a significantly more rapid rejection together with increased IFN-γ levels and enhanced recruitment of effector T cells in the grafts. Furthermore, it was shown in the same studies that graft-borne APC from PD-L1$^{-/-}$ mice did not play a significant role in corneal allograft rejection which provides further evidence that allorejection is not mediated by the direct pathway in this model. However, expression of PD-L1 on parenchymal cells is essential for limiting the allospecific T effector response in the corneal graft and regulating the induction of host alloreactive cells (42).

As described previously, expression of EGFP or lentiviral transduction itself was shown to initiate minimal or moderate immune responses in mouse models (190, 191). In this study, we did not observe rejection of LV.EGFP transduced syngeneic corneas (n=5) (Fig. 4.2 A) suggesting only a negligible influence of LV gene transfer on the rejection process. Moreover, LV-transduction and EGFP expression did not change the opacity dynamics, an indicator of cell infiltration and endothelial dysfunction, compared to untreated controls in syngeneic transplantation (Fig. 4.2B). Therefore, our study indicates that neither EGFP expression nor lentiviral transduction caused significant changes in observed parameters during graft rejection or survival. Similar results were described in the application of EGFP expressing stem cells or LV based gene therapy in other rat models (191, 192).

Next, the influence of PD-L1 overexpression on allogeneic corneal graft survival was determined. Allogeneic LV.PD-L1 transduced corneas showed a high percentage (83%) of graft survival (MST >30d, n=5, 15d, n=1) when compared to allogeneic or LV.EGFP control groups (Fig. 4.2A). LV.PD-L1 transduced corneas when observed at the time of rejection of allogeneic control grafts showed opacity scores in the range of 1 to 2.5 but this was not accompanied with changes in the geometry of the

transplant e.g. convex contour, shrinking and surface roughness. In contrast, all allogeneic controls and EGFP expressing corneas displayed signs of rejection as described above. Evidence of edema development was confirmed by histological analysis of corneas in allogeneic controls which was profoundly reduced in LV.PD-L1 transduced corneas on the average day of rejection (Fig. 4.3 and 4.4).

In summary these data suggest that the local overexpression of PD-L1 does not fully protect the allogeneic cornea from opacification but rather from rejection (41, 178). Gene transfer of PD-L1 led to significantly prolonged survival upon transplantation in allogeneic recipients, which has only rarely been observed following local gene therapy (88, 114, 193).

In order to study the influence of PD-L1 overexpression on inflammatory cell populations within the allografts, allogeneic transplants were collected from three experimental groups at a time-point corresponding to the average day of maximal rejection of the control group (between day 13 and 14). Moreover, cells from ipsi-lateral and contra-lateral submandibular and superficial cervical LNs and PBMCs were collected from the same animals and subjected to flow cytometric analysis.

The primary effector cells in the cornea rejection process are $CD4^+$ T cells. To delineate the impact of PD-L1 overexpression on $CD4^+$ T cell infiltration into the graft, as well as the changes in LNs and PBMCs the frequency of $CD4^+$ T cells and $CD4^+CD134^+$ T cells (activated $CD4^+$ cells) were analyzed between the experimental groups. According to the results from El Annan and colleagues, a significant increase in T-cell homing into PD-$L1^{-/-}$ corneas was observed which suggests regulation of T-cell chemotaxis by PD-L1 (177). Interestingly, overexpression of PD-L1 did not result in a decreased infiltration of $CD4^+$ T cells in the graft. There were no significant changes between allogeneic controls and the PD-L1 transduced group in either corneal grafts or LNs and PBMC. Similarly, the percentage of $CD4^+CD134^+$ cells was also quantified and no significant changes were observed between all allogeneic groups. However, there was a significant increase in activated $CD4^+$ subpopulation frequency in rejected rat corneas compared to LNs and PBMC (Fig. 4.9 right panel). These results confirmed that $CD4^+$ T cells play an important role in the allograft

rejection process, although PD-L1 treatment did not affect the alloreactive $CD4^+$ T-cell subset frequency.

The other subtype that has been proposed to mediate corneal graft rejection is $CD8^+$ cytotoxic T lymphocytes (CTL). Indeed, this study showed a significant reduction of infiltrating cells in LV.PD-L1 transduced corneas in the $CD3^+CD8^+CD161^-$ (cytotoxic T cells) compartment (Fig. 4.6 upper-right panel). These findings are interesting when compared to other studies demonstrating the impact of the PD-1/PD-L1 pathway on T cell alloreactivity. It was shown that PD-1 is highly upregulated on both activated $CD4^+$ and $CD8^+$ T cells (194), however, the PD-1/PD-L1 pathway is involved in a rapid allotolerance induction of donor-specific alloreactive $CD8^+$ T cells, but not $CD4^+$ T cells, as early as 4 days after allogeneic bone marrow transplantation (BMT). Furthermore, the blockade of the PD-L1 molecule alone was shown to be sufficient to prevent $CD8^+$ cell tolerance (195). Surprisingly, it was demonstrated that PD-L1 plays a crucial role in a selective regulation of the accumulation and deletion of cytotoxic $CD8^+$ T cells in the liver which is associated with the induction of hepatic tolerance. These findings were strengthened by the discovery that there was increased accumulation of antigen-activated $CD8^+$ T cells, but not $CD4^+$ T cells, selectively in the liver of naïve PD-L1 deficient mice (196). Taken together, it was suggested that PD-L1 plays a role in the deletion of activated $CD8^+$ T cells and tolerance induction which could contribute to the mechanism of long-term corneal graft survival after over-expression of the PD-L1 protein.

Several studies have also shown a rapid increase in the $CD3^+CD161^+$ or $CD3^-CD161^+$ cell population in aqueous humor (AH) and in the corneal allograft during the rejection process (77, 78). Interestingly, a rapid and constant increase in the percentage of $CD161^+$ cells within the $CD3^+$ population in the AH but not in draining lymph nodes was observed during rejection (77). Similarly, we could show a significantly higher frequency of $CD3^+CD8^+CD161^+$, $CD3^-CD8^+CD161^+$ and $CD3^-CD8^+CD161^{++}$ cells which correspond to NKT, NK and activated NK cells, respectively, in rejecting control grafts when compared to their presence in the LNs and PBMCs (Fig. 4.6 and 4.7). This increase in cell numbers may indicate a preferential

infiltration or clonal expansion within the target organ and confirm the important role of innate immunity in the corneal graft rejection process as described previously (77, 78, 197). However, the most striking difference in infiltrating cell populations was found in the $CD3^+CD8^+CD161^+$ (NKT cells) compartment which may play a “dual role” in eye immunology. In some conditions, NKT cells can function as cytolytic cells or play a role in shaping adaptive immune responses together with NK cells. However, NKT cells also contribute to the induction of ACAID and Treg cells (198). Further investigation will be required in upcoming research for a thorough characterization of the NKT cell population due to their potential importance in corneal allograft rejection. In this study it was demonstrated that the frequency of $CD3^+CD8^+CD161^+$ cells was significantly reduced from 18.7±5.8% in control or 15.5±2.0% in LV.EGFP transduced allografts to 10.4±1.7% in LV.PD-L1 transduced corneas (Fig. 4.6). This reflects an overall reduction of 44% in graft infiltration by this particular cell population. Moreover, a profound, albeit not significant, reduction in $CD3^-CD8^+CD161^+$ (NK cells) cells was observed in LV.PD-L1 transduced corneas compared to untreated and LV.EGFP transduced corneas. No significant differences in cellular distribution were observed in draining LNs and PBMCs (Fig. 4.6) which was expected due to the nature of the local gene therapeutic application. Additionally, histological analysis of corneal tissue sections showed a significant reduction of absolute cell numbers in LV.PD-L1 transduced corneas compared to the control group (Fig. 4.3 and 4.4).

In summary, our data indicate that local over-expression of PD-L1 reduces corneal graft immune cell infiltration. In general, a modulation of graft-infiltrating cell populations both of innate (NKT) and adaptive (cytotoxic T cells) immunity was detected by analyzing the percentage of graft-infiltrating cells. The results shown here are also supported by the previous reports on the role of PD-L1 in tumour immunology (199). It was shown that NKT cells constitutively express PD-1 and after primary activation may become hyporesponsive toward their ligands. Blocking of the PD-1/PD-L1 pathway not only diminishes anergy of NKT cells but may also prevent its induction. Combining abrogation of the PD-L1 pathway together with

NKT activation can overcome the immunosuppressive effects of B16F10 tumor by enhancement of tumor-specific T cells (199, 200).

Although overexpression of PD-L1 on the corneal endothelium significantly prolonged allograft survival, it has to be considered that a continuous expression might be undesirable. Indeed, in the setting chronic inflammation conditions stable expression of PD-L1 may result in tumor escape from immune surveillance and contribute to cancerous changes (181, 182). This problem could be overcome by utilizing an inducible promoter which could be inactivated if necessary. However, corneal endothelial cells are terminally differentiated and the risk of mutagenesis is greatly reduced. Hence, further studies will be required in the future to optimize the conditions of LV-mediated PD-L1 overexpression in the cornea. Specifically, better control over the transduction process will be necessary to derive the maximal therapeutic benefit from the minimal viral dose.

Finally, the B-cells were characterized as CD45R-bearing cells and was gated on lymphocytes from LNs and PBMCs as presented in Fig. 4.10 A and B. In contrast to other cell types, B-cells are not necessary in mediating rejection of allogeneic corneas in mice (80). However, according to other investigators the role of B cells can be masked by robust T-cell-mediated effector mechanisms (81). Interestingly, it was described that B cells are important during the maintenance of ocular immune-privilege by inducing $CD8^+$ suppressor T cells and establishment of peripheral tolerance (83, 84, 201). In this study it was shown that the frequency of $CD45R^+$ cells in allogeneic control subjects, LV.EGFP and PD-L1 treated animals was not significantly altered in any analyzed LNs and comprised 35.4±3.8, 33.8±11.2 and 44.4±9.8% of lymphocytes in ipsi-lateral LN, respectively. There was also no significant difference in the B-cell population between groups in PBMCs.

As mentioned above, it was demonstrated that prolongation of corneal graft survival by LV.PD-L1 transduction of allografts is associated with a decreased frequency of $CD3^+CD8^+CD161^+$ cells in the graft which occurs without prevention of general infiltration. Histological analysis showed massive infiltration in control and LV.EGFP transduced corneas, however, cell infiltration in LV.PD-L1 transduced corneas was markedly reduced which correlates with the severity of opacity score

(Fig. 4.2 B). Local overexpression of PD-L1 in corneal allografts may, in addition to the endogenous expression of PD-L1 on corneal cells, aid the further development of an immunomodulatory milieu after trauma or cornea transplantation (41). Taken together these results demonstrate that lentivirus-mediated local overexpression of the therapeutic gene PD-L1 was efficient in prolonging corneal graft survival through the modulation of $CD3^+CD8^+CD161^-$ and $CD3^+CD8^+CD161^+$ cells which revealed the importance of these cells in the process of corneal allograft rejection.

Chapter 5:

General discussion

5 General discussion

There are several issues that have to be considered before applying a gene therapy approach for human diseases. The biosafety issue and the efficiency of gene transfer are the most important aspects from a research perspective. Lentivirus-based vectors (LV) are capable of transducing both dividing and post-mitotic cells such as corneal endothelial cells. Several different LV vectors have been tested in preclinical ocular studies including both primate and non-primate vectors (92). However, only vectors based on human immunodeficiency virus type 1 (HIV-1) and equine infectious anaemia virus (EIAV) pseudotyped with the vesicular stomatitis virus G (VSV-G) protein were applied for efficient gene delivery to the cornea (202, 203).

The main concern for bio-safety of LV in clinical application, although very unlikely, is the generation of replication-competent lentivirus (RCL) during vector production. The public tension increases when HIV vectors are considered for use, particularly for non-life threatening diseases such as perforating keratoplasty. The advantage of using non-primate LV is due to the negligible probability of non-primate RCL generation in human cells because of high species-specificity of lentivirus (204, 205).

The risk of insertional mutagenesis (IM) has to be considered before any clinical application of lentiviral-based gene therapy. The incident of tumorigenesis in patients with X-linked Severe Combined Immunodeficiency treated with *ex vivo* gene-modified $CD34^+$ hematopoietic stem cells with a MuLV vector highlighted the risk of IM (206, 207). Recent data have shown that LV typically favours integration into active coding regions in dividing human cells rather than transcriptional promoter sites similarly to oncogenic vectors which minimize the risk of IM (208, 209). Additionally, human corneal endothelium is a terminally differentiated cell layer which may reduce the risk of IM even more in comparison to mitotically active cells. Indeed, HIV-1 vector integration in post-mitotic murine RPE *in vivo* demonstrated near random and uniform frequency of integration into genes and gene spare long interspersed nuclear elements (LINE) (210). Moreover, application

of non-integrative LV for long-term treatment of post-mitotic cells would further improve the biosafety of corneal endothelium gene therapy (211). A non-integrating SIV vector, that has been described recently (212), is a compromising solution for biosafety enhancement by reduction the risk of IM and the potential advantages of non-primate vectors in terms of possible generation of replication-competent lentivirus during vector production (92).

The successful application of HIV-based vectors in well-described rodent models of ocular gene therapy and the potential for clinical application were the main criteria for using LV in these studies. There is also a wealth of knowledge on lentivirus biology that will give confidence for gene therapy application. Lentiviral vectors can be manufactured to high titres in a fully controlled environment with repeatable quality of generated batches. In addition, LV are able to target a broad range of organs as well as dividing and non-dividing cells. The latter feature, as mentioned before, is important for gene transfer into the corneal endothelium. Although not of relevance for this project, lentiviral-based vectors have a relatively large capacity for carrying transgenes. This may allow for further opportunities and more specific applications including multi-cistronic delivery of several therapeutic agents or delivery of large genes. Additionally, expression kinetics after LV gene transfer is known to have greater consistency, typically producing rapid and sustained transgene expression. However, as discussed before, LV-delivered gene expression kinetics might be influenced by several factors like titer, tropism determined by surface envelope proteins, target cells or organs, site of vector delivery and the species (92). In the context of cornea transplantation, it was shown in several studies that LV pseudotyped by VSV-G envelope have tropism to the endothelium (107), however, under specific conditions stromal cells may also be transduced when vectors are injected into the corneal pocket created by the femtosecond laser cut (213). It was also demonstrated that therapeutic gene expression, driven by LV vectors, is strictly dependent on the species and was significantly delayed in the ovine cornea in comparison to the human cornea (154).

To further improve the biosafety of HIV-based vectors highly advanced 3rd generation self-inactivating (SIN) vectors are currently available (214). This was

achieved by deletion of the pro-inflammatory and pathogenic viral components from the vector genome. Despite profound vector modification and the low pro-inflammatory profile of lentivirus vector, host immune responses against the viral vector or the transgene product may result in the clearance of transduced cells or neutralization of the therapeutic product. Indeed, an early mild inflammatory response was described after LV administration to the anterior segment, however, no signs of reduced corneal clarity or increased thickness was reported suggesting this was a transient episode (202, 215). Moreover, no toxicity on ocular cells arising from vector administration was reported. These observations are in accordance with the results presented in this thesis. LV-transduction and reporter gene (EGFP) expression did not change the opacification compared to untreated controls in syngeneic transplantation. Furthermore, it was shown that neither EGFP expression nor lentiviral transduction caused changes in observed parameters during graft rejection or its survival. Similar results were described in the application of EGFP expressing stem cells or LV based gene therapy in other rat models (191, 192).

Due to the anatomically compartmentalized nature of the eye the vector dispersion is greatly limited and highly depends on site and method of vector delivery. Therefore, the cornea is an attractive organ for gene therapy presenting a unique opportunity for *ex vivo* manipulations. The protocol based on *ex-vivo* vector delivery further increases a biosafety by minimizing the risk of viral vector spread to other tissues. Together with rigorous biosafety derived from wider understanding of vector toxicity, a safer *ex vivo* gene delivery and successful preclinical therapeutic applications of LV-based cornea gene therapy, that has been evaluated in the transplantation model by several investigators (106, 193, 216), these data indicate the potential of lentivirus vector-based therapies as a valuable clinical approach for treatment corneal endothelium failure and graft rejection.

This project explored novel gene therapy approaches to prolong corneal graft survival. The two different strategies were investigated using LV vectors for therapeutic gene transfer to endothelium.

The first approach was based on the anti-apoptotic properties of NGF to protect endothelium from immune mediated cell loss. However, while the main goal of this

part of the project could not be achieved, this method still has some therapeutic potential. It is possible that many factors contributed to a failure of this concept, however, the precise reason remains unknown. It is possible that immortalized HCECs were not suitable for *in vitro* studies of cytoprotection. This cell line seems to be resistant to apoptosis induction (156) or may have altered signalling pathways. The clear weakness of this model was the utilization of compounds from different species (i.e. mouse NGF, human endothelial cells, rat PC12 cell line). As proposed earlier, primary corneal endothelial cells isolated from rat corneas could be a better and more suitable model for this project. To provide comprehensive studies on endothelial cell apoptosis, different and more physiological inducers of programmed death cells might have been utilized. It was shown that the proinflammatory cytokines TNFα and INFγ are involved in endothelium damage during allograft rejection (35). Using these cytokines to induce apoptosis would provide a means to generate a relevant *in vitro* model for investigating the cytoprotective effects of NGF. The other neurotrophins that are present in the aqueous humor might have also been considered as potential anti-apoptotic agents. Calcitonin gene-related peptide (CGRP) seems to be a good candidate in the context of local overexpression by endothelial cells because it contributes to the inhibition of the production of NO^- which is thought to be responsible for apoptosis of corneal endothelium during the rejection process (34). Furthermore, its expression and release is regulated by NGF in many different cell types (217-219). The cytoprotective effect of CGRP was described against stress induced apoptosis in rat retinal cells (220) but also in cultured rat cardiomyocytes (221) and in human osteoblasts (222). Moreover, it was shown that Ad-mediated CGRP gene transfer to rat descending thoracic aortas before transplantation averted rejection and suppressed allograft vasculopathy and encroachment by inflammatory cells (223).

The difficulties arising in the *in vivo* experiments of LV-mediated NGF gene transfer may be overcome by using different strain combination with low-responder characteristics to avoid a rapid and destructive rejection. This could be performed using a rat model described by Maenz *et al.* (78). The other option could be a mouse model of cornea transplantation. This would give the opportunity to select more

strain combinations and give a broad access to many reagents or transgenic animals that might be beneficial to the project.

The second part of the project explored immunomodulatory properties of PD-L1. The results showed a great potential as a future therapeutic approach, however, many other issues have to be evaluated before any clinical application could be considered. Firstly, there is a need to characterize the expression kinetics and to determine the optimal dose for the best treatment conditions. In this study only one dose of LV vectors was tested to overexpress the PD-L1 gene. There is a need to investigate the relevance of titer on long term graft survival and the level of PD-L1 expression in the endothelial cells. It was difficult to predict the expression level because transduction efficiency was not fully determined. The protocol that was established during this project provided information on a percentage of transduced cells in a single cell suspension from whole corneal buttons (Fig. 3.11), however, mostly endothelial cells are transduced by LV vectors (107). To evaluate the efficiency of gene transfer and subsequently the quality of the corneal endothelium, laser scanning microscopy (Leica TCS SP2) could be used as it was described in other studies (111). Secondly, to further delineate a mechanism underlying long-term graft survival after PD-L1 gene transfer, PD-L1 knockout animals or local suppression of PD-L1 using targeted RNAi could have been utilized. This project revealed the importance of $CD8^+$ T cells and NKT cells in the process of corneal allograft rejection and the involvement of PD-L1 on these cell populations, however, the interactions are poorly understood. On the other hand, the results showed that PD-L1 plays an important role in down-regulating local immune responses and is responsible for maintaining immune privilege by inducing apoptosis of the infiltrating cells (41, 42), however, the exact mechanism was not described. The protocol of rapid isolation of graft infiltrating cells (78) used in these studies could be beneficial to further investigation of the impact of PD-L1 overexpression on infiltrating lymphocytes and their apoptosis and whether allograft acceptance is due to tolerance induction or as a consequence of continuous PD-L1 overexpression.

Bibliography

Bibliography

1. Wang, X., B. Appukuttan, S. Ott, R. Patel, J. Irvine, J. Song, J. H. Park, R. Smith, and J. T. Stout. 2000. Efficient and sustained transgene expression in human corneal cells mediated by a lentiviral vector. *Gene Ther* 7: 196-200.
2. HANNA, C., D. S. BICKNELL, and J. E. O'BRIEN. 1961. Cell turnover in the adult human eye. *Arch Ophthalmol* 65: 695-698.
3. George, A. J., and D. F. Larkin. 2004. Corneal transplantation: the forgotten graft. *Am J Transplant* 4: 678-685.
4. Zhao, X. C., R. W. Yee, E. Norcom, H. Burgess, A. S. Avanesov, J. P. Barrish, and J. Malicki. 2006. The zebrafish cornea: structure and development. *Invest Ophthalmol Vis Sci* 47: 4341-4348.
5. Joyce, N. C., B. Meklir, S. J. Joyce, and J. D. Zieske. 1996. Cell cycle protein expression and proliferative status in human corneal cells. *Invest Ophthalmol Vis Sci* 37: 645-655.
6. Maurice, D. M. 1972. The location of the fluid pump in the cornea. *J Physiol* 221: 43-54.
7. Fitch, K. L., and M. J. Nadakavukaren. 1986. Age-related changes in the corneal endothelium of the mouse. *Exp Gerontol* 21: 31-35.
8. Sherrard, E. S., P. Novakovic, and L. Speedwell. 1987. Age-related changes of the corneal endothelium and stroma as seen in vivo by specular microscopy. *Eye (Lond)* 1 (Pt 2): 197-203.
9. Fitch, K. L., M. J. Nadakavukaren, and A. Richardson. 1982. Age-related changes in the corneal endothelium of the rat. *Exp Gerontol* 17: 179-183.
10. Bell, K. D., R. J. Campbell, and W. M. Bourne. 2000. Pathology of late endothelial failure: late endothelial failure of penetrating keratoplasty: study with light and electron microscopy. *Cornea* 19: 40-46.
11. Bourne, W. M. 2001. Cellular changes in transplanted human corneas. *Cornea* 20: 560-569.
12. Claerhout, I., H. Beele, D. De Bacquer, and P. Kestelyn. 2003. Factors influencing the decline in endothelial cell density after corneal allograft rejection. *Invest Ophthalmol Vis Sci* 44: 4747-4752.
13. Claerhout, I., H. Beele, and P. Kestelyn. 2008. Graft failure: I. Endothelial cell loss. *Int Ophthalmol* 28: 165-173.
14. Plskova, J., L. Kuffova, M. Filipec, V. Holan, and J. V. Forrester. 2004. Quantitative evaluation of the corneal endothelium in the mouse after grafting. *Br J Ophthalmol* 88: 1209-1216.
15. Streilein, J. W. 2003. Ocular immune privilege: therapeutic opportunities from an experiment of nature. *Nat Rev Immunol* 3: 879-889.
16. Niederkorn, J. Y., and D. F. Larkin. 2010. Immune privilege of corneal allografts. *Ocul Immunol Inflamm* 18: 162-171.
17. Williams, K. A., A. J. Esterman, C. Bartlett, H. Holland, N. B. Hornsby, and D. J. Coster. 2006. How effective is penetrating corneal transplantation? Factors influencing long-term outcome in multivariate analysis. *Transplantation* 81: 896-901.

18. Tan, Y., F. Cruz-Guilloty, C. A. Medina-Mendez, N. J. Cutrufello, R. E. Martinez, M. Urbieta, D. Wilson, Y. Li, and V. L. Perez. 2012. Immunological disruption of antiangiogenic signals by recruited allospecific T cells leads to corneal allograft rejection. *J Immunol* 188: 5962-5969.
19. Dana, M. R., and J. W. Streilein. 1996. Loss and restoration of immune privilege in eyes with corneal neovascularization. *Invest Ophthalmol Vis Sci* 37: 2485-2494.
20. Ambati, B. K., M. Nozaki, N. Singh, A. Takeda, P. D. Jani, T. Suthar, R. J. Albuquerque, E. Richter, E. Sakurai, M. T. Newcomb, M. E. Kleinman, R. B. Caldwell, Q. Lin, Y. Ogura, A. Orecchia, D. A. Samuelson, D. W. Agnew, J. St Leger, W. R. Green, P. J. Mahasreshti, D. T. Curiel, D. Kwan, H. Marsh, S. Ikeda, L. J. Leiper, J. M. Collinson, S. Bogdanovich, T. S. Khurana, M. Shibuya, M. E. Baldwin, N. Ferrara, H. P. Gerber, S. De Falco, J. Witta, J. Z. Baffi, B. J. Raisler, and J. Ambati. 2006. Corneal avascularity is due to soluble VEGF receptor-1. *Nature* 443: 993-997.
21. Hori, J., and J. W. Streilein. 2001. Role of recipient epithelium in promoting survival of orthotopic corneal allografts in mice. *Invest Ophthalmol Vis Sci* 42: 720-726.
22. Cursiefen, C., L. Chen, M. Saint-Geniez, P. Hamrah, Y. Jin, S. Rashid, B. Pytowski, K. Persaud, Y. Wu, J. W. Streilein, and R. Dana. 2006. Nonvascular VEGF receptor 3 expression by corneal epithelium maintains avascularity and vision. *Proc Natl Acad Sci U S A* 103: 11405-11410.
23. Albuquerque, R. J., T. Hayashi, W. G. Cho, M. E. Kleinman, S. Dridi, A. Takeda, J. Z. Baffi, K. Yamada, H. Kaneko, M. G. Green, J. Chappell, J. Wilting, H. A. Weich, S. Yamagami, S. Amano, N. Mizuki, J. S. Alexander, M. L. Peterson, R. A. Brekken, M. Hirashima, S. Capoor, T. Usui, B. K. Ambati, and J. Ambati. 2009. Alternatively spliced vascular endothelial growth factor receptor-2 is an essential endogenous inhibitor of lymphatic vessel growth. *Nat Med* 15: 1023-1030.
24. Dietrich, T., F. Bock, D. Yuen, D. Hos, B. O. Bachmann, G. Zahn, S. Wiegand, L. Chen, and C. Cursiefen. 2010. Cutting edge: lymphatic vessels, not blood vessels, primarily mediate immune rejections after transplantation. *J Immunol* 184: 535-539.
25. Sugita, S., and J. W. Streilein. 2003. Iris pigment epithelium expressing CD86 (B7-2) directly suppresses T cell activation in vitro via binding to cytotoxic T lymphocyte-associated antigen 4. *J Exp Med* 198: 161-171.
26. Apte, R. S., D. Sinha, E. Mayhew, G. J. Wistow, and J. Y. Niederkorn. 1998. Cutting edge: role of macrophage migration inhibitory factor in inhibiting NK cell activity and preserving immune privilege. *J Immunol* 160: 5693-5696.
27. Cousins, S. W., M. M. McCabe, D. Danielpour, and J. W. Streilein. 1991. Identification of transforming growth factor-beta as an immunosuppressive factor in aqueous humor. *Invest Ophthalmol Vis Sci* 32: 2201-2211.
28. Koh, S. W., A. Rutzen, T. Coll, R. Hemady, and E. Higginbotham. 2005. VIP immunoreactivity in human aqueous humor. *Curr Eye Res* 30: 189-194.
29. Koh, S. W., and J. A. Waschek. 2000. Corneal endothelial cell survival in organ cultures under acute oxidative stress: effect of VIP. *Invest Ophthalmol Vis Sci* 41: 4085-4092.
30. Koh, S. W., J. Cheng, R. M. Dodson, C. Y. Ku, and C. J. Abbondandolo. 2009. VIP down-regulates the inflammatory potential and promotes survival

of dying (neural crest-derived) corneal endothelial cells ex vivo: necrosis to apoptosis switch and up-regulation of Bcl-2 and N-cadherin. *J Neurochem* 109: 792-806.

31. Taylor, A. W., J. W. Streilein, and S. W. Cousins. 1994. Alpha-melanocyte-stimulating hormone suppresses antigen-stimulated T cell production of gamma-interferon. *Neuroimmunomodulation* 1: 188-194.
32. Taylor, A. W., and D. J. Lee. 2011. The alpha-melanocyte stimulating hormone induces conversion of effector T cells into treg cells. *J Transplant* 2011: 246856.
33. Hamrah, P., Z. Haskova, A. W. Taylor, Q. Zhang, B. R. Ksander, and M. R. Dana. 2009. Local treatment with alpha-melanocyte stimulating hormone reduces corneal allorejection. *Transplantation* 88: 180-187.
34. Taylor, A. W., D. G. Yee, and J. W. Streilein. 1998. Suppression of nitric oxide generated by inflammatory macrophages by calcitonin gene-related peptide in aqueous humor. *Invest Ophthalmol Vis Sci* 39: 1372-1378.
35. Sagoo, P., G. Chan, D. F. Larkin, and A. J. George. 2004. Inflammatory cytokines induce apoptosis of corneal endothelium through nitric oxide. *Invest Ophthalmol Vis Sci* 45: 3964-3973.
36. Stuart, P. M., X. Yin, S. Plambeck, F. Pan, and T. A. Ferguson. 2005. The role of Fas ligand as an effector molecule in corneal graft rejection. *Eur J Immunol* 35: 2591-2597.
37. Aoki, K., M. Kurooka, J. J. Chen, J. Petryniak, E. G. Nabel, and G. J. Nabel. 2001. Extracellular matrix interacts with soluble CD95L: retention and enhancement of cytotoxicity. *Nat Immunol* 2: 333-337.
38. Griffith, T. S., T. Brunner, S. M. Fletcher, D. R. Green, and T. A. Ferguson. 1995. Fas ligand-induced apoptosis as a mechanism of immune privilege. *Science* 270: 1189-1192.
39. Hargrave, S. L., E. Mayhew, S. Hegde, and J. Niederkorn. 2003. Are corneal cells susceptible to antibody-mediated killing in corneal allograft rejection? *Transpl Immunol* 11: 79-89.
40. Sohn, J. H., H. J. Kaplan, H. J. Suk, P. S. Bora, and N. S. Bora. 2000. Chronic low level complement activation within the eye is controlled by intraocular complement regulatory proteins. *Invest Ophthalmol Vis Sci* 41: 3492-3502.
41. Hori, J., M. Wang, M. Miyashita, K. Tanemoto, H. Takahashi, T. Takemori, K. Okumura, H. Yagita, and M. Azuma. 2006. B7-H1-induced apoptosis as a mechanism of immune privilege of corneal allografts. *J Immunol* 177: 5928-5935.
42. Shen, L., Y. Jin, G. J. Freeman, A. H. Sharpe, and M. R. Dana. 2007. The function of donor versus recipient programmed death-ligand 1 in corneal allograft survival. *J Immunol* 179: 3672-3679.
43. Cunnusamy, K., K. Paunicka, N. Reyes, W. Yang, P. W. Chen, and J. Y. Niederkorn. 2010. Two different regulatory T cell populations that promote corneal allograft survival. *Invest Ophthalmol Vis Sci* 51: 6566-6574.
44. Cunnusamy, K., P. W. Chen, and J. Y. Niederkorn. 2010. IL-17 promotes immune privilege of corneal allografts. *J Immunol* 185: 4651-4658.
45. Cunnusamy, K., P. W. Chen, and J. Y. Niederkorn. 2011. IL-17A-dependent CD4+CD25+ regulatory T cells promote immune privilege of corneal allografts. *J Immunol* 186: 6737-6745.

46. Krieger, N. R., D. P. Yin, and C. G. Fathman. 1996. CD4+ but not CD8+ cells are essential for allorejection. *J Exp Med* 184: 2013-2018.
47. Hornick, P. I., P. D. Mason, R. J. Baker, M. Hernandez-Fuentes, L. Frasca, G. Lombardi, K. Taylor, L. Weng, M. L. Rose, M. H. Yacoub, R. Batchelor, and R. I. Lechler. 2000. Significant frequencies of T cells with indirect anti-donor specificity in heart graft recipients with chronic rejection. *Circulation* 101: 2405-2410.
48. Vella, J. P., M. Spadafora-Ferreira, B. Murphy, S. I. Alexander, W. Harmon, C. B. Carpenter, and M. H. Sayegh. 1997. Indirect allorecognition of major histocompatibility complex allopeptides in human renal transplant recipients with chronic graft dysfunction. *Transplantation* 64: 795-800.
49. Vella, J. P., L. Vos, C. B. Carpenter, and M. H. Sayegh. 1997. Role of indirect allorecognition in experimental late acute rejection. *Transplantation* 64: 1823-1828.
50. Niederkorn, J. Y. 1990. Immune privilege and immune regulation in the eye. *Adv Immunol* 48: 191-226.
51. Boisgérault, F., Y. Liu, N. Anosova, R. Dana, and G. Benichou. 2009. Differential roles of direct and indirect allorecognition pathways in the rejection of skin and corneal transplants. *Transplantation* 87: 16-23.
52. Sano, Y., B. R. Ksander, and J. W. Streilein. 1996. Minor H, rather than MHC, alloantigens offer the greater barrier to successful orthotopic corneal transplantation in mice. *Transpl Immunol* 4: 53-56.
53. Liu, Y., P. Hamrah, Q. Zhang, A. W. Taylor, and M. R. Dana. 2002. Draining lymph nodes of corneal transplant hosts exhibit evidence for donor major histocompatibility complex (MHC) class II-positive dendritic cells derived from MHC class II-negative grafts. *J Exp Med* 195: 259-268.
54. Huq, S., Y. Liu, G. Benichou, and M. R. Dana. 2004. Relevance of the direct pathway of sensitization in corneal transplantation is dictated by the graft bed microenvironment. *J Immunol* 173: 4464-4469.
55. Sano, Y., B. R. Ksander, and J. W. Streilein. 1997. Murine orthotopic corneal transplantation in high-risk eyes. Rejection is dictated primarily by weak rather than strong alloantigens. *Invest Ophthalmol Vis Sci* 38: 1130-1138.
56. Dana, M. R., J. Yamada, and J. W. Streilein. 1997. Topical interleukin 1 receptor antagonist promotes corneal transplant survival. *Transplantation* 63: 1501-1507.
57. Niederkorn, J. Y. 2006. See no evil, hear no evil, do no evil: the lessons of immune privilege. *Nat Immunol* 7: 354-359.
58. Ljunggren, H. G., and K. Kärre. 1990. In search of the 'missing self': MHC molecules and NK cell recognition. *Immunol Today* 11: 237-244.
59. Ayliffe, W., Y. Alam, E. B. Bell, D. McLeod, and I. V. Hutchinson. 1992. Prolongation of rat corneal graft survival by treatment with anti-CD4 monoclonal antibody. *Br J Ophthalmol* 76: 602-606.
60. Pleyer, U., J. K. Milani, A. Dukes, J. Chou, S. Lutz, D. Rückert, H. J. Thiel, and B. J. Mondino. 1995. Effect of topically applied anti-CD4 monoclonal antibodies on orthotopic corneal allografts in a rat model. *Invest Ophthalmol Vis Sci* 36: 52-61.
61. He, Y. G., J. Ross, and J. Y. Niederkorn. 1991. Promotion of murine orthotopic corneal allograft survival by systemic administration of anti-CD4 monoclonal antibody. *Invest Ophthalmol Vis Sci* 32: 2723-2728.

62. Yamada, J., I. Kurimoto, and J. W. Streilein. 1999. Role of CD4+ T cells in immunobiology of orthotopic corneal transplants in mice. *Invest Ophthalmol Vis Sci* 40: 2614-2621.
63. Haskova, Z., N. Usiu, J. S. Pepose, T. A. Ferguson, and P. M. Stuart. 2000. CD4+ T cells are critical for corneal, but not skin, allograft rejection. *Transplantation* 69: 483-487.
64. Torres, P. F., A. F. De Vos, R. van der Gaag, B. Martins, and A. Kijlstra. 1996. Cytokine mRNA expression during experimental corneal allograft rejection. *Exp Eye Res* 63: 453-461.
65. Rayner, S. A., W. J. King, R. M. Comer, J. D. Isaacs, G. Hale, A. J. George, and D. F. Larkin. 2000. Local bioactive tumour necrosis factor (TNF) in corneal allotransplantation. *Clin Exp Immunol* 122: 109-116.
66. Pleyer, U., J. K. Milani, D. Rückert, P. Rieck, and B. J. Mondino. 1997. Determinations of serum tumor necrosis factor alpha in corneal allografts. *Ocul Immunol Inflamm* 5: 149-155.
67. Goldberg, M. F., T. A. Ferguson, and J. S. Pepose. 1994. Detection of cellular adhesion molecules in inflamed human corneas. *Ophthalmology* 101: 161-168.
68. Hargrave, S. L., C. Hay, J. Mellon, E. Mayhew, and J. Y. Niederkorn. 2004. Fate of MHC-matched corneal allografts in Th1-deficient hosts. *Invest Ophthalmol Vis Sci* 45: 1188-1193.
69. Yamada, J., M. Yoshida, A. W. Taylor, and J. W. Streilein. 1999. Mice with Th2-biased immune systems accept orthotopic corneal allografts placed in "high risk" eyes. *J Immunol* 162: 5247-5255.
70. Hargrave, S. L., J. Mellon, and J. Niederkorn. 2002. MHC matching improves corneal allograft survival in mice with Th2-immune bias. *Transplant Proc* 34: 3413-3415.
71. Hargrave, S., Y. Chu, D. Mendelblatt, E. Mayhew, and J. Niederkorn. 2003. Preliminary findings in corneal allograft rejection in patients with keratoconus. *Am J Ophthalmol* 135: 452-460.
72. Larkin, D. F., V. L. Calder, and S. L. Lightman. 1997. Identification and characterization of cells infiltrating the graft and aqueous humour in rat corneal allograft rejection. *Clin Exp Immunol* 107: 381-391.
73. Callanan, D. G., M. W. Luckenbach, B. J. Fischer, J. S. Peeler, and J. Y. Niederkorn. 1989. Histopathology of rejected orthotopic corneal grafts in the rat. *Invest Ophthalmol Vis Sci* 30: 413-424.
74. Callanan, D., J. Peeler, and J. Y. Niederkorn. 1988. Characteristics of rejection of orthotopic corneal allografts in the rat. *Transplantation* 45: 437-443.
75. Niederkorn, J. Y., C. Stevens, J. Mellon, and E. Mayhew. 2006. CD4+ T-cell-independent rejection of corneal allografts. *Transplantation* 81: 1171-1178.
76. Ksander, B. R., Y. Sano, and J. W. Streilein. 1996. Role of donor-specific cytotoxic T cells in rejection of corneal allografts in normal and high-risk eyes. *Transpl Immunol* 4: 49-52.
77. Claerhout, I., P. Kestelyn, V. Debacker, H. Beele, and G. Leclercq. 2004. Role of natural killer cells in the rejection process of corneal allografts in rats. *Transplantation* 77: 676-682.
78. Maenz, M., M. Morcos, and T. Ritter. 2011. A comprehensive flow-cytometric analysis of graft infiltrating lymphocytes, draining lymph nodes

and serum during the rejection phase in a fully allogeneic rat cornea transplant model. *Mol Vis* 17: 420-429.

79. Schwartzkopff, J., S. L. Schlereth, M. Berger, L. Bredow, F. Birnbaum, D. Böhringer, and T. Reinhard. 2010. NK cell depletion delays corneal allograft rejection in baby rats. *Mol Vis* 16: 1928-1935.
80. Goslings, W. R., J. Yamada, M. R. Dana, J. W. Streilein, E. van Beelen, A. P. Prodeus, M. C. Carroll, and M. J. Jager. 1999. Corneal transplantation in antibody-deficient hosts. *Investigative Ophthalmology & Visual Science* 40: 250-253.
81. Hegde, S., J. K. Mellon, S. L. Hargrave, and J. Y. Niederkorn. 2002. Effect of alloantibodies on corneal allograft survival. *Invest Ophthalmol Vis Sci* 43: 1012-1018.
82. Hahn, A. B., G. N. Foulks, C. Enger, N. Fink, W. J. Stark, K. A. Hopkins, and F. Sanfilippo. 1995. The association of lymphocytotoxic antibodies with corneal allograft rejection in high risk patients. The Collaborative Corneal Transplantation Studies Research Group. *Transplantation* 59: 21-27.
83. D'Orazio, T. J., E. Mayhew, and J. Y. Niederkorn. 2001. Ocular immune privilege promoted by the presentation of peptide on tolerogenic B cells in the spleen. II. Evidence for presentation by Qa-1. *J Immunol* 166: 26-32.
84. D'Orazio, T. J., and J. Y. Niederkorn. 1998. Splenic B cells are required for tolerogenic antigen presentation in the induction of anterior chamber-associated immune deviation (ACAID). *Immunology* 95: 47-55.
85. Ritter, T., and U. Pleyer. 2009. Novel gene therapeutic strategies for the induction of tolerance in cornea transplantation. *Expert Rev Clin Immunol* 5: 749-764.
86. Kampik, D., R. R. Ali, and D. F. Larkin. 2012. Experimental gene transfer to the corneal endothelium. *Exp Eye Res* 95: 54-59.
87. Parker, D. G., H. M. Brereton, D. J. Coster, and K. A. Williams. 2009. The potential of viral vector-mediated gene transfer to prolong corneal allograft survival. *Curr Gene Ther* 9: 33-44.
88. Klebe, S., P. J. Sykes, D. J. Coster, R. Krishnan, and K. A. Williams. 2001. Prolongation of sheep corneal allograft survival by ex vivo transfer of the gene encoding interleukin-10. *Transplantation* 71: 1214-1220.
89. Larkin, D. F., H. B. Oral, C. J. Ring, N. R. Lemoine, and A. J. George. 1996. Adenovirus-mediated gene delivery to the corneal endothelium. *Transplantation* 61: 363-370.
90. Ritter, T., K. Vogt, P. Rieck, A. Schilling-Schon, J. Kolls, C. Hartmann, H. D. Volk, and U. Pleyer. 1999. Adenovirus-mediated gene transfer of interleukin-4 to corneal endothelial cells and organ cultured corneas leads to high IL-4 expression. *Exp Eye Res* 69: 563-568.
91. Qian, Y., F. L. Leong, A. Kazlauskas, and M. R. Dana. 2004. Ex vivo adenovirus-mediated gene transfer to corneal graft endothelial cells in mice. *Invest Ophthalmol Vis Sci* 45: 2187-2193.
92. Balaggan, K. S., and R. R. Ali. 2012. Ocular gene delivery using lentiviral vectors. *Gene Ther* 19: 145-153.
93. Ward, P., and C. E. Walsh. 2012. Targeted integration of a rAAV vector into the AAVS1 region. *Virology* 433: 356-366.

94. Fischer, A., S. Hacein-Bey-Abina, and M. Cavazzana-Calvo. 2011. Gene therapy for primary adaptive immune deficiencies. *The Journal of allergy and clinical immunology* 127: 1356-1359.
95. Banerjee, S., and A. D. Dick. 2003. Recent developments in the pharmacological treatment and prevention of corneal graft rejection. *Expert Opin Investig Drugs* 12: 29-37.
96. Cideciyan, A. V., T. S. Aleman, S. L. Boye, S. B. Schwartz, S. Kaushal, A. J. Roman, J. J. Pang, A. Sumaroka, E. A. Windsor, J. M. Wilson, T. R. Flotte, G. A. Fishman, E. Heon, E. M. Stone, B. J. Byrne, S. G. Jacobson, and W. W. Hauswirth. 2008. Human gene therapy for RPE65 isomerase deficiency activates the retinoid cycle of vision but with slow rod kinetics. *Proc Natl Acad Sci U S A* 105: 15112-15117.
97. Bainbridge, J. W., A. J. Smith, S. S. Barker, S. Robbie, R. Henderson, K. Balaggan, A. Viswanathan, G. E. Holder, A. Stockman, N. Tyler, S. Petersen-Jones, S. S. Bhattacharya, A. J. Thrasher, F. W. Fitzke, B. J. Carter, G. S. Rubin, A. T. Moore, and R. R. Ali. 2008. Effect of gene therapy on visual function in Leber's congenital amaurosis. *N Engl J Med* 358: 2231-2239.
98. Maguire, A. M., F. Simonelli, E. A. Pierce, E. N. Pugh, F. Mingozzi, J. Bennicelli, S. Banfi, K. A. Marshall, F. Testa, E. M. Surace, S. Rossi, A. Lyubarsky, V. R. Arruda, B. Konkle, E. Stone, J. Sun, J. Jacobs, L. Dell'Osso, R. Hertle, J. X. Ma, T. M. Redmond, X. Zhu, B. Hauck, O. Zelenaia, K. S. Shindler, M. G. Maguire, J. F. Wright, N. J. Volpe, J. W. McDonnell, A. Auricchio, K. A. High, and J. Bennett. 2008. Safety and efficacy of gene transfer for Leber's congenital amaurosis. *N Engl J Med* 358: 2240-2248.
99. Bennett, J., M. Ashtari, J. Wellman, K. A. Marshall, L. L. Cyckowski, D. C. Chung, S. McCague, E. A. Pierce, Y. Chen, J. L. Bennicelli, X. Zhu, G. S. Ying, J. Sun, J. F. Wright, A. Auricchio, F. Simonelli, K. S. Shindler, F. Mingozzi, K. A. High, and A. M. Maguire. 2012. AAV2 gene therapy readministration in three adults with congenital blindness. *Sci Transl Med* 4: 120ra115.
100. Gong, N., U. Pleyer, J. Yang, K. Vogt, M. Hill, I. Anegon, H. D. Volk, and T. Ritter. 2006. Influence of local and systemic CTLA4Ig gene transfer on corneal allograft survival. *J Gene Med* 8: 459-467.
101. Fabian, D., N. Gong, K. Vogt, H. D. Volk, U. Pleyer, and T. Ritter. 2007. The influence of inducible costimulator fusion protein (ICOSIg) gene transfer on corneal allograft survival. *Graefes Arch Clin Exp Ophthalmol* 245: 1515-1521.
102. Beutelspacher, S. C., P. H. Tan, M. O. McClure, D. F. Larkin, R. I. Lechler, and A. J. George. 2006. Expression of indoleamine 2,3-dioxygenase (IDO) by endothelial cells: implications for the control of alloresponses. *Am J Transplant* 6: 1320-1330.
103. Klebe, S., D. J. Coster, P. J. Sykes, S. Swinburne, P. Hallsworth, J. P. Scheerlinck, R. Krishnan, and K. A. Williams. 2005. Prolongation of sheep corneal allograft survival by transfer of the gene encoding ovine IL-12-p40 but not IL-4 to donor corneal endothelium. *J Immunol* 175: 2219-2226.
104. Ritter, T., J. Yang, H. Dannowski, K. Vogt, H. D. Volk, and U. Pleyer. 2007. Effects of interleukin-12p40 gene transfer on rat corneal allograft survival. *Transpl Immunol* 18: 101-107.

105. Sonoda, Y., and J. W. Streilein. 1992. Orthotopic corneal transplantation in mice--evidence that the immunogenetic rules of rejection do not apply. *Transplantation* 54: 694-704.
106. Murthy, R. C., T. J. McFarland, J. Yoken, S. Chen, C. Barone, D. Burke, Y. Zhang, B. Appukuttan, and J. T. Stout. 2003. Corneal transduction to inhibit angiogenesis and graft failure. *Invest Ophthalmol Vis Sci* 44: 1837-1842.
107. Barcia, R. N., M. R. Dana, and A. Kazlauskas. 2007. Corneal graft rejection is accompanied by apoptosis of the endothelium and is prevented by gene therapy with bcl-xL. *Am J Transplant* 7: 2082-2089.
108. Armitage, W. J., and D. L. Easty. 1997. Factors influencing the suitability of organ-cultured corneas for transplantation. *Invest Ophthalmol Vis Sci* 38: 16-24.
109. Williams, K. A., M. Lowe, C. Bartlett, T. L. Kelly, D. J. Coster, and A. Contributors. 2008. Risk factors for human corneal graft failure within the Australian corneal graft registry. *Transplantation* 86: 1720-1724.
110. Fuchsluger, T. A., U. Jurkunas, A. Kazlauskas, and R. Dana. 2011. Anti-apoptotic gene therapy prolongs survival of corneal endothelial cells during storage. *Gene Ther* 18: 778-787.
111. Fuchsluger, T. A., U. Jurkunas, A. Kazlauskas, and R. Dana. 2011. Corneal endothelial cells are protected from apoptosis by gene therapy. *Hum Gene Ther* 22: 549-558.
112. Hoffman, L. M., A. M. Maguire, and J. Bennett. 1997. Cell-mediated immune response and stability of intraocular transgene expression after adenovirus-mediated delivery. *Invest Ophthalmol Vis Sci* 38: 2224-2233.
113. Tripathy, S. K., H. B. Black, E. Goldwasser, and J. M. Leiden. 1996. Immune responses to transgene-encoded proteins limit the stability of gene expression after injection of replication-defective adenovirus vectors. *Nat Med* 2: 545-550.
114. Gong, N., U. Pleyer, K. Vogt, I. Anegon, A. Flügel, H. D. Volk, and T. Ritter. 2007. Local overexpression of nerve growth factor in rat corneal transplants improves allograft survival. *Invest Ophthalmol Vis Sci* 48: 1043-1052.
115. Yang, W., H. Li, P. W. Chen, H. Alizadeh, Y. He, R. N. Hogan, and J. Y. Niederkorn. 2009. PD-L1 expression on human ocular cells and its possible role in regulating immune-mediated ocular inflammation. *Invest Ophthalmol Vis Sci* 50: 273-280.
116. Riccardi, C., and I. Nicoletti. 2006. Analysis of apoptosis by propidium iodide staining and flow cytometry. *Nat Protoc* 1: 1458-1461.
117. Mnich, K., D. P. Finn, E. Dowd, and A. M. Gorman. 2010. Inhibition by anandamide of 6-hydroxydopamine-induced cell death in PC12 cells. *Int J Cell Biol* 2010: 818497.
118. Livak, K. J., and T. D. Schmittgen. 2001. Analysis of relative gene expression data using real-time quantitative PCR and the 2(-Delta Delta C(T)) Method. *Methods* 25: 402-408.
119. LEVI-MONTALCINI, R., and S. COHEN. 1960. Effects of the extract of the mouse submaxillary salivary glands on the sympathetic system of mammals. *Ann N Y Acad Sci* 85: 324-341.
120. Barde, Y. A., D. Edgar, and H. Thoenen. 1982. Purification of a new neurotrophic factor from mammalian brain. *EMBO J* 1: 549-553.

121. Hohn, A., J. Leibrock, K. Bailey, and Y. A. Barde. 1990. Identification and characterization of a novel member of the nerve growth factor/brain-derived neurotrophic factor family. *Nature* 344: 339-341.
122. Hallböök, F., C. F. Ibáñez, and H. Persson. 1991. Evolutionary studies of the nerve growth factor family reveal a novel member abundantly expressed in Xenopus ovary. *Neuron* 6: 845-858.
123. Berkemeier, L. R., J. W. Winslow, D. R. Kaplan, K. Nikolics, D. V. Goeddel, and A. Rosenthal. 1991. Neurotrophin-5: a novel neurotrophic factor that activates trk and trkB. *Neuron* 7: 857-866.
124. Huber, L. J., and M. V. Chao. 1995. A potential interaction of p75 and trkA NGF receptors revealed by affinity crosslinking and immunoprecipitation. *J Neurosci Res* 40: 557-563.
125. Chao, M. V., and B. L. Hempstead. 1995. p75 and Trk: a two-receptor system. *Trends Neurosci* 18: 321-326.
126. Lambiase, A., S. Bonini, A. Micera, P. Rama, and L. Aloe. 1998. Expression of nerve growth factor receptors on the ocular surface in healthy subjects and during manifestation of inflammatory diseases. *Invest Ophthalmol Vis Sci* 39: 1272-1275.
127. You, L., F. E. Kruse, and H. E. Völcker. 2000. Neurotrophic factors in the human cornea. *Invest Ophthalmol Vis Sci* 41: 692-702.
128. Lambiase, A., L. Manni, S. Bonini, P. Rama, A. Micera, and L. Aloe. 2000. Nerve growth factor promotes corneal healing: structural, biochemical, and molecular analyses of rat and human corneas. *Invest Ophthalmol Vis Sci* 41: 1063-1069.
129. Lu, B., C. R. Buck, C. F. Dreyfus, and I. B. Black. 1989. Expression of NGF and NGF receptor mRNAs in the developing brain: evidence for local delivery and action of NGF. *Exp Neurol* 104: 191-199.
130. Kokaia, Z., J. Bengzon, M. Metsis, M. Kokaia, H. Persson, and O. Lindvall. 1993. Coexpression of neurotrophins and their receptors in neurons of the central nervous system. *Proc Natl Acad Sci U S A* 90: 6711-6715.
131. Ehrhard, P. B., P. Erb, U. Graumann, and U. Otten. 1993. Expression of nerve growth factor and nerve growth factor receptor tyrosine kinase Trk in activated CD4-positive T-cell clones. *Proc Natl Acad Sci U S A* 90: 10984-10988.
132. Kruse, F. E., and S. C. Tseng. 1993. Growth factors modulate clonal growth and differentiation of cultured rabbit limbal and corneal epithelium. *Invest Ophthalmol Vis Sci* 34: 1963-1976.
133. Lambiase, A., P. Rama, S. Bonini, G. Caprioglio, and L. Aloe. 1998. Topical treatment with nerve growth factor for corneal neurotrophic ulcers. *N Engl J Med* 338: 1174-1180.
134. Lambiase, A., S. Bonini, L. Manni, E. Ghinelli, P. Tirassa, P. Rama, and L. Aloe. 2002. Intraocular production and release of nerve growth factor after iridectomy. *Invest Ophthalmol Vis Sci* 43: 2334-2340.
135. Sornelli, F., A. Lambiase, F. Mantelli, and L. Aloe. 2010. NGF and NGF-receptor expression of cultured immortalized human corneal endothelial cells. *Mol Vis* 16: 1439-1447.
136. Casaccia-Bonnefil, P., C. Gu, and M. V. Chao. 1999. Neurotrophins in cell survival/death decisions. *Adv Exp Med Biol* 468: 275-282.

137. Thompson, C. B. 1995. Apoptosis in the pathogenesis and treatment of disease. *Science* 267: 1456-1462.
138. Kale, J., Q. Liu, B. Leber, and D. W. Andrews. 2012. Shedding light on apoptosis at subcellular membranes. *Cell* 151: 1179-1184.
139. Albon, J., A. B. Tullo, S. Aktar, and M. E. Boulton. 2000. Apoptosis in the endothelium of human corneas for transplantation. *Invest Ophthalmol Vis Sci* 41: 2887-2893.
140. Boisgérault, F., Y. Liu, N. Anosova, E. Ehrlich, M. R. Dana, and G. Benichou. 2001. Role of CD4+ and CD8+ T cells in allorecognition: lessons from corneal transplantation. *J Immunol* 167: 1891-1899.
141. Chang, E. J., Y. S. Im, E. P. Kay, J. Y. Kim, J. E. Lee, and H. K. Lee. 2008. The role of nerve growth factor in hyperosmolar stress induced apoptosis. *J Cell Physiol* 216: 69-77.
142. Ebendal, T. 1992. Function and evolution in the NGF family and its receptors. *J Neurosci Res* 32: 461-470.
143. Szegezdi, E., K. R. Herbert, E. T. Kavanagh, A. Samali, and A. M. Gorman. 2008. Nerve growth factor blocks thapsigargin-induced apoptosis at the level of the mitochondrion via regulation of Bim. *J Cell Mol Med* 12: 2482-2496.
144. Papadakis, E. D., S. A. Nicklin, A. H. Baker, and S. J. White. 2004. Promoters and control elements: designing expression cassettes for gene therapy. *Curr Gene Ther* 4: 89-113.
145. Weber, E. L., and P. M. Cannon. 2007. Promoter choice for retroviral vectors: transcriptional strength versus trans-activation potential. *Hum Gene Ther* 18: 849-860.
146. Fehervari, Z., S. A. Rayner, H. B. Oral, A. J. George, and D. F. Larkin. 1997. Gene transfer to ex vivo stored corneas. *Cornea* 16: 459-464.
147. Oral, H. B., D. F. Larkin, Z. Fehervari, A. P. Byrnes, A. M. Rankin, D. O. Haskard, M. J. Wood, M. J. Dallman, and A. J. George. 1997. Ex vivo adenovirus-mediated gene transfer and immunomodulatory protein production in human cornea. *Gene Ther* 4: 639-647.
148. Brooks, A. R., R. N. Harkins, P. Wang, H. S. Qian, P. Liu, and G. M. Rubanyi. 2004. Transcriptional silencing is associated with extensive methylation of the CMV promoter following adenoviral gene delivery to muscle. *J Gene Med* 6: 395-404.
149. Gopalkrishnan, R. V., K. A. Christiansen, N. I. Goldstein, R. A. DePinho, and P. B. Fisher. 1999. Use of the human EF-1alpha promoter for expression can significantly increase success in establishing stable cell lines with consistent expression: a study using the tetracycline-inducible system in human cancer cells. *Nucleic Acids Res* 27: 4775-4782.
150. Challa, P., C. Luna, P. B. Liton, B. Chamblin, J. Wakefield, R. Ramabhadran, D. L. Epstein, and P. Gonzalez. 2005. Lentiviral mediated gene delivery to the anterior chamber of rodent eyes. *Mol Vis* 11: 425-430.
151. Gong, N., I. Ecke, S. Mergler, J. Yang, S. Metzner, S. Schu, H. D. Volk, U. Pleyer, and T. Ritter. 2007. Gene transfer of cyto-protective molecules in corneal endothelial cells and cultured corneas: analysis of protective effects in vitro and in vivo. *Biochem Biophys Res Commun* 357: 302-307.
152. Fleury, S., E. Simeoni, C. Zuppinger, N. Déglon, L. K. von Segesser, L. Kappenberger, and G. Vassalli. 2003. Multiply attenuated, self-inactivating

lentiviral vectors efficiently deliver and express genes for extended periods of time in adult rat cardiomyocytes in vivo. *Circulation* 107: 2375-2382.

153. Parker, D. G., C. Kaufmann, H. M. Brereton, D. S. Anson, L. Francis-Staite, C. F. Jessup, K. Marshall, C. Tan, R. Koldej, D. J. Coster, and K. A. Williams. 2007. Lentivirus-mediated gene transfer to the rat, ovine and human cornea. *Gene Ther* 14: 760-767.
154. Parker, D. G., D. J. Coster, H. M. Brereton, P. H. Hart, R. Koldej, D. S. Anson, and K. A. Williams. 2010. Lentivirus-mediated gene transfer of interleukin 10 to the ovine and human cornea. *Clin Experiment Ophthalmol* 38: 405-413.
155. Lambiase, A., M. Sacchetti, and S. Bonini. 2012. Nerve growth factor therapy for corneal disease. *Curr Opin Ophthalmol* 23: 296-302.
156. Fuchsluger T.A., J. U., Kazlauskas A., Dana R. 2009. Characteristics of Primary Human Corneal Endothelial Cells (pHCEC) and Immortalized HCEC (iHCEC) Studying Early Apoptosis and Gene Transfer. In *ARVO 2009 Annual Meeting*, Fort Lauderdale, Fl.
157. Tatard, V. M., M. C. Venier-Julienne, J. P. Benoit, P. Menei, and C. N. Montero-Menei. 2004. In vivo evaluation of pharmacologically active microcarriers releasing nerve growth factor and conveying PC12 cells. *Cell Transplant* 13: 573-583.
158. Allen, S. J., J. J. Watson, and D. Dawbarn. 2011. The neurotrophins and their role in Alzheimer's disease. *Curr Neuropharmacol* 9: 559-573.
159. Allen, S. J., J. J. Watson, D. K. Shoemark, N. U. Barua, and N. K. Patel. 2013. GDNF, NGF and BDNF as therapeutic options for neurodegeneration. *Pharmacol Ther*.
160. Nagahara, A. H., T. Bernot, R. Moseanko, L. Brignolo, A. Blesch, J. M. Conner, A. Ramirez, M. Gasmi, and M. H. Tuszynski. 2009. Long-term reversal of cholinergic neuronal decline in aged non-human primates by lentiviral NGF gene delivery. *Exp Neurol* 215: 153-159.
161. Tuszynski, M. H., L. Thal, M. Pay, D. P. Salmon, H. S. U, R. Bakay, P. Patel, A. Blesch, H. L. Vahlsing, G. Ho, G. Tong, S. G. Potkin, J. Fallon, L. Hansen, E. J. Mufson, J. H. Kordower, C. Gall, and J. Conner. 2005. A phase 1 clinical trial of nerve growth factor gene therapy for Alzheimer disease. *Nat Med* 11: 551-555.
162. Katami, M., P. W. Madden, D. J. White, P. G. Watson, and N. Kamada. 1989. The extent of immunological privilege of orthotopic corneal grafts in the inbred rat. *Transplantation* 48: 371-376.
163. del Rio, M. L., L. Buhler, C. Gibbons, J. Tian, and J. I. Rodriguez-Barbosa. 2008. PD-1/PD-L1, PD-1/PD-L2, and other co-inhibitory signaling pathways in transplantation. *Transpl Int* 21: 1015-1028.
164. Salomon, B., and J. A. Bluestone. 2001. Complexities of CD28/B7: CTLA-4 costimulatory pathways in autoimmunity and transplantation. *Annu Rev Immunol* 19: 225-252.
165. Walunas, T. L., D. J. Lenschow, C. Y. Bakker, P. S. Linsley, G. J. Freeman, J. M. Green, C. B. Thompson, and J. A. Bluestone. 1994. CTLA-4 can function as a negative regulator of T cell activation. *Immunity* 1: 405-413.
166. Nishimura, H., N. Minato, T. Nakano, and T. Honjo. 1998. Immunological studies on PD-1 deficient mice: implication of PD-1 as a negative regulator for B cell responses. *Int Immunol* 10: 1563-1572.

167. Fife, B. T., and J. A. Bluestone. 2008. Control of peripheral T-cell tolerance and autoimmunity via the CTLA-4 and PD-1 pathways. *Immunol Rev* 224: 166-182.
168. Nishimura, H., M. Nose, H. Hiai, N. Minato, and T. Honjo. 1999. Development of lupus-like autoimmune diseases by disruption of the PD-1 gene encoding an ITIM motif-carrying immunoreceptor. *Immunity* 11: 141-151.
169. Nishimura, H., T. Okazaki, Y. Tanaka, K. Nakatani, M. Hara, A. Matsumori, S. Sasayama, A. Mizoguchi, H. Hiai, N. Minato, and T. Honjo. 2001. Autoimmune dilated cardiomyopathy in PD-1 receptor-deficient mice. *Science* 291: 319-322.
170. Nishimura, H., and T. Honjo. 2001. PD-1: an inhibitory immunoreceptor involved in peripheral tolerance. *Trends Immunol* 22: 265-268.
171. Dong, H., G. Zhu, K. Tamada, and L. Chen. 1999. B7-H1, a third member of the B7 family, co-stimulates T-cell proliferation and interleukin-10 secretion. *Nat Med* 5: 1365-1369.
172. Latchman, Y., C. R. Wood, T. Chernova, D. Chaudhary, M. Borde, I. Chernova, Y. Iwai, A. J. Long, J. A. Brown, R. Nunes, E. A. Greenfield, K. Bourque, V. A. Boussiotis, L. L. Carter, B. M. Carreno, N. Malenkovich, H. Nishimura, T. Okazaki, T. Honjo, A. H. Sharpe, and G. J. Freeman. 2001. PD-L2 is a second ligand for PD-1 and inhibits T cell activation. *Nat Immunol* 2: 261-268.
173. Ishida, M., Y. Iwai, Y. Tanaka, T. Okazaki, G. J. Freeman, N. Minato, and T. Honjo. 2002. Differential expression of PD-L1 and PD-L2, ligands for an inhibitory receptor PD-1, in the cells of lymphohematopoietic tissues. *Immunol Lett* 84: 57-62.
174. Yamazaki, T., H. Akiba, H. Iwai, H. Matsuda, M. Aoki, Y. Tanno, T. Shin, H. Tsuchiya, D. M. Pardoll, K. Okumura, M. Azuma, and H. Yagita. 2002. Expression of programmed death 1 ligands by murine T cells and APC. *J Immunol* 169: 5538-5545.
175. Ozkaynak, E., L. Wang, A. Goodearl, K. McDonald, S. Qin, T. O'Keefe, T. Duong, T. Smith, J. C. Gutierrez-Ramos, J. B. Rottman, A. J. Coyle, and W. W. Hancock. 2002. Programmed death-1 targeting can promote allograft survival. *J Immunol* 169: 6546-6553.
176. Watson, M. P., A. J. George, and D. F. Larkin. 2006. Differential effects of costimulatory pathway modulation on corneal allograft survival. *Invest Ophthalmol Vis Sci* 47: 3417-3422.
177. El Annan, J., S. Goyal, Q. Zhang, G. J. Freeman, A. H. Sharpe, and R. Dana. 2010. Regulation of T-cell chemotaxis by programmed death-ligand 1 (PD-L1) in dry eye-associated corneal inflammation. *Invest Ophthalmol Vis Sci* 51: 3418-3423.
178. Sugita, S., Y. Usui, S. Horie, Y. Futagami, Y. Yamada, J. Ma, T. Kezuka, H. Hamada, T. Usui, M. Mochizuki, and S. Yamagami. 2009. Human corneal endothelial cells expressing programmed death-ligand 1 (PD-L1) suppress PD-1+ T helper 1 cells by a contact-dependent mechanism. *Invest Ophthalmol Vis Sci* 50: 263-272.
179. Benson, D. M., C. E. Bakan, A. Mishra, C. C. Hofmeister, Y. Efebera, B. Becknell, R. A. Baiocchi, J. Zhang, J. Yu, M. K. Smith, C. N. Greenfield, P. Porcu, S. M. Devine, R. Rotem-Yehudar, G. Lozanski, J. C. Byrd, and M. A.

Caligiuri. 2010. The PD-1/PD-L1 axis modulates the natural killer cell versus multiple myeloma effect: a therapeutic target for CT-011, a novel monoclonal anti-PD-1 antibody. *Blood* 116: 2286-2294.

180. Iwai, Y., M. Ishida, Y. Tanaka, T. Okazaki, T. Honjo, and N. Minato. 2002. Involvement of PD-L1 on tumor cells in the escape from host immune system and tumor immunotherapy by PD-L1 blockade. *Proc Natl Acad Sci U S A* 99: 12293-12297.
181. Cao, Y., L. Zhang, Y. Kamimura, P. Ritprajak, M. Hashiguchi, S. Hirose, and M. Azuma. 2011. B7-H1 overexpression regulates epithelial-mesenchymal transition and accelerates carcinogenesis in skin. *Cancer Res* 71: 1235-1243.
182. Cao, Y., L. Zhang, P. Ritprajak, F. Tsushima, P. Youngnak-Piboonratanakit, Y. Kamimura, M. Hashiguchi, and M. Azuma. 2011. Immunoregulatory molecule B7-H1 (CD274) contributes to skin carcinogenesis. *Cancer Res* 71: 4737-4741.
183. Billerbeck, E., Y. H. Kang, L. Walker, H. Lockstone, S. Grafmueller, V. Fleming, J. Flint, C. B. Willberg, B. Bengsch, B. Seigel, N. Ramamurthy, N. Zitzmann, E. J. Barnes, J. Thevanayagam, A. Bhagwanani, A. Leslie, Y. H. Oo, S. Kollnberger, P. Bowness, O. Drognitz, D. H. Adams, H. E. Blum, R. Thimme, and P. Klenerman. 2009. Analysis of CD161 expression on human CD8+ T cells defines a distinct functional subset with tissue-homing properties. *Proc Natl Acad Sci U S A* 107: 3006-3011.
184. Takahashi, T., S. Dejbakhsh-Jones, and S. Strober. 2006. Expression of CD161 (NKR-P1A) defines subsets of human CD4 and CD8 T cells with different functional activities. *J Immunol* 176: 211-216.
185. Wang, L., R. Han, and W. W. Hancock. 2007. Programmed cell death 1 (PD-1) and its ligand PD-L1 are required for allograft tolerance. *Eur J Immunol* 37: 2983-2990.
186. Wang, W., K. Carper, F. Malone, Y. Latchman, J. Perkins, Y. Fu, J. Reyes, and W. Li. 2008. PD-L1/PD-1 signal deficiency promotes allogeneic immune responses and accelerates heart allograft rejection. *Transplantation* 86: 836-844.
187. Gao, W., G. Demirci, T. B. Strom, and X. C. Li. 2003. Stimulating PD-1-negative signals concurrent with blocking CD154 co-stimulation induces long-term islet allograft survival. *Transplantation* 76: 994-999.
188. Fiorina, P., M. Jurewicz, A. Vergani, A. Petrelli, M. Carvello, F. D'Addio, J. G. Godwin, K. Law, E. Wu, Z. Tian, G. Thoma, J. Kovarik, S. La Rosa, C. Capella, S. Rodig, H. G. Zerwes, M. H. Sayegh, and R. Abdi. 2011. Targeting the CXCR4-CXCL12 axis mobilizes autologous hematopoietic stem cells and prolongs islet allograft survival via programmed death ligand 1. *J Immunol* 186: 121-131.
189. Cheng, X., H. Dai, N. Wan, Y. Moore, R. Vankayalapati, and Z. Dai. 2009. Interaction of programmed death-1 and programmed death-1 ligand-1 contributes to testicular immune privilege. *Transplantation* 87: 1778-1786.
190. Rosenzweig, M., M. Connole, R. Glickman, S. P. Yue, B. Noren, M. DeMaria, and R. P. Johnson. 2001. Induction of cytotoxic T lymphocyte and antibody responses to enhanced green fluorescent protein following transplantation of transduced CD34(+) hematopoietic cells. *Blood* 97: 1951-1959.

191. Baekelandt, V., K. Eggermont, M. Michiels, B. Nuttin, and Z. Debyser. 2003. Optimized lentiviral vector production and purification procedure prevents immune response after transduction of mouse brain. *Gene Ther* 10: 1933-1940.
192. Moloney, T. C., P. Dockery, A. J. Windebank, F. P. Barry, L. Howard, and E. Dowd. Survival and immunogenicity of mesenchymal stem cells from the green fluorescent protein transgenic rat in the adult rat brain. *Neurorehabil Neural Repair* 24: 645-656.
193. Beutelspacher, S. C., R. Pillai, M. P. Watson, P. H. Tan, J. Tsang, M. O. McClure, A. J. George, and D. F. Larkin. 2006. Function of indoleamine 2,3-dioxygenase in corneal allograft rejection and prolongation of allograft survival by over-expression. *Eur J Immunol* 36: 690-700.
194. Sharpe, A. H., E. J. Wherry, R. Ahmed, and G. J. Freeman. 2007. The function of programmed cell death 1 and its ligands in regulating autoimmunity and infection. *Nat Immunol* 8: 239-245.
195. Haspot, F., T. Fehr, C. Gibbons, G. Zhao, T. Hogan, T. Honjo, G. J. Freeman, and M. Sykes. 2008. Peripheral deletional tolerance of alloreactive CD8 but not CD4 T cells is dependent on the PD-1/PD-L1 pathway. *Blood* 112: 2149-2155.
196. Dong, H., G. Zhu, K. Tamada, D. B. Flies, J. M. van Deursen, and L. Chen. 2004. B7-H1 determines accumulation and deletion of intrahepatic CD8(+) T lymphocytes. *Immunity* 20: 327-336.
197. Flynn, T. H., N. A. Mitchison, S. J. Ono, and D. F. Larkin. 2008. Aqueous humor alloreactive cell phenotypes, cytokines and chemokines in corneal allograft rejection. *Am J Transplant* 8: 1537-1543.
198. Niederkorn, J. Y. 2009. Role of NKT cells in anterior chamber-associated immune deviation. *Expert Rev Clin Immunol* 5: 137-144.
199. Chang, W. S., J. Y. Kim, Y. J. Kim, Y. S. Kim, J. M. Lee, M. Azuma, H. Yagita, and C. Y. Kang. 2008. Cutting edge: Programmed death-1/programmed death ligand 1 interaction regulates the induction and maintenance of invariant NKT cell anergy. *J Immunol* 181: 6707-6710.
200. Durgan, K., M. Ali, P. Warner, and Y. E. Latchman. 2011. Targeting NKT cells and PD-L1 pathway results in augmented anti-tumor responses in a melanoma model. *Cancer Immunol Immunother* 60: 547-558.
201. Skelsey, M. E., E. Mayhew, and J. Y. Niederkorn. 2003. Splenic B cells act as antigen presenting cells for the induction of anterior chamber-associated immune deviation. *Invest Ophthalmol Vis Sci* 44: 5242-5251.
202. Balaggan, K. S., K. Binley, M. Esapa, S. Iqball, Z. Askham, O. Kan, M. Tschernutter, J. W. Bainbridge, S. Naylor, and R. R. Ali. 2006. Stable and efficient intraocular gene transfer using pseudotyped EIAV lentiviral vectors. *J Gene Med* 8: 275-285.
203. Beutelspacher, S. C., N. Ardjomand, P. H. Tan, G. S. Patton, D. F. Larkin, A. J. George, and M. O. McClure. 2005. Comparison of HIV-1 and EIAV-based lentiviral vectors in corneal transduction. *Exp Eye Res* 80: 787-794.
204. Maury, W. 1998. Regulation of equine infectious anemia virus expression. *J Biomed Sci* 5: 11-23.
205. Miskin, J., D. Chipchase, J. Rohll, G. Beard, T. Wardell, D. Angell, H. Roehl, D. Jolly, S. Kingsman, and K. Mitrophanous. 2006. A replication competent

lentivirus (RCL) assay for equine infectious anaemia virus (EIAV)-based lentiviral vectors. *Gene Ther* 13: 196-205.

206. Li, Z., J. Düllmann, B. Schiedlmeier, M. Schmidt, C. von Kalle, J. Meyer, M. Forster, C. Stocking, A. Wahlers, O. Frank, W. Ostertag, K. Kühlcke, H. G. Eckert, B. Fehse, and C. Baum. 2002. Murine leukemia induced by retroviral gene marking. *Science* 296: 497.
207. Hacein-Bey-Abina, S., C. von Kalle, M. Schmidt, F. Le Deist, N. Wulffraat, E. McIntyre, I. Radford, J. L. Villeval, C. C. Fraser, M. Cavazzana-Calvo, and A. Fischer. 2003. A serious adverse event after successful gene therapy for X-linked severe combined immunodeficiency. *N Engl J Med* 348: 255-256.
208. Hacker, C. V., C. A. Vink, T. W. Wardell, S. Lee, P. Treasure, S. M. Kingsman, K. A. Mitrophanous, and J. E. Miskin. 2006. The integration profile of EIAV-based vectors. *Mol Ther* 14: 536-545.
209. Schröder, A. R., P. Shinn, H. Chen, C. Berry, J. R. Ecker, and F. Bushman. 2002. HIV-1 integration in the human genome favors active genes and local hotspots. *Cell* 110: 521-529.
210. Bartholomae, C. C., A. Arens, K. S. Balaggan, R. J. Yáñez-Muñoz, E. Montini, S. J. Howe, A. Paruzynski, B. Korn, J. U. Appelt, A. Macneil, D. Cesana, U. Abel, H. Glimm, L. Naldini, R. R. Ali, A. J. Thrasher, C. von Kalle, and M. Schmidt. 2011. Lentiviral vector integration profiles differ in rodent postmitotic tissues. *Mol Ther* 19: 703-710.
211. Banasik, M. B., and P. B. McCray. 2010. Integrase-defective lentiviral vectors: progress and applications. *Gene Ther* 17: 150-157.
212. Michelini, Z., D. R. Negri, S. Baroncelli, M. Spada, P. Leone, R. Bona, M. E. Klotman, and A. Cara. 2009. Development and use of SIV-based Integrase defective lentiviral vector for immunization. *Vaccine* 27: 4622-4629.
213. Bemelmans, A. P., Y. Arsenijevic, and F. Majo. 2009. Efficient lentiviral gene transfer into corneal stroma cells using a femtosecond laser. *Gene Ther* 16: 933-938.
214. Dull, T., R. Zufferey, M. Kelly, R. J. Mandel, M. Nguyen, D. Trono, and L. Naldini. 1998. A third-generation lentivirus vector with a conditional packaging system. *J Virol* 72: 8463-8471.
215. Yáñez-Muñoz, R. J., K. S. Balaggan, A. MacNeil, S. J. Howe, M. Schmidt, A. J. Smith, P. Buch, R. E. MacLaren, P. N. Anderson, S. E. Barker, Y. Duran, C. Bartholomae, C. von Kalle, J. R. Heckenlively, C. Kinnon, R. R. Ali, and A. J. Thrasher. 2006. Effective gene therapy with nonintegrating lentiviral vectors. *Nat Med* 12: 348-353.
216. Nosov, M., M. Wilk, M. Morcos, M. Cregg, L. O'Flynn, O. Treacy, and T. Ritter. 2012. Role of Lentivirus-Mediated Overexpression of Programmed Death-Ligand 1 on Corneal Allograft Survival. *Am J Transplant*.
217. Park, K. A., J. C. Fehrenbacher, E. L. Thompson, D. B. Duarte, C. M. Hingtgen, and M. R. Vasko. 2010. Signaling pathways that mediate nerve growth factor-induced increase in expression and release of calcitonin gene-related peptide from sensory neurons. *Neuroscience* 171: 910-923.
218. Bracci-Laudiero, L., L. Aloe, P. Buanne, A. Finn, C. Stenfors, E. Vigneti, E. Theodorsson, and T. Lundeberg. 2002. NGF modulates CGRP synthesis in human B-lymphocytes: a possible anti-inflammatory action of NGF? *J Neuroimmunol* 123: 58-65.

219. Bracci-Laudiero, L., L. Aloe, M. C. Caroleo, P. Buanne, N. Costa, G. Starace, and T. Lundeberg. 2005. Endogenous NGF regulates CGRP expression in human monocytes, and affects HLA-DR and CD86 expression and IL-10 production. *Blood* 106: 3507-3514.
220. Yang, J. H., Y. Q. Zhang, and Z. Guo. 2011. Endogenous CGRP protects retinal cells against stress induced apoptosis in rats. *Neurosci Lett* 501: 83-85.
221. Zhao, F. P., Z. Guo, and P. F. Wang. 2010. Calcitonin gene related peptide (CGRP) inhibits norepinephrine induced apoptosis in cultured rat cardiomyocytes not via PKA or PKC pathways. *Neurosci Lett* 482: 163-166.
222. Mrak, E., F. Guidobono, G. Moro, G. Fraschini, A. Rubinacci, and I. Villa. 2010. Calcitonin gene-related peptide (CGRP) inhibits apoptosis in human osteoblasts by β-catenin stabilization. *J Cell Physiol* 225: 701-708.
223. Zhang, X. N., D. Z. Chen, Y. H. Zheng, J. G. Liang, H. X. Yang, X. W. Lin, and J. Zhuang. 2009. Gene transfer of calcitonin gene-related peptide suppresses development of allograft vasculopathy. *Transplant Proc* 41: 1900-1905.

Appendix

Appendix

I. Publications by the author

Role of lentivirus-mediated overexpression of programmed death-ligand 1 on corneal allograft survival.

Nosov M*, **Wilk M***, Morcos M, Cregg M, O'Flynn L, Treacy O, Ritter T. Am J Transplant. 2012 May;12(5):1313-22. * Both authors contributed equally to this manuscript.

Available from: http:doi: http://dx.doi.org/10.1111/j.1600-6143.2011.03948.x

Adenoviral transduction of mesenchymal stem cells: *in vitro* responses and *in vivo* immune responses after cell transplantation.

Treacy O, Ryan A, Heinzl T, O'Flynn L, Cregg M, **Wilk M**, Odoardi F, Lohan P, O'Brien, Nosov M, Ritter T. PLOS One. 2012;7(8).

Available from: http://dx.doi.org/10.1371/journal.pone.0042662

Gene therapy approaches to prevent corneal graft rejection: Where do we stand?

Ritter T, **Wilk M,** Nosov M. Ophthalmic Research

Manuscript in press